E. L. Wilson

REPORT NO.
SESM-66-17

STRUCTURES AND MATERIALS RESEARCH
DEPARTMENT OF CIVIL ENGINEERING

ANALYSIS OF SIMPLY SUPPORTED BOX GIRDER BRIDGES

BY

A. C. SCORDELIS

Report to the Sponsors: Division of Highways, Department of Public Works, State of California, and the Bureau of Public Roads.

OCTOBER 1966

COLLEGE OF ENGINEERING
OFFICE OF RESEARCH SERVICES
UNIVERSITY OF CALIFORNIA
BERKELEY CALIFORNIA

Structures and Materials Research
Department of Civil Engineering
Division of Structural Engineering
and Structural Mechanics

ANALYSIS OF SIMPLY SUPPORTED BOX GIRDER BRIDGES

A Report of an Investigation

by

A. C. Scordelis
Professor of Civil Engineering

to

The Division of Highways
Department of Public Works
State of California
Under California Standard Agreement
No. 14685
and
U. S. Department of Commerce
Bureau of Public Roads

College of Engineering
Office of Research Services
University of California
Berkeley, California

October 1966

TABLE OF CONTENTS

LIST OF TABLES

LIST OF FIGURES

I. INTRODUCTION

1. Objective

The objective of this investigation was the development of a general method of analysis for simply supported box girder bridges. The study was concerned with the elastic analysis of these structures by methods suited to the application of digital computers. Ultimate goal of the investigation was the development of a general computer program capable of determining displacements and internal forces in multi-celled, simply supported box girder bridges subjected to a variety of loading and boundary conditions.

2. General Remarks

Bridge systems form an important part of much of the modern highway system being constructed in California, as well as throughout the United States. In recent years, the use of reinforced concrete box girder bridges has increased such that in 1965, approximately 60% of the total deck area of the bridges constructed in California were of this type. This increase is primarily due to the box girder's pleasing aesthetic appearance, its structural efficiency and its favorable economic position as contractors have become familiar with its construction. Because of the large annual volume of box girder bridge construction in California, it is obvious that research on box girder bridges leading to improved design methods and more economical structures could result in substantial savings in the total dollars spent for bridge construction in California.

A box girder bridge (Fig. 1) consists of a top and bottom slab connected by vertical webs to form a cellular or box-like structure. Present design

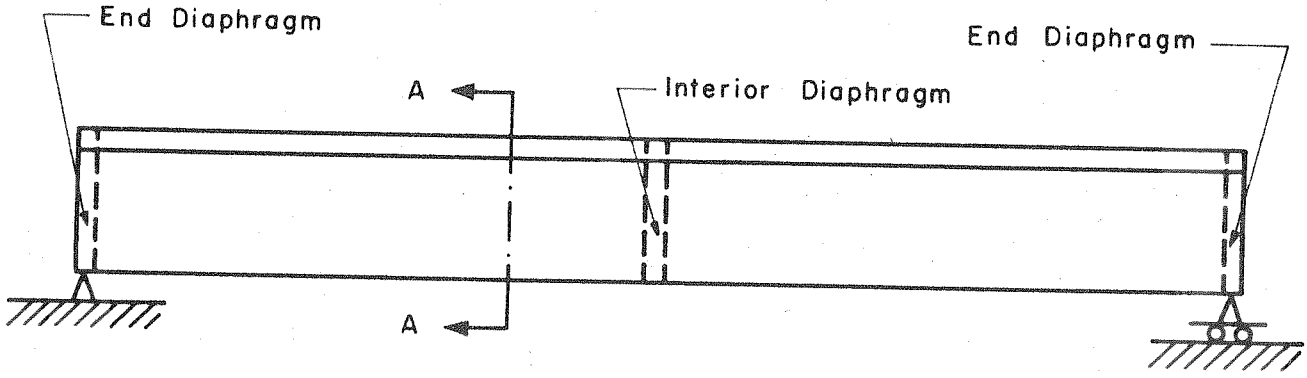

(a) SIDE ELEVATION

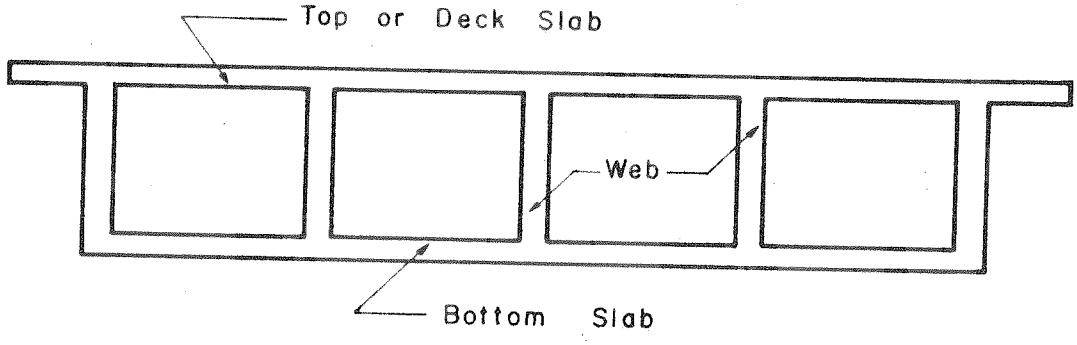

(b) CROSS - SECTION A - A

FIG. 1 TYPICAL BOX GIRDER BRIDGE

methods are generally based on empirical methods in which a typical repeating I shaped member consisting of a web and a top and bottom flange, equal in width to the web spacing, is taken from the structure and is analyzed as an independent beam. For wheel loads placed on the bridge, empirical formulae, based on the web spacing, are used to determine the load distribution to the independent longitudinal beams. Longitudinal and diagonal tension reinforcement are then provided to resist the tensile stresses developed in these beams. Additional reinforcement is also provided in the slabs to carry transverse and longitudinal slab bending moments, calculated again by empirical formulae.

An analytical solution of the true response of a box girder bridge under load is complicated by the usual factors common to other reinforced concrete structural systems. It is a highly indeterminate structure; it is made of two materials, concrete and steel; under increasing load it experiences cracking and thus a redistribution of internal forces; and also the internal forces are time-dependent because of creep and shrinkage in the concrete. Notwithstanding these complexities, as an initial step, the development of a general solution for box girders based on an elastic analysis of an uncracked homogeneous system should prove of considerable value in studying structures with a wide range of variables for interpretation purposes concerning wheel load distribution, distribution of internal forces and moments, deflections, economical dimensional relationships and general behavior.

3. Previous Studies

Numerous analytical and experimental studies have been made on the problem of wheel load distribution on slab bridges or on bridges with slabs supported

by longitudinal beams. On the contrary, information on the distribution of wheel loads on fully monolithic reinforced concrete box girder bridges is very meager.

Many investigators during the past thirty years have attempted to simplify the problem of analyzing a slab, or a slab on a network of beams, subjected to loads. Among these investigators are Hetenyi [1], Leonhardt [2,3], Pippard and deWaele [4], Guyon [5], Massonet [6,7,8], Morice, Little and Rowe [9,10,11, 12,13,14,15], and Hendry and Jaeger [16,17,18,19,20]. In all of these cases the slab and beam system is converted to an equivalent gridwork of beams or to an equivalent anisotropic slab. Once this is done the method of analysis varies depending on the investigator. Among the methods used are distribution and relaxation techniques, plate theory, and harmonic analysis. None of the methods involved are directly applicable to the problem of the box girder structure since they do not adequately represent the interaction of the individual plates and they do not yield answers for all of the important internal forces and moments in each plate.

The problem of a box beam is frequently encountered in aircraft structures. Textbooks by Niles and Newell [21], or Bruhn [22], and a paper by Nieman [23] outline procedures for the analysis of box beams. These procedures assume that due to the presence of transverse stiffeners or bulkheads, no transverse distortion of the beam cross-section occurs. Since, in general, the box girder system does experience transverse distortion, the above procedure cannot be used for this problem.

An accurate solution for simply supported box girder bridges can be obtained using the theory of prismatic folded plate structures. This approach, which

forms the basis of the present investigation, requires an enormous amount of computation and thus has become practicable only with the advent of fast digital computers with large storage capacities. Many papers have been written on the analysis of folded plates. A comprehensive bibliography on this subject is given in the report of the ASCE Task Committee on Folded Plate Construction [24]. Particularly pertinent to the present study are the papers by Goldberg and Leve [25] and De Fries and Scordelis [26].

The only previous comprehensive experimental and analytical investigation specifically on reinforced concrete box girder bridges is that reported on by Davis, Kozak, and Scheffey [27]. In this research program an extensive test program was conducted on a prototype, 4-cell, box girder bridge having an 80 ft. simple span. These experimental results were then correlated with analytical studies based on folded plate theory.

A number of other papers have been written on various aspects of box girder structures of various types and for reference they have been included in the selected bibliography, covering the past 30 years, at the end of this report.

4. Scope of Present Investigation

This investigation was concerned with the elastic analysis of a simply supported box girder bridge. This type of bridge may be thought of as a series of rectangular plates interconnected along longitudinal joints to form a cellular structure supported at end diaphragms. Conceptually, this type of structure is similar to folded plate structures which have often been used for roof systems. The roof system is somewhat simpler than the box girder

bridge since the connected plates do not form a closed cellular structure.

In the present study a direct stiffness solution for box girder bridges using a folded plate harmonic analysis based on the elasticity method [26] was developed. In this method, elastic plate theory is used for loads normal to the plane of the plates and two-dimensional plane stress theory is used for loads in the plane of the plates. Using this method, solutions for box girder bridges, with and without intermediate diaphragms, under concentrated or distributed loads anywhere on the bridge were obtained.

These solutions were then used to write general computer programs in which the basic input consists of the span; the geometry and material properties of the plates; the loading conditions; and the boundary conditions along each longitudinal joint. Final output from the programs include joint displacements, reactions, and all of the internal forces, moments and displacements at selected points in the structure.

On the basis of data supplied by the Bridge Department of the State of California, a review was made of over 200 simple span box girder bridges which have been constructed in California during the past ten years. Among the information collected and studied for each bridge were the span, width, depth, number of cells, spacing of webs, and thickness of top and bottom slabs and webs. This data was summarized and used to select the basic dimensions of example bridges used in parameter studies with respect to load distribution in box girder bridges. The examples, all analyzed by the computer programs developed, included two spans, 60 ft. and 80 ft., four cross-sections, 3, 4, 6, and 8 cells; and four loading conditions involving a single unit load at mid-span placed at four lateral positions on the bridge.

II. ANALYTICAL MODELS AND METHODS

1. Basic Assumptions

Various analytical models may be used to represent the simply supported box girder bridge. In this chapter the following assumptions are common to all of the analytical models discussed.

a. Each plate of the box girder is rectangular, of uniform thickness and is made of an elastic, isotropic and homogeneous material.

b. The relation between forces and deformations is linear, so that superposition is valid.

c. The structure is completely monolithic.

d. End support and intermediate diaphragms are infinitely stiff in their own plane, but perfectly flexible normal to their own plane.

The objective of the analysis may be stated simply as follows: given, a structure with known geometry, loading, boundary conditions and material properties; find, the resulting internal forces, moments, displacements and reactions. Several possible analytical models and methods will now be discussed.

2. Beam Method

The simplest approach for determining the longitudinal stresses in a box girder is to consider the entire cross-section to act as a beam and calculate the longitudinal stresses on the basis of the flexure formula from

elementary beam theory. The assumptions of this theory are:

a. The longitudinal fiber strains and stresses have a planar distribution over the entire cross-section.

b. As a result of assumption a, all points on a given cross-section experience the same resultant deflection and therefore, there is no transverse distortion of the cross-section.

c. The resultant of the external loads passes through the shear center.

Since the box girder is made up of relatively thin plates the assumption that no transverse distortion occurs is not generally satisfied and thus the beam method can give results which are considerably in error. Also in most cases the resultant load does not pass through the shear center, in which case the effect of torsion must be considered.

3. Equivalent Gridwork

In this approach each plate in the structure is replaced by a series of orthogonal slab strips that are taken as an equivalent gridwork of beam type members (Fig. 2). These grid members are assigned axial, bending, and torsional stiffnesses to approximate the two way plate behavior and are considered rigidly connected at the joints to form a three-dimensional rigid frame. The equivalent structure is then analyzed for the given loading to determine the internal forces and moments in the grid members which in turn are interpreted and converted to corresponding quantities in each of the actual two-dimensional plates. Since the rigid frame analyzed is three dimensional, each joint has six degrees of freedom, thus from a practical

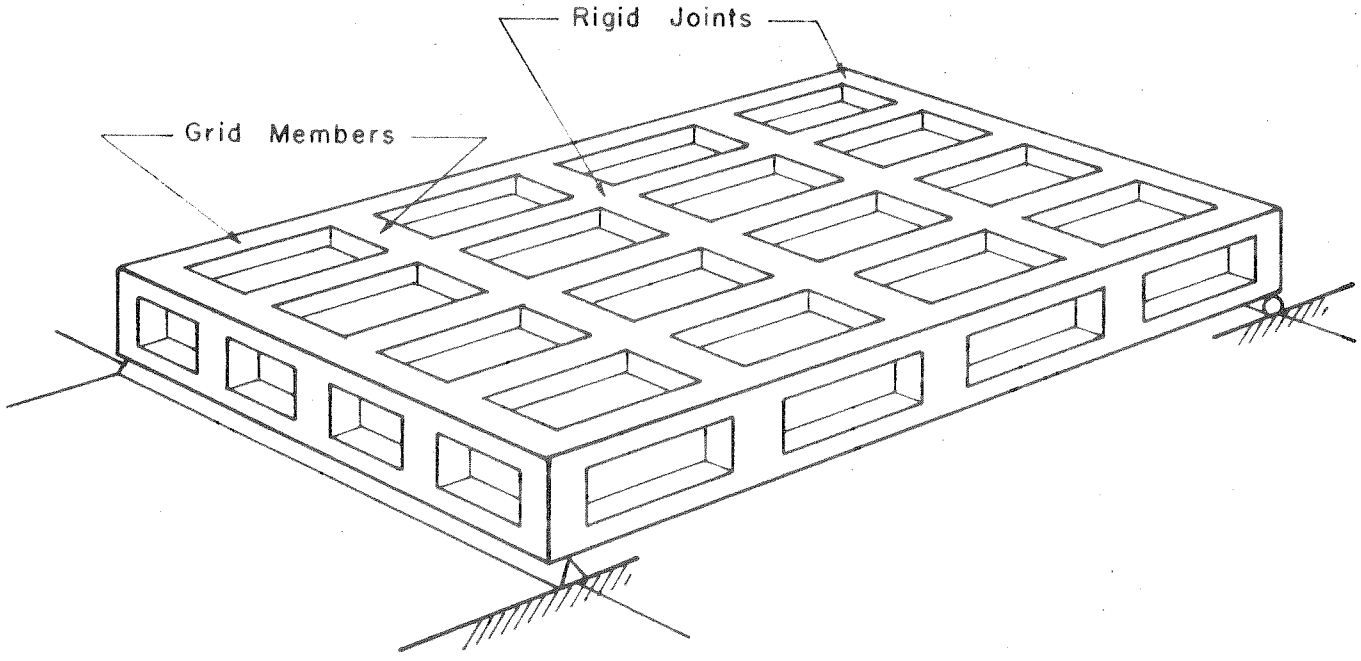

FIG. 2 EQUIVALENT GRIDWORK ANALYTICAL MODEL

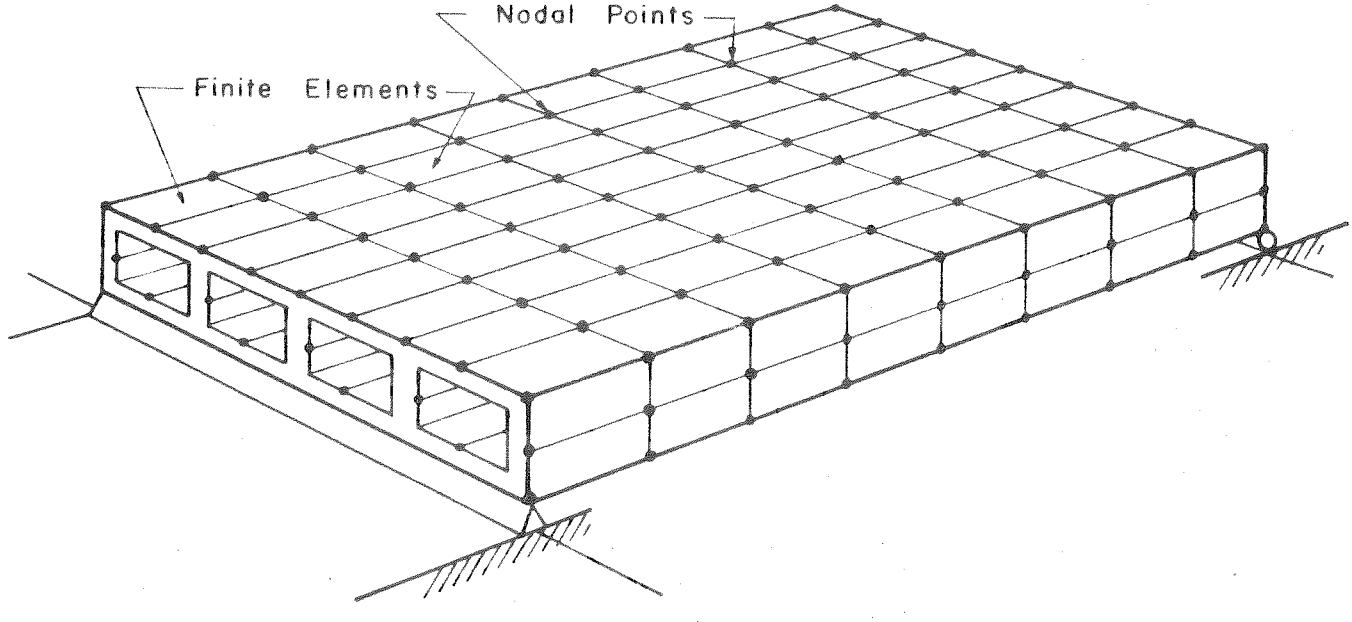

FIG. 3 FINITE ELEMENT ANALYTICAL MODEL

standpoint the analysis can only be performed using a digital computer. Even then the size of matrices, and the computation time required in the solution are considerable. Another disadvantage is that the gridwork is only an approximation of the true structure.

4. Finite Difference Method

The finite difference method for the analysis of the box girder system involves the representation of the governing differential equations for thin plates loaded in their own plane and normal to their own plane by a system of finite difference equations. A system of grid points or nodes is established on the structure and the various derivatives in the differential equations for the continuum are expressed in terms of differences of selected quantities at adjacent grid points. This leads to a large system of algebraic equations which requires a digital computer for solution. The accuracy of the solution is dependent on the fineness of the mesh size used. While this method is generally versatile, it becomes somewhat involved in application, especially in the interpretation and incorporation of certain boundary conditions.

5. Finite Element Method

In this method each plate is physically subdivided into a number of discrete finite elements interconnected at nodal points (Fig. 3). At each nodal point there are six degrees of freedom and for each of these a known force or a known displacement may exist. If a certain force is known the corresponding displacement is unknown, and vice versa. A direct stiffness solution can be used to find all of the unknown nodal point displacements and

forces. Once these are known the internal forces and stresses may be determined. The key step in this approach is the development of element stiffness matrices for the individual finite elements which can accurately approximate the behavior of the continuum.

This method is perhaps the most versatile of those presently available. It can be used for arbitrary loadings and boundary conditions. It also can treat the cases of varying dimensional and material properties throughout the structure, as well as the case of cutouts in the plates. It has the disadvantage that it involves the solution of a very large system of equations for structures of the complexity of the box girder bridge. The size of the problem is large even for present day computers, in terms of storage and computer time required for solution. In addition the method is approximate with its accuracy being dependent on the fineness of the subdivision used in dividing the structure into finite elements.

6. Folded Plate Method

This method is ideally suited to box girder bridges which have simple supports at the two ends, since a harmonic analysis using Fourier series can be used to analyze structures for both concentrated and distributed loads on the bridge. The bridge is treated as a series of rectangular plates interconnected along the longitudinal joints. Each plate is first analyzed independently by elastic plate theory for loads normal to the plane of the plate and by two-dimensional plane stress theory for loads in the plane of the plate. The stiffness matrix for a single plate can then be expressed in terms of the harmonics of a Fourier series. For each harmonic, the plate has

only four degrees of freedom at each longitudinal edge. A direct stiffness solution is used to analyze the total structure consisting of the interconnected plates.

This method also requires the use of a digital computer for solution, but it is considerably faster and requires less storage than the finite element method, since it involves a fewer number of degrees of freedom. Any loading can be treated as long as it can be represented by a Fourier series and the solution is exact within the assumptions of the elasticity theory.

All the analyses and computer programs discussed in this report have been based on the "Folded Plate Method" and a more detailed description of these will be given in the next chapter.

III. THEORETICAL ANALYSIS OF CELLULAR FOLDED PLATES

1. Introduction

A structure may be thought of as an assemblage of structural elements interconnected at joints. In the case of a cellular folded plate structure (Fig. 4), simply supported at its two ends, the structural elements can be taken as the individual rectangular plates which are interconnected at longitudinal joints and frame into transverse end diaphragms. Such a structure can be effectively analyzed by an extension of the direct stiffness method described by De Fries and Scordelis [26] as outlined below.

2. Solution of Cellular Folded Plates Without Interior Diaphragms

Because of the simple supports at the two ends of the structure, an analysis for applied loads with any arbitrary longitudinal distribution may be performed using a harmonic analysis. The applied forces are first resolved into Fourier series components. An analysis is carried out for all of the loading components of each particular harmonic and then the final results are obtained by summing the results for all of the harmonics used to represent the load. Once the solution technique, which involves extensive computations, has been developed for a single harmonic it can be reused for any harmonic, and thus the approach is well suited to the application of a digital computer.

The analysis for each harmonic load has the advantage that such loads will produce displacements of the same variation and vice versa and thus a single characteristic value may be used to describe any force or displacement

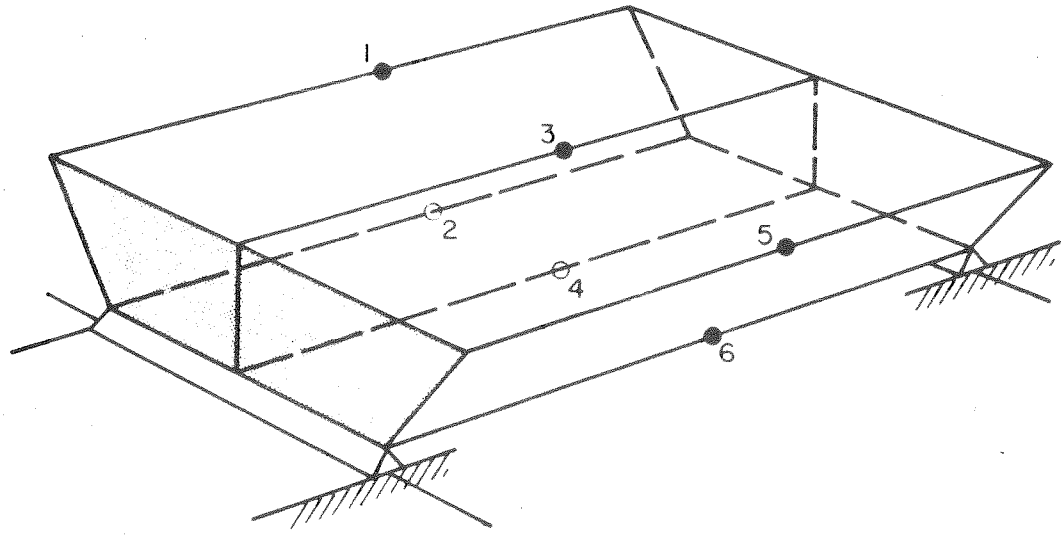

FIG. 4 SIMPLY SUPPORTED CELLULAR FOLDED PLATE

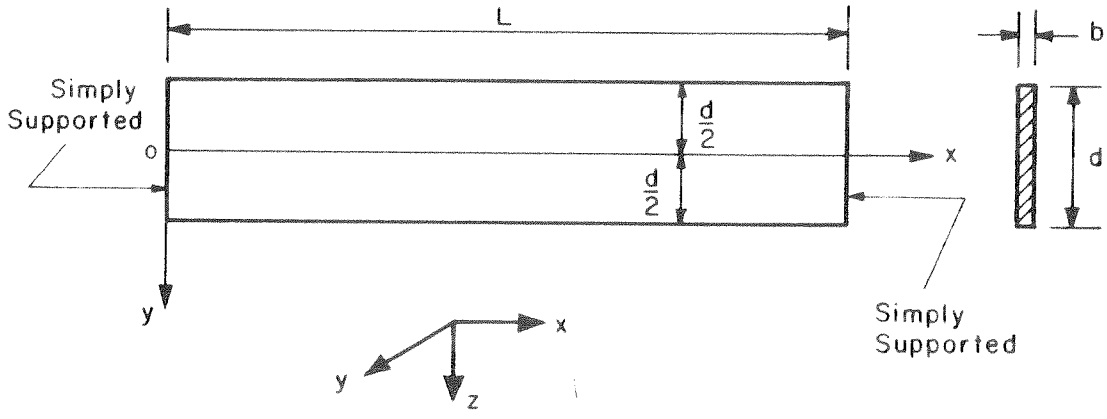

FIG. 5 PLATE ELEMENT COORDINATE SYSTEM

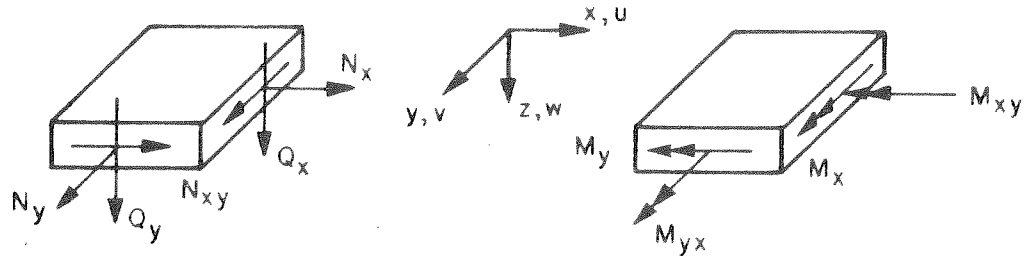

FIG. 6 POSITVE INTERNAL FORCES AND DISPLACEMENTS IN PLATE ELEMENT

pattern. For example the displacement pattern:

$$r(x) = r_o \sin \frac{n\pi x}{L} \tag{1}$$

may be described by the single value r_o. This makes it possible to treat an entire joint as a single nodal point and to operate with single forces and displacements instead of functions. If the condition of static equilibrium and geometric compatability are maintained at a nodal point, they will automatically be satisfied along the entire longitudinal joint.

Each joint or nodal point has four degrees of freedom, it can displace vertically and horizontally in a plane parallel to the end diaphragms; it can move longitudinally parallel to the joint; and it can rotate about an axis parallel to the joint. The structure in Fig. 4 has 6 nodal points and thus a total of 6x4 = 24 degrees of freedom.

Each individual plate (Fig. 5) taken as a free body will be subjected to surface loads and will experience displacements and forces along its two longitudinal edges. Due to these effects, internal forces and displacements (Fig. 6) will be developed throughout the plate. Using classical thin plate theory for loading normal to the plate and the elasticity equations defining the plane stress problem for loads in the plane of the plate, expressions can be derived for internal and edge forces due to surface loads, for the case of the longitudinal edges fixed against displacement. These are termed fixed edge forces and at each edge consist of a transverse membrane force, a longitudinal membrane shear force, a shear force normal to the plate, and a moment about the longitudinal edge (Fig. 7). Expressions relating these same four forces at each edge in terms of each of the corresponding edge displacements

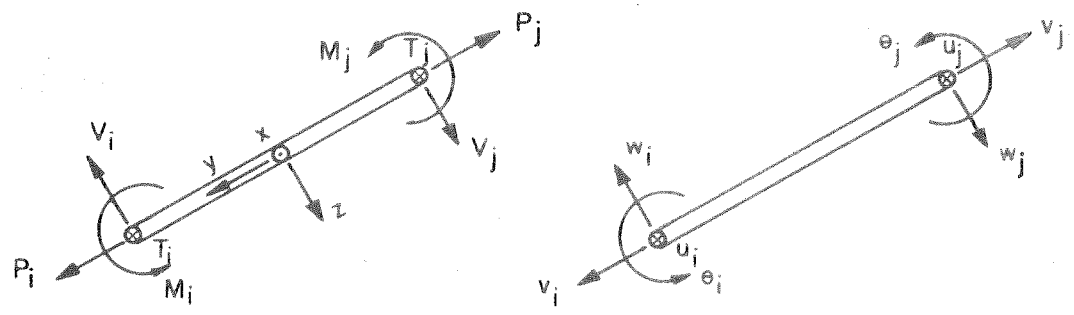

FIG. 7 POSITIVE ELEMENT EDGE FORCES AND DISPLACEMENTS IN THE RELATIVE COORDINATE SYSTEM

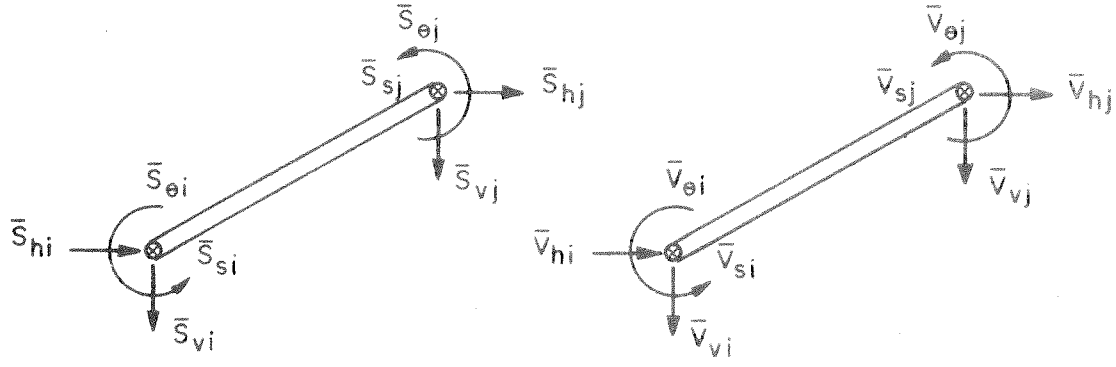

FIG. 8 POSITIVE ELEMENT EDGE FORCES AND DISPLACEMENTS IN THE FIXED COORDINATE SYSTEM

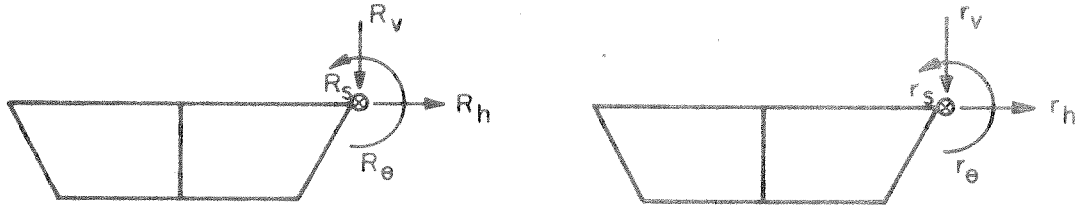

FIG. 9 POSITIVE JOINT FORCES AND DISPLACEMENTS IN THE FIXED COORDINATE SYSTEM

can also be derived to yield an element stiffness matrix. Internal forces at any point can also be stated in terms of each of the edge displacements. All of these necessary formulae have been derived and presented by Lo [71] and by Goldberg and Leve [25]. Since both the formulae and their derivations are quite lengthy, they will not be repeated here.

With the above formulae available, the direct stiffness solution for a typical harmonic can proceed as follows:

a. Fixed edge solution for surface loads.

   (1) Resolve the given surface loading on each plate into normal and tangential components.

   (2) Determine the internal and fixed edge forces due to the surface loading with edges fixed against displacements.

   (3) Resolve the fixed edge forces from all plates coming into a common joint into components corresponding to a fixed or global coordinate system for the structure (Fig. 8).

   (4) Sum the forces in (3) to determine the total external joint restraint or holding forces at each joint.

b. Solution for structure subjected to joint loads only.

   (1) Add to the given external joint forces a set of forces equal and opposite to the joint restraint forces found for the fixed edge solution above. Treat this sum as the total external loading R at the joints, referred to a fixed coordinate system (Fig. 9).

(2) Determine the corresponding joint displacements r for the structure by means of the following steps of a standard direct stiffness solution [26].

(3) The element stiffness matrix k is formed for each plate relating element edge forces S to element edge displacements v, referred to a relative or element coordinate system. (Fig. 7).

$$\{S\} = [k]\ \{v\} \tag{2}$$

(4) The edge forces S and displacements v in Eq. (2) are resolved into a fixed coordinate system (Fig. 8), $\bar{S}$ and $\bar{v}$, by means of a displacement transformation matrix A and its transpose A^T.

$$\{v\} = [A]\ \{\bar{v}\} \tag{3}$$

$$\{\bar{S}\} = [A]^T\ \{S\} \tag{4}$$

(5) By substituting Eqs. (3) and (4) into (2) the following is found.

$$\{\bar{S}\} = [A]^T\ [k]\ [A]\ \{\bar{v}\} \tag{5a}$$

or $$\{\bar{S}\} = [\bar{k}]\ \{\bar{v}\} \tag{5b}$$

where $$[\bar{k}] = [A]^T\ [k]\ [A] \tag{6}$$

The matrix $\bar{k}$ is an 8x8 element stiffness matrix in the fixed coordinate system.

(6) Eq. (5b) is partitioned as follows

$$\begin{Bmatrix} \bar{S}_i \\ \bar{S}_j \end{Bmatrix} = \begin{bmatrix} \bar{k}_i & \bar{k}_{ij} \\ \bar{k}_{ji} & \bar{k}_j \end{bmatrix} \begin{Bmatrix} \bar{v}_i \\ \bar{v}_j \end{Bmatrix} \tag{7}$$

where i and j refer to the joint numbers at the two edges of the plate. The above procedure is repeated for each plate element.

(7) Static equilibrium of any joint requires that the joint forces must equal the sum of the element forces acting on the plate edges that form that particular joint. For illustration, assume three elements are connected at joint i.

$$\{R_i\} = \{\bar{S}_i^{\,1}\} + \{\bar{S}_i^{\,2}\} + \{\bar{S}_i^{\,3}\} \tag{8}$$

(8) Geometric compatibility of the joint requires that the joint displacements must be equal to the plate edge displacements

$$\{r_i\} = \{\bar{v}_i^{\,1}\} = \{\bar{v}_i^{\,2}\} = \{\bar{v}_i^{\,3}\} \tag{9}$$

(9) The stiffness matrix K for the entire structure can now be assembled by properly adding the element stiffness matrices of Eq. (7). The size of the K matrix for m joints, will be 4mx4m. As an example, the structure shown in Fig. 4 will have a 24x24 K matrix which will take the following form.

$$\begin{Bmatrix} R_1 \\ R_2 \\ R_3 \\ R_4 \\ R_5 \\ R_6 \end{Bmatrix} = \begin{bmatrix} K_1 & K_{12} & K_{13} & 0 & 0 & 0 \\ K_{12}^T & K_2 & 0 & K_{24} & 0 & 0 \\ K_{13}^T & 0 & K_3 & K_{34} & K_{35} & 0 \\ 0 & K_{24}^T & K_{34}^T & K_4 & 0 & K_{46} \\ 0 & 0 & K_{35}^T & 0 & K_5 & K_{56} \\ 0 & 0 & 0 & K_{46}^T & K_{56}^T & K_6 \end{bmatrix} \begin{Bmatrix} r_1 \\ r_2 \\ r_3 \\ r_4 \\ r_5 \\ r_6 \end{Bmatrix} \tag{10}$$

In symbolic form this equation may be written for a general structure as

$$\{R\} = [K]\ \{r\} \tag{10a}$$

In Eq. (10) the subscripts refer to joint number. The diagonal submatrix K_i represents the forces developed at joint i due to unit displacements applied at the same joint. Each diagonal term is the sum of the plate element stiffnesses $\bar{k}_i$ of all of the plate elements connected to joint i.

$$K_i = \sum_e \bar{k}_i^e \tag{11}$$

in which the superscript e represents plate element number.

The off-diagonal submatrix K_{ij} represents a coupling effect, that is the forces developed at joint i due to unit displacements at joint j. Two joints are coupled only if there is a plate element between them. In general,

there is at most only one such element

$$K_{ij} = \bar{k}_{ij} \tag{12}$$

The joint numbers assigned are arbitrary, but should be arranged to minimize the maximum difference in the joint numbers of any plate. In this manner the K matrix will have the narrowest band width possible and result in a more rapid solution in the computer.

(10) Once the structure stiffness matrix is formed, Eq. (10) can be solved for the unknown displacements using a recursive procedure similar to that presented by Clough, Wilson and King [68] for tri-diagonal matrices.

(11) With the joint displacements r known, the plate edge displacements v in the element coordinate system are determined through the use of Eqs. (9) and (3).

(12) Internal forces and displacements in each plate are calculated by the expressions described earlier relating these quantities to plate edge displacements.

c. Final Results.

(1) These are obtained by adding the results of paragraph a, fixed edge solution for surface loads only, to those of paragraph b, solution for structure subjected to joint loads only.

3. Solution of Cellular Folded Plates with Interior Rigid Diaphragms

In structures such as box girder bridges, interior diaphragms may be added to the cellular folded plates structure described in the preceding section in order to improve its load distributing properties. In the following discussion these diaphragms will be assumed to be infinitely rigid in their own plane, but perfectly flexible normal to their own plane. For simplicity consider the structure shown in Fig. 10, which is a one cell structure with one rigid diaphragm at midspan.

A force method of analysis is used in which the redundants are taken as the interaction forces between the folded plate and the rigid diaphragm. These are represented by a set of three joint forces at each longitudinal joint, consisting of vertical, horizontal and rotational components and a set of four plate forces for each plate, consisting of distributed normal and tangential forces having triangular variations between the two longitudinal edges of the plate. The structure shown in Fig. 10 would have a total of 28 redundants. All of the interaction forces are assumed to be uniformly distributed in the span direction over a length equal to the diaphragm thickness.

The redundant interaction forces are determined as those required to establish compatibility between the folded plate and the rigid diaphragm at the longitudinal joints in the vertical, horizontal and rotational directions and at third points between joints in directions normal and tangential to the plane of the plate.

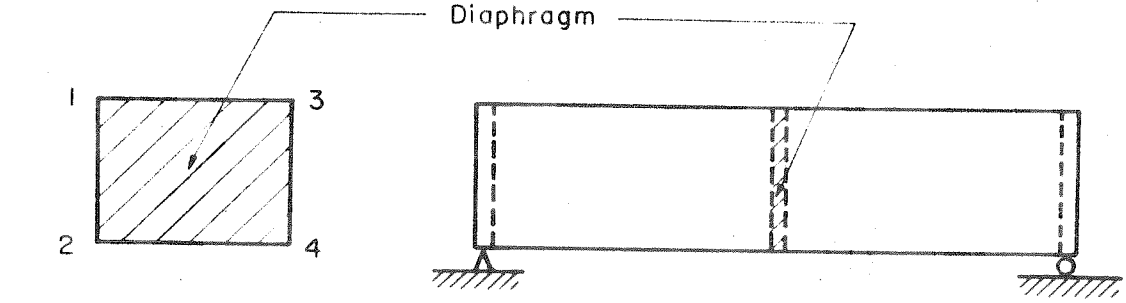

FIG. 10 CELLULAR FOLDED PLATE STRUCTURE WITH ONE DIAPHRAGM

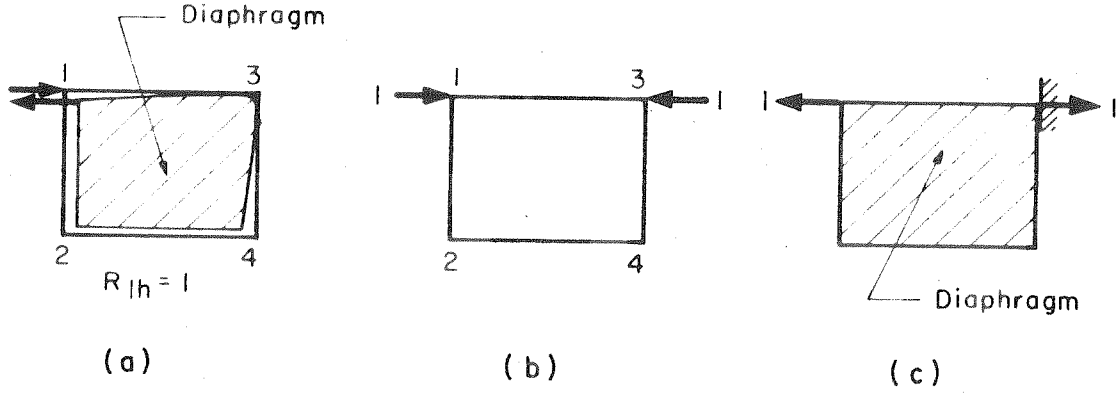

FIG. 11 INTERACTION BETWEEN MOVABLE DIAPHRAGM AND FOLDED PLATE SYSTEM

Once the magnitude of the redundant forces are known the cellular folded plate can be analyzed, by the method already discribed for structures without diaphragms, for both the external loading and the redundants acting together, to obtain the final results.

A distinction must be made between the case of an interior rigid diaphragm which is externally supported so that it cannot displace and the case in which it is not externally supported so that it can displace as a rigid body and thus be termed a movable diaphragm. In the first case compatibility requires that the total or absolute displacement of the folded plate structure at each of the points where the redundants exist must be equal to zero, while in the second case the relative displacement between the folded plate structure and the movable diaphragm at each of these points must be equal to zero. The procedure for solutions in each case is described below.

a. Interior diaphragm externally supported.

(1) With the redundants set equal to zero, the structure is analyzed under the given external loading. This is the same as the case without diaphragms already described. A displacement vector is found for this case, which defines the displacements at the points where the redundants are to act.

$$\{\delta\}_o = \begin{Bmatrix} \delta_1 \\ \delta_2 \\ \vdots \\ \delta_c \end{Bmatrix}_o \qquad (13)$$

(2) The folded plate structure without a diaphragm is analyzed for unit values of each of the redundant forces X and the corresponding flexibility matrix is formed.

$$\begin{Bmatrix} \delta_1 \\ \delta_2 \\ \vdots \\ \delta_c \end{Bmatrix}_X = \begin{bmatrix} F_{11} & F_{12} & \cdots & F_{1c} \\ F_{21} & F_{22} & \cdots & F_{2c} \\ \vdots & \vdots & \cdots & \vdots \\ F_{c1} & F_{c2} & \cdots & F_{cc} \end{bmatrix} \begin{Bmatrix} X_1 \\ X_2 \\ \vdots \\ X_c \end{Bmatrix} \tag{14}$$

or simply

$$\{\delta\}_X = [F]\,[X] \tag{14a}$$

(3) Since the diaphragm does not displace for this case, the total or absolute displacement of the folded plate structure at each of the points where redundants exist must equal zero

$$\{\delta\} = \{\delta\}_o + \{\delta\}_X = 0 \tag{15}$$

(4) Substituting Eq. (14a) into (15) the redundants may be found

$$\begin{aligned} \{\delta\}_o + [F]\,\{X\} &= 0 \\ \{X\} &= -[F]^{-1}\,\{\delta\}_o \end{aligned} \tag{16}$$

b. Interior diaphragm not externally supported (movable diaphragm).

(1) Since the rigid diaphragm is not externally supported, but is supported directly by the folded plate structure (Fig. 11a), each redundant force pattern must be self-equilibrating when considering the diaphragm as a free body alone (Fig. 11c).

(2) The relationship between the new redundant force patterns $\bar{X}$ and the individual redundant forces X used in the preceding section, is defined by a force transformation matrix B.

$$\{X\} = [B]\ \{\bar{X}\} \tag{17}$$

In the usual case in which the rigid diaphragm can experience three rigid body displacements (two translations and a rotation in the plane of the diaphragm) X will have 3 more elements than $\bar{X}$. The B matrix is formed by assuming the rigid diaphragm is connected in a statically determinate manner to the folded plate system, such as by a rigid connection at joint 3 of Fig. 11a. The interaction forces between the diaphragm and the folded plate at the remaining joints 1, 2, 4 as well as those distributed along the plate between the joints make up the new set of redundants. Applying each of these redundants $\bar{X}$ to the diaphragm alone (Fig. 11c), the necessary equilibrating support forces at joint 3

are found and the resulting forces on the folded plate system (Fig. 11b) corresponding to the original X redundant system are found to form the B matrix.

Matrices B and $\bar{X}$ depend on how the diaphragm is assumed to be initially statically connected to the folded plate system. For example, the diaphragm could be assumed connected to the system by one pinned joint (two restraints) and another roller joint (one restraint) rather than the fixed joint (three restraints) used above.

(3) The transpose of the B matrix will also relate the relative displacements $\bar{\delta}$ between the movable diaphragm and the folded plate system to the total or absolute displacements δ of the folded plate system.

$$\{\bar{\delta}\} = [B]^T \{\delta\} \tag{18a}$$

$$\{\bar{\delta}\}_o = [B]^T \{\delta\}_o \tag{18b}$$

$$\{\bar{\delta}\}_x = [B]^T \{\delta\}_x \tag{18c}$$

(4) Substituting Eqs. (14a) and (17) into Eq. (18c) yields

$$\{\bar{\delta}\}_x = [B]^T [F] [B] \{\bar{X}\}$$

$$= [\bar{F}] \{\bar{X}\} \tag{19}$$

where $$[\bar{F}] = [B]^T [F] [B] \tag{20}$$

which is the modified flexibility matrix for unit interactions between the movable diaphragm and the folded plate structure.

(5) The redundants $\bar{X}$ may then be found by setting the relative displacements between the movable diaphragm and the folded plate structure equal to zero.

$$\{\bar{\delta}\} = \{\bar{\delta}\}_o + \{\bar{\delta}\}_x = 0 \tag{21}$$

substituting Eq. (19) into (21)

$$\begin{aligned} &\{\bar{\delta}\}_o + [\bar{F}]\ \{\bar{X}\} = 0 \\ &\{\bar{X}\} = -\ [\bar{F}]^{-1}\ \{\bar{\delta}\}_o \end{aligned} \tag{22}$$

The individual redundant forces X in the original system may then be found from Eq. (17).

(6) If there are more diaphragms than one in the structure, the procedure for analysis is essentially the same except the redundants at each diaphragm must be included. However, the force transformation matrix requires additional attention. Suppose there are c diaphragms, Eq. (17) should then be written in the following generalized form.

$$\begin{Bmatrix} X_I \\ X_{II} \\ \vdots \\ X_c \end{Bmatrix} = \begin{bmatrix} B_I & 0 & \cdots & 0 \\ 0 & B_{II} & \cdots & 0 \\ \vdots & \vdots & \ddots & \vdots \\ 0 & 0 & \cdots & B_c \end{bmatrix} \begin{Bmatrix} \bar{X}_I \\ \bar{X}_{II} \\ \vdots \\ \bar{X}_c \end{Bmatrix} \tag{23}$$

The subscript refers to the diaphragm number. In case all diaphragms are similar, the force transformation submatrices are identical.

$$B_I = B_{II} = \ldots\ldots = B_c \tag{24}$$

On the other hand, when any diaphragm (say diaphragm i) is supported externally so it can not displace, the corresponding transformation submatrix, B_i becomes a unit matrix so that $\bar{X}_i = X_i$.

4. Computer Programs

Two general computer programs have been written to perform the analyses described in this chapter. The first program, entitled MULTPL, is for the solution of cellular folded plates without interior diaphragms and the second program, entitled MUPDI, is for the solution of cellular folded plates with interior diaphragms. Both programs were written in FORTRAN IV language for the IBM 7094 computer. Detailed descriptions of the input, output, sign conventions, and limitations and restrictions for these programs are given in Appendices A and B. A brief description of these is given below.

a. Input Data

(1) Geometry and dimensions of the structure in terms of the number of plates, joints, diaphragms, etc.

(2) Dimensions and material properties for each plate element.

(3) Magnitudes and locations of uniform and partial surface loads.

(4) Boundary conditions at the longitudinal joints. Any combination of known forces and given zero displacements may be used.

(5) Magnitudes and locations of additional concentrated joint loads.

(6) Location and thickness of each diaphragm and indices for restraint conditions on each joint and plate element. This is used only in the MUPDI program.

(7) Desired locations for final results in output.

b. Output Data

(1) The complete input data is properly labelled and printed as a check.

(2) For a solution by the MUPDI program, the interaction (restraint) joint and plate forces between each diaphragm and the folded plate system are printed.

(3) Resulting horizontal vertical, rotational and longitudinal joint displacements are given at specified locations.

(4) For each element all internal forces and displacements are printed for each transverse section specified across the plate width and at the x-coordinates specified along the plate length.

c. Limitations, Restrictions and Remarks.

(1) The maximum number of plate elements and joints for MULTPL are 150 and 100 and for MUPDI are 30 and 20.

(2) Up to 100 non-zero terms of the appropriate Fourier series may be used to express the loads.

(3) The maximum absolute difference between the two joint numbers of any plate element is 4.

(4) All surface loads are uniformly distributed over the loaded area. They may be distributed over any length of the plate desired.

(5) Joint loads may be concentrated or uniformly distributed line loads over any length of the joint desired.

(6) For the MUPDI program, restraint conditions on joints and plate elements are indicated by input restraint indices. If there are more diaphragms than one, the restraint conditions are the same for all diaphragms, but each diaphragm can be either supported externally or unsupported (movable).

(7) For the MUPDI program, the maximum number of interactions (connections) between the folded plate system and all of the diaphragms must not exceed 120. The maximum number of diaphragms is 4.

(8) Computer time required for the solution of typical cases is given at the end of Chapter VI.

IV. EXAMPLES

1. General Remarks

The computer programs described in the preceding chapter provide a powerful means for the analysis of a wide variety of problems. Numerous examples have been run and studied to check the validity of the results obtained. In all cases the comparisons with existing solutions were excellent. These have included individual plates subjected to loads either normal to the plane of plate or in the plane of the plate. These results were compared to those obtained by classical plate theory by Timoshenko [69]. In addition a large number of folded plate problems were run and checked against existing known solutions. Statics checks were also performed on the results from a number of cases and again these were found to be excellent.

At the request of the State Bridge Department several actual bridges completed or under design were analyzed for special loading cases. To illustrate the variety of problems which can be treated, each of these will be briefly described and discussed.

2. Harrison Street Undercrossing

This bridge, Fig. 12a, was the prototype bridge used in the study by Davis, Kozak and Scheffey [27]. As part of their study analyses were made by Davis using a special computer program, based on the Goldberg-Leve [25] plate equations, which was developed specifically for the prototype bridge. Several load cases used in that study were analyzed using the general computer program developed in the present study. Since the basic assumptions

used in the analyses in the two studies were the same, the final answers obtained should be essentially the same, even though different procedures and computer programs were used to arrive at these answers. This proved to be the case.

A typical comparison for longitudinal stresses σ_x at the 5/12th span section is given in Table 1 for the points shown in Fig. 12b for the case of two test vehicles located on the bridge in the positions indicated in Fig. 12c. In Table 1, Col. (1) represents the results obtained by Davis using the first 8 harmonics to represent each concentrated wheel load; and Cols. (2) and (3) represent results obtained using 8 and 50 harmonics respectively with the computer program developed in the present study.

TABLE 1. LONGITUDINAL STRESSES σ_x (PSI) AT 5/12th SPAN OF HARRISON STREET BRIDGE FOR LOADING SHOWN IN FIG. 12c

Location (see Fig. 12b)	Top Slab			Bottom Slab		
	(1)	(2)	(3)	(1)	(2)	(3)
A	-139	-135	-134	176	170	169
1	-140	-138	-137	173	170	169
B	-149	-147	-142	180	179	172
2	-147	-146	-145	178	177	175
C	-153	-153	-148	184	185	178
3	-150	-150	-148	181	182	180
D	-155	-155	-149	190	189	183
4	-149	-148	-148	187	186	185
E	-152	-151	-147	195	195	187

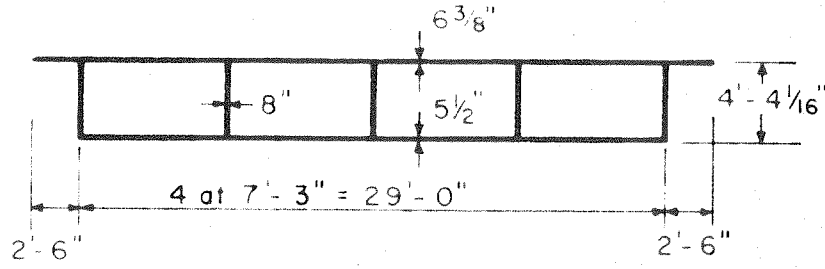

(a) CROSS-SECTIONAL CENTERLINE DIMENSIONS. LONGITUDINAL SIMPLE SPAN = 80 ft.

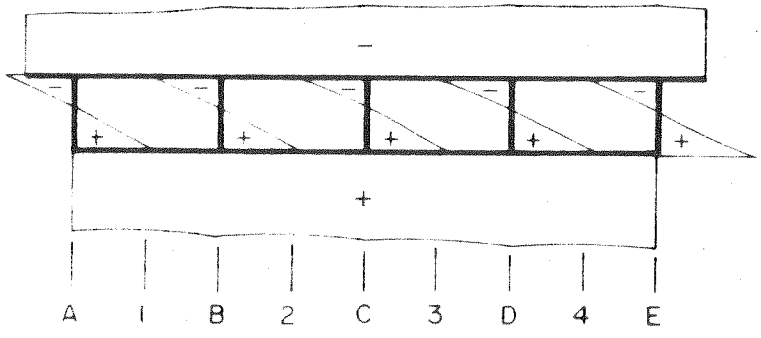

(b) LONGITUDINAL STRESS DISTRIBUTION AT SECTION A-A (5/12 TH SPAN) FOR LOADING SHOWN IN (c)

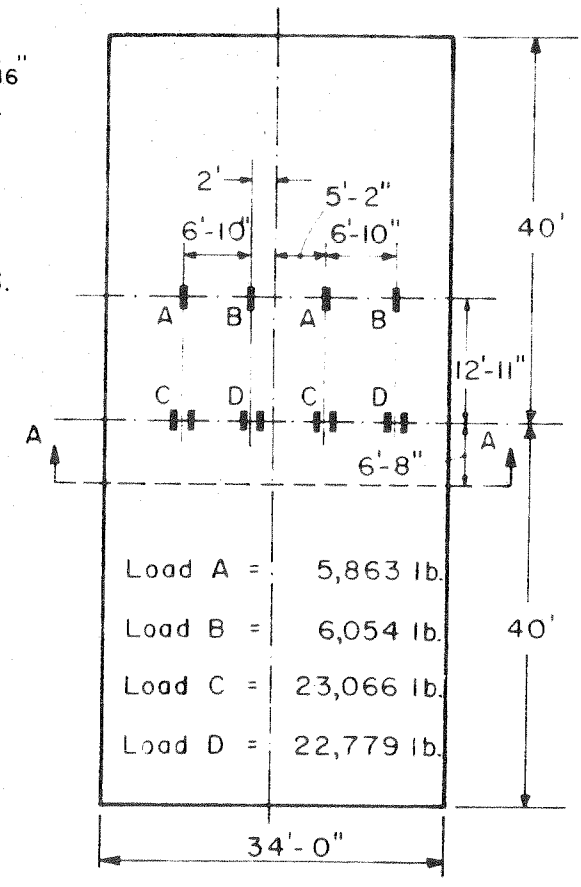

(c) PLAN OF BRIDGE AND LOACATION AND MAGNITUDE OF TEST VEHICLE WHEEL LOADS

FIG. 12 DIMENSIONS, STRESSES AND LOADING FOR HARRISON STREET UNDERCROSSING

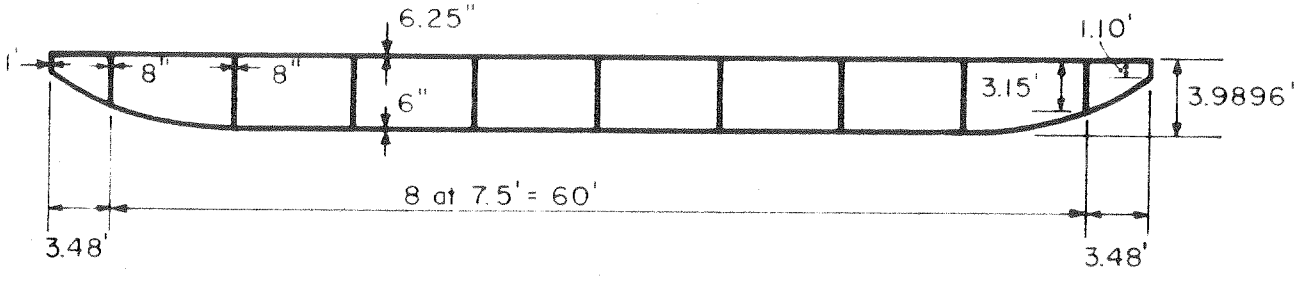

FIG. 13 CROSS-SECTIONAL CENTERLINE DIMENSIONS FOR LA BARRANCA WAY UNDERCROSSING. LONGITUDINAL SIMPLE SPAN = 82.2 FT.

Results in all three cols. are in quite close agreement, first, indicating a check between the two studies and second, that the use of additional harmonics to represent the concentrated loads does not change the stresses appreciably for this loading case because the section at which the stresses are found is some distance away from the concentrated wheel loads.

3. La Barranca Way Undercrossing

This example illustrates the application of the program to a bridge with a curved bottom soffit, Fig. 13. The curved soffit near the exterior edges of the bridge was approximated by a series of short flat plates, and analyses were carried out for dead load and for the case of shrinkage in the top slab only. In the latter case, since the top slab is cast separately at an interval of one week to ten days after the bottom portion of the bridge, different moduli of elasticity E_c equal to 1.5×10^5 psi and 2.5×10^6 psi respectively are assumed for these two parts in the analysis. The shrinkage case was analyzed as follows:

a. All longitudinal joint were assumed locked in position and the transverse joint forces due to shrinkage required to hold them in this position were determined. These forces can be found by first allowing the assumed free transverse shrinkage strain to occur in each plate and then finding the transverse elastic tensile force required to bring the plates back to their original position. Algebraically summing the tensile forces from the plates framing into a particular joint gives the required joint holding forces.

b. The complete structure is then analyzed for joint loads equal and opposite to the above holding forces, using the proper assumed E_c for each plate.

c. The final results are obtained by the superposition of a and b.

It should be apparent that problems involving differential temperature changes in the plates can be handled in the same way.

4. College Avenue Undercrossing

In order to determine the live load distribution for the exterior girder of this bridge, Fig. 14a which had a sloping soffit, two analyses were run using equivalent single axle loadings at midspan of 16 and 12 kips placed at each of the load points shown in Figs. 14b and 14c, respectively. Resulting midspan longitudinal stresses are also shown, in Figs. 14b and 14c. It should be noted that even though for compatibility the longitudinal strains in all plates meeting at a common joint must be the same, the longitudinal stresses will differ slightly due to the contribution of different transverse strains in the plates and Poisson's ratio. Modulus of elasticity E_c and Poisson's ratio ν were taken equal to 3.0×10^6 psi and 0.15 respectively.

5. Sacramento River Bridge and Overhead

This bridge consists of a top slab of concrete integrally cast with a steel system consisting of top flange plates, stiffened web plates, and a stiffened bottom plate used to form the box girder system idealized in Fig. 15a. The system has 23 plates and 16 longitudinal joints. Detailed makeup

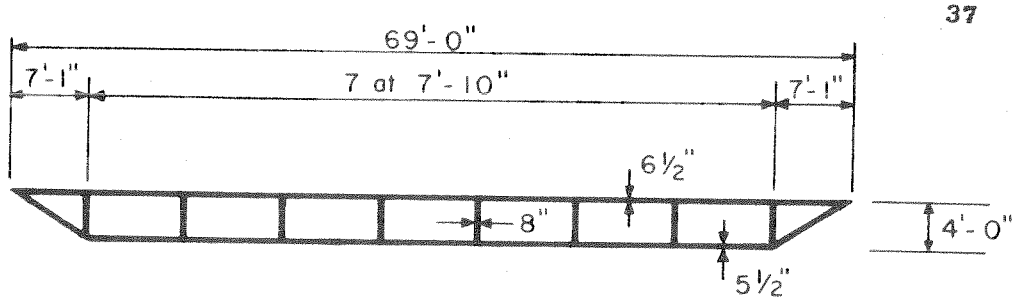

(a) CROSS-SECTIONAL CENTERLINE DIMENSIONS.
EQUIVALENT LONGITUDINAL SIMPLE SPAN = 90 FT.

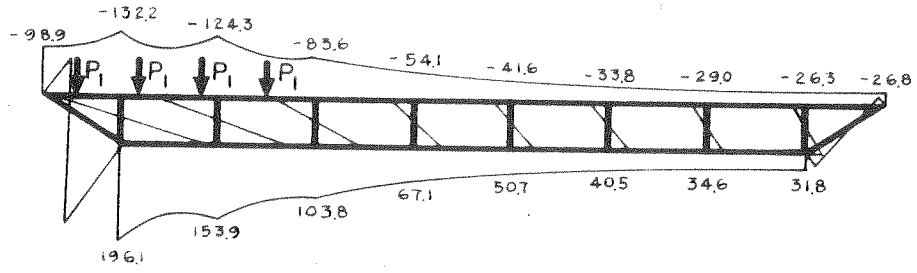

(b) MIDSPAN LONGITUDINAL STRESSES σ_x (PSI)
LOADING NO. I, P_1 = 16 KIPS

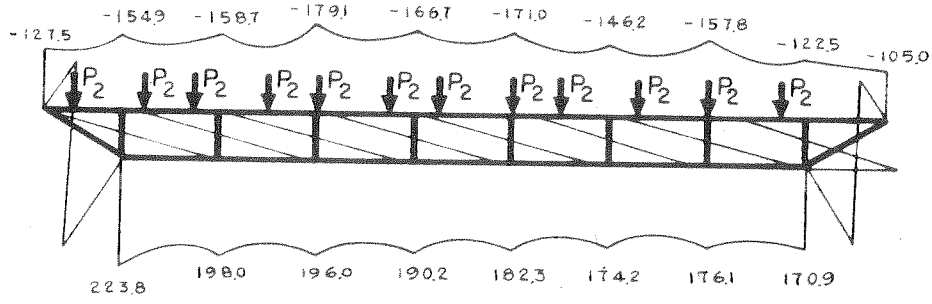

(c) MIDSPAN LONGITUDINAL STESSES σ_x (PSI)
LOADING NO. II, P_2 = 12 KIPS

FIG. 14 DIMENSIONS, STRESSES AND LOADING FOR COLLEGE AVENUE UNDERCROSSING

and dimensions of the actual bridge are not given because of the complexity of the system. In addition, this bridge is to have several transverse, truss-type, steel cross-frames which act as diaphragms.

Several cases were analyzed for this complex bridge. The loading for one case in which equivalent concentrated loads were used to represent the actual truck loads is shown in Fig. 15b. Results for longitudinal stresses σ_x at midspan due to this loading are shown in Figs. 16a and 16b. In Fig. 16a no cross-frame diaphragms were assumed in the analysis and in Fig. 16b the bridge was analyzed with four cross-frames assumed to be rigid diaphragms. The beneficial effect of the diaphragms in distributing the load more uniformly across the width of the bridge is evident.

6. Summary

It should be emphasized that much more additional information is obtained from the computer analyses than that indicated in the brief descriptions given above. This includes all of the internal forces, moments and displacements at any desired points in the structure. These detailed results can be used to give a total picture of the behavior of the bridge.

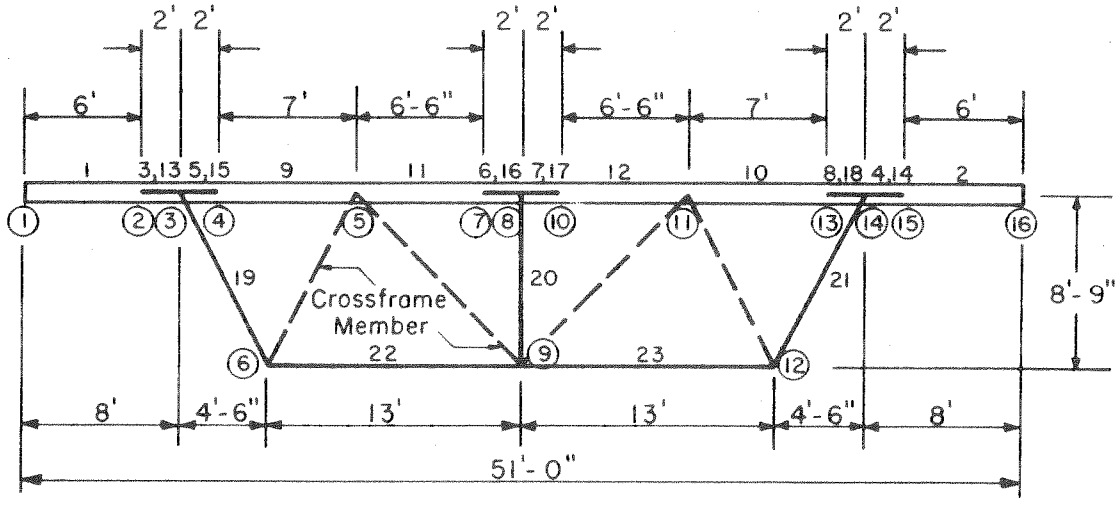

(a) CROSS-SECTIONAL DIMENSIONS SHOWING IDEALIZED SYSTEM USED FOR ANALYSIS

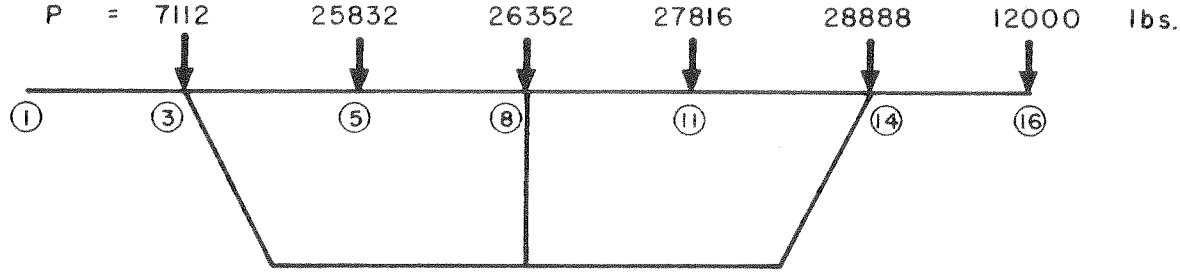

(b) TRANSVERSE POSITION OF EQUIVALENT CONCENTRATED LOADS

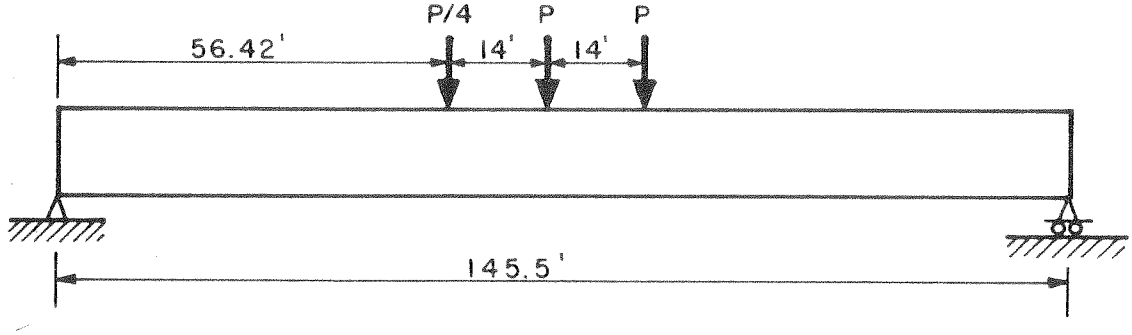

(c) LONGITUDINAL POSITION OF EQUIVALENT CONCENTRATED LOADS

FIG. 15 DIMENSIONS AND LOADING FOR SACRAMENTO RIVER BRIDGE AND OVERHEAD

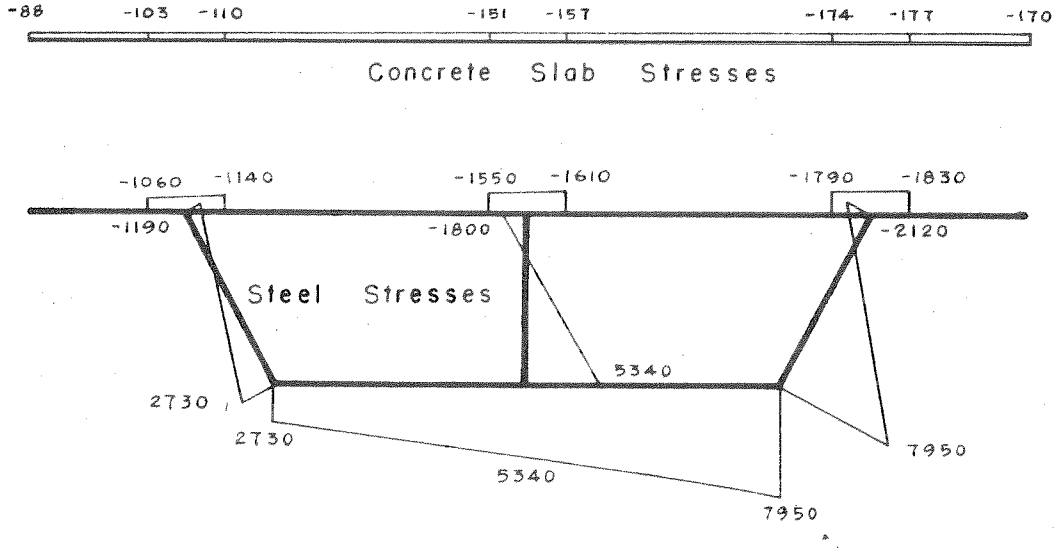

(a) NO CROSSFRAMES USED

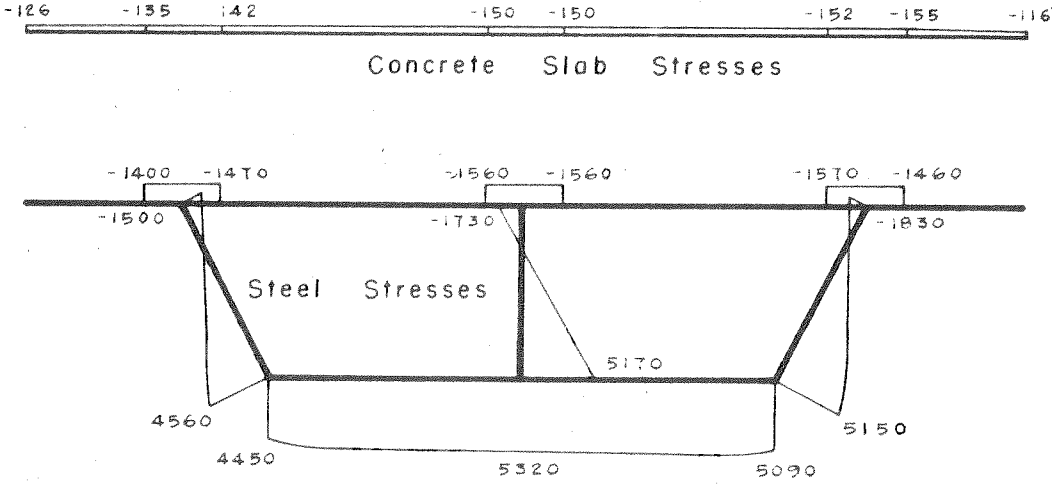

(b) FOUR CROSSFRAMES USED

FIG. 16 MIDSPAN LONGITUDINAL STRESSES σ_x (PSI) FOR SACRAMENTO RIVER BRIDGE AND OVERHEAD

V. REVIEW OF EXISTING BOX GIRDER BRIDGES

1. General Remarks

Box girder construction in California was initiated and developed primarily in the Los Angeles area as a desirable bridge type for a freeway system in highly developed residential and commercial areas. Its pleasing aesthetic appearance due to its smooth continuous lines and its ability to conceal and carry utilities in its cells were its prime advantages. As contractors throughout the State became familiar with box girder construction and consistently bid favorably on it, its use spread rapidly. At present it is by far the most widely used bridge type in California.

In order to ascertain the range of variables used in designing existing box girder bridges a review was made by the State Bridge Department of over 200 simple span box girder bridges constructed during the past ten years in California. Available data on spans, widths, depths, depth-span ratios, number of cells, width of cells, and thicknesses of top and bottom slabs and webs are summarized in Figs. 17 through 25. For some of these categories, data on certain bridges was unavailable and thus is not included in the figures. The figures give totals for all bridges with or without interior diaphragms and also separately indicate values for bridges without diaphragms. 74 of the bridges had no interior diaphragms, 129 had one, 26 had two, 1 had three, 1 had four, and the remainder were unspecified.

2. Span Lengths (Fig. 17)

For all bridges a heavy clustering exists in the 50 to 90 ft. span range. For bridges without diaphragms this is particularly true and it can be seen that for spans above 85 ft., all bridges had at least one interior diaphragm.

The concentration of bridges in the 50 to 90 ft. span range is primarily a result of economics. In this regard the Bridge Department's "Manual of Bridge Department Practice" [70] (p. 6-5) states:

> "For average cases with ample headroom the box girder and T-beam cost approximately the same at spans of 80 ft. Under 80 ft. the T-beam is cheaper; over 80 ft. the box girder is more economical. Where structure depth is limited, the economic range of the box girder is lowered to as little as 50 ft."

Undoubtedly, the latter factor as well as considerations of appearance have prompted the widespread use of the box girder for spans below 80 ft.

3. Overall Widths (Fig. 18)

The overall widths are a direct function of the number of bridge lanes and tend to be concentrated at certain widths for this reason.

4. Overall Depths (Fig. 19) and Depth-Span Ratios (Fig. 20)

Of these two factors, the latter is perhaps most relevant and Fig. 20 shows a heavy use of depth-span ratios, in the .050 to .065 range. It is interesting to note in this respect that the Bridge Department's design manual [68] recommends a normal use of .065 for simple spans and cautions

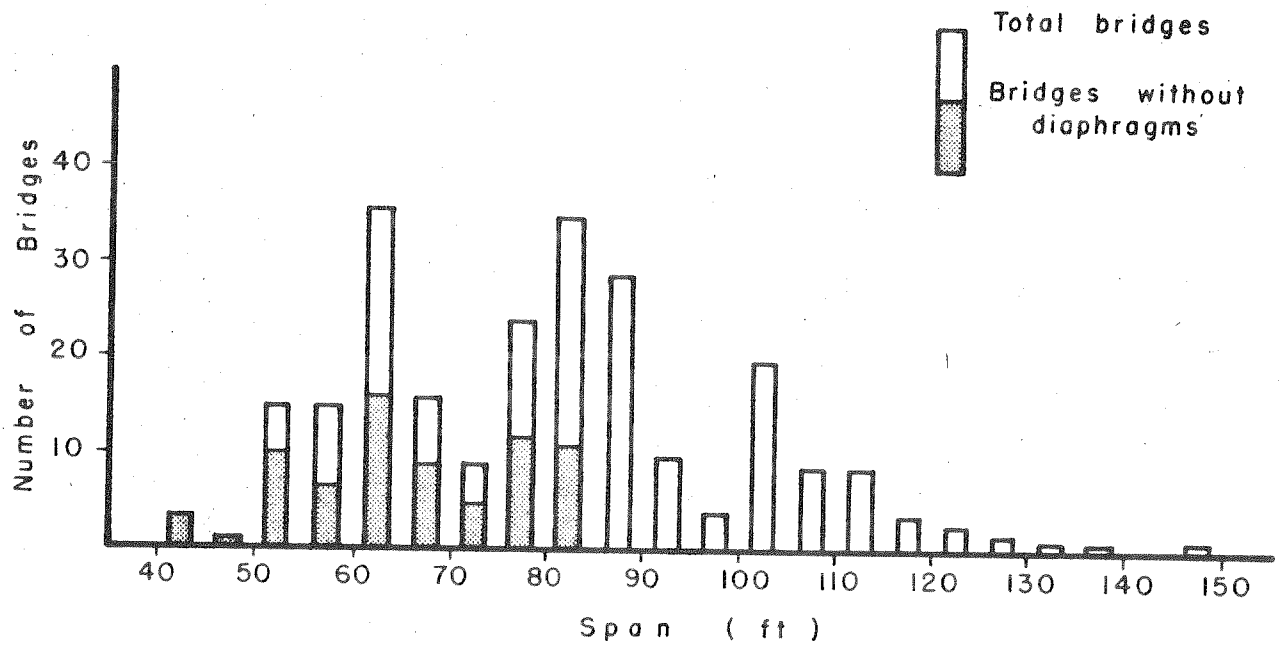

FIG. 17 SPAN LENGTHS

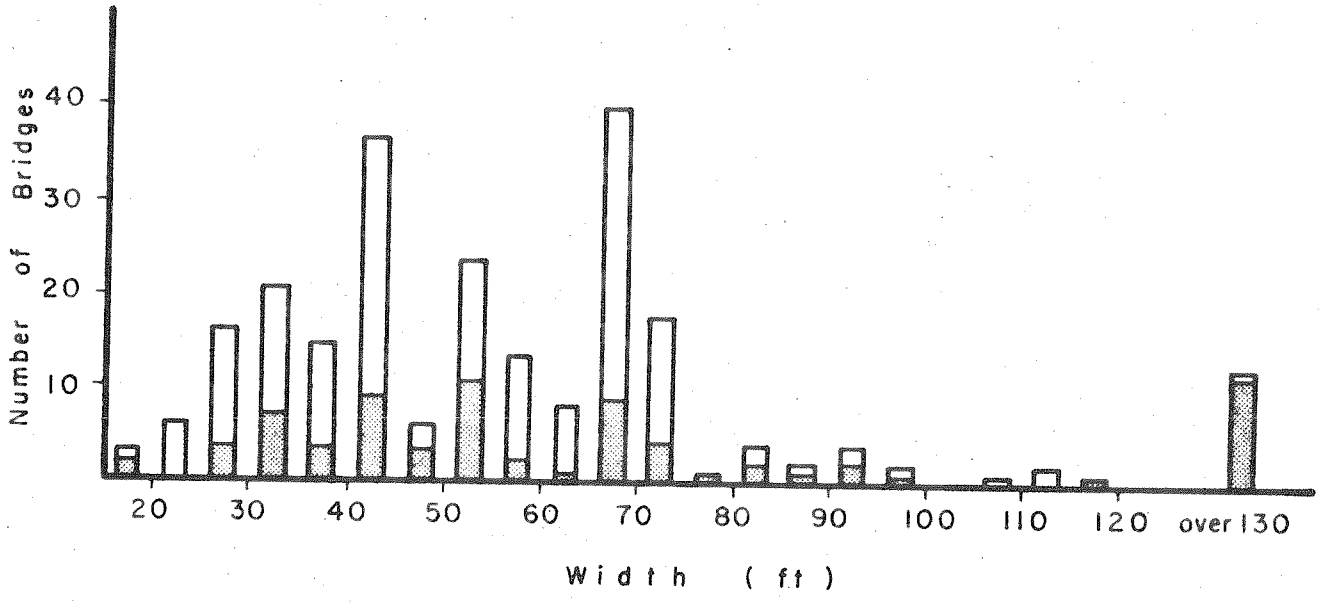

FIG. 18 OVERALL WIDTHS

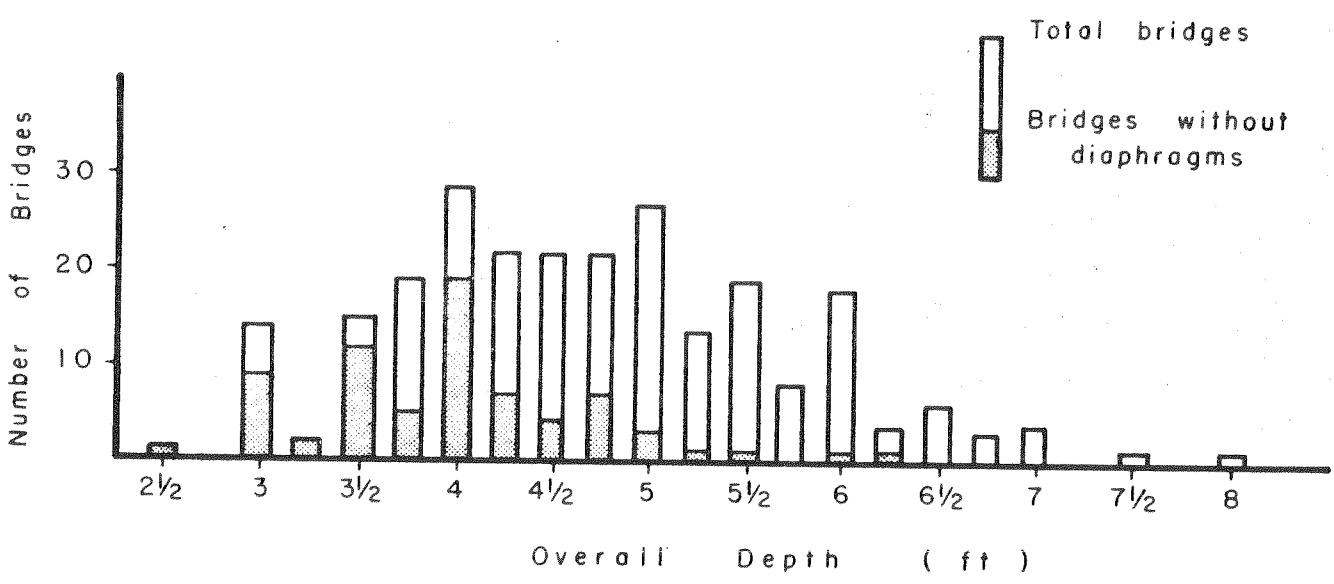

FIG. 19 OVERALL DEPTHS

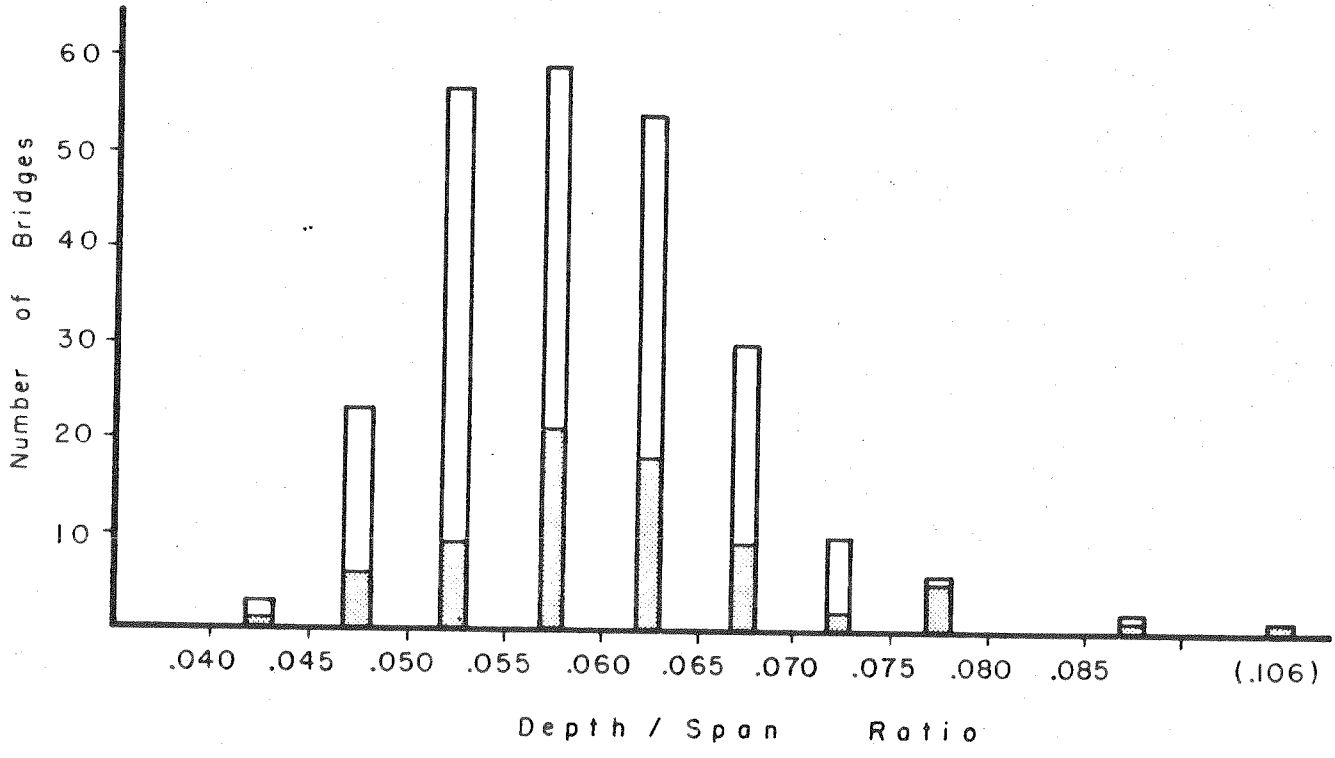

FIG. 20 DEPTH / SPAN RATIOS

against the use of values below .053 without prestressing, because of the excessive plastic flow in these shallower bridges.

5. Width of Cells (Fig. 21) and Number of Cells (Fig. 22)

The width of cells (web spacing) used varies to fit different roadway width requirements, but as seen in Fig. 21 a spacing between 7 and 8 ft. is most often used. As the width becomes greater the top slab bending moments due to wheel loads become larger, but on the other hand the number of girder webs become fewer. Generally, within the range 7 to 9 ft., the width of cells which gives the least number of webs is considered to be the most economical. The number of cells is of course a function of overall width and width of cells, but it can be seen from Fig. 22 that the majority of bridges have from 4 to 9 cells.

6. Top Slab (Fig. 23), Bottom Slab (Fig. 24), and Web Thicknesses (Fig. 25)

The top slab thickness is governed by the slab moments produced by dead load and concentrated wheel loads. These moments are in turn a function of the web spacing. In Fig. 23 it can be seen that almost all of the bridges had a top slab thickness between 6 and 7 in. with a large percentage being 6-1/2 in. thick.

The bottom slab thickness is generally designed on the basis of a minimum thickness of 1/16 of the clear span between the webs. Fig. 24 shows that a 5-1/2 in. thickness seems to be a standard adopted by many designers.

The web thickness, Fig. 25, is governed by shear at the supports and by an arbitrary practical minimum of 8 in. at midspan specified in the Bridge Departments design manual [67]. At the support the thickness is increased by flaring to carry the necessary shear.

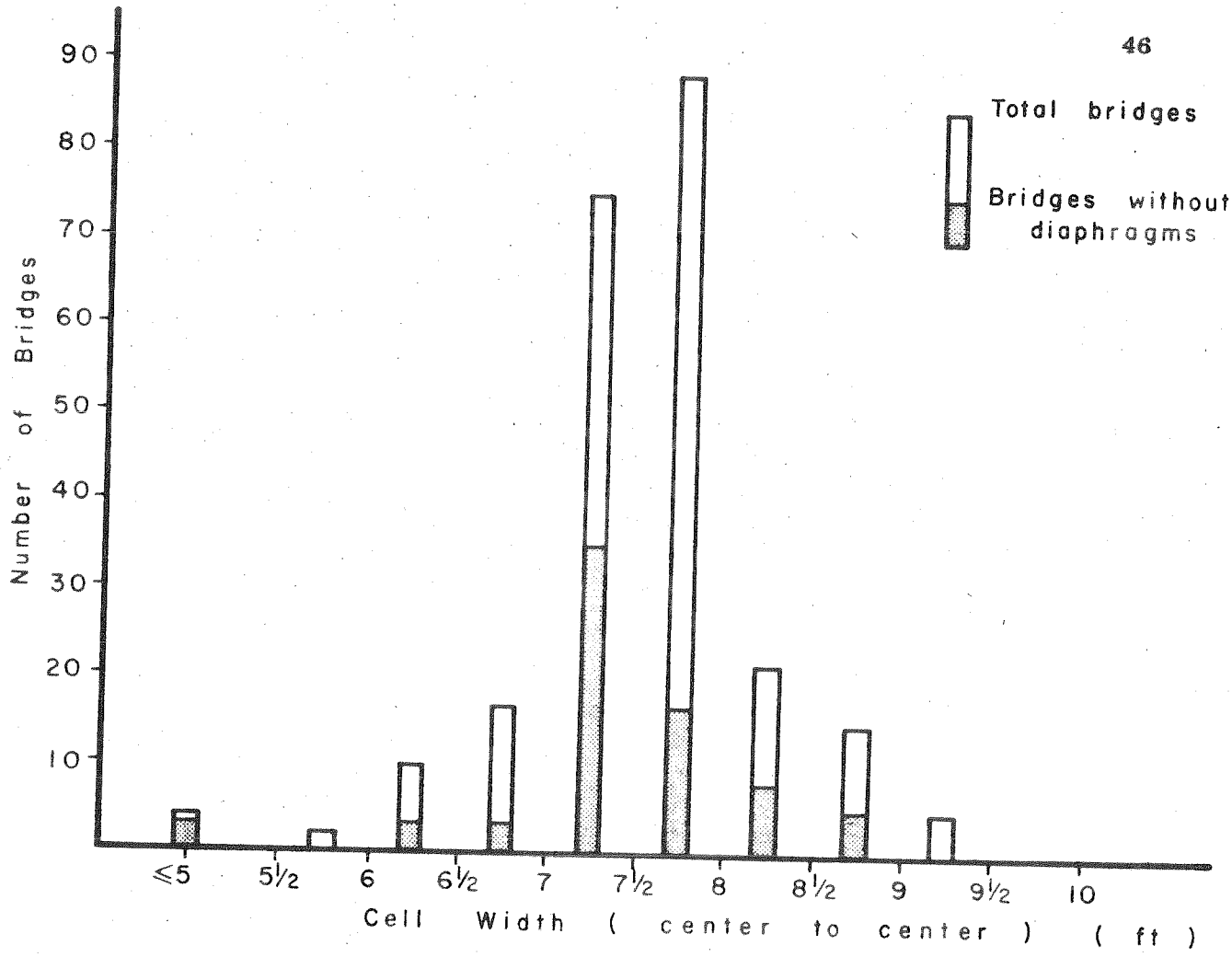

FIG. 21 WIDTH OF CELLS

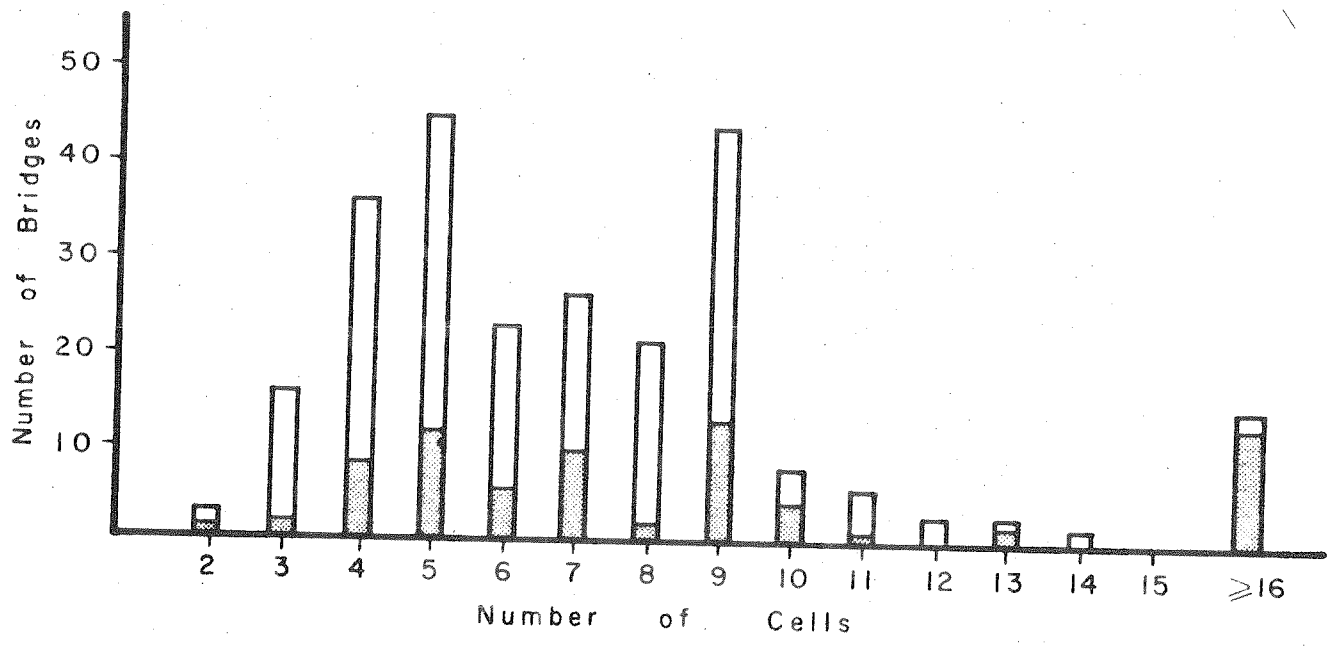

FIG. 22 NUMBER OF CELLS

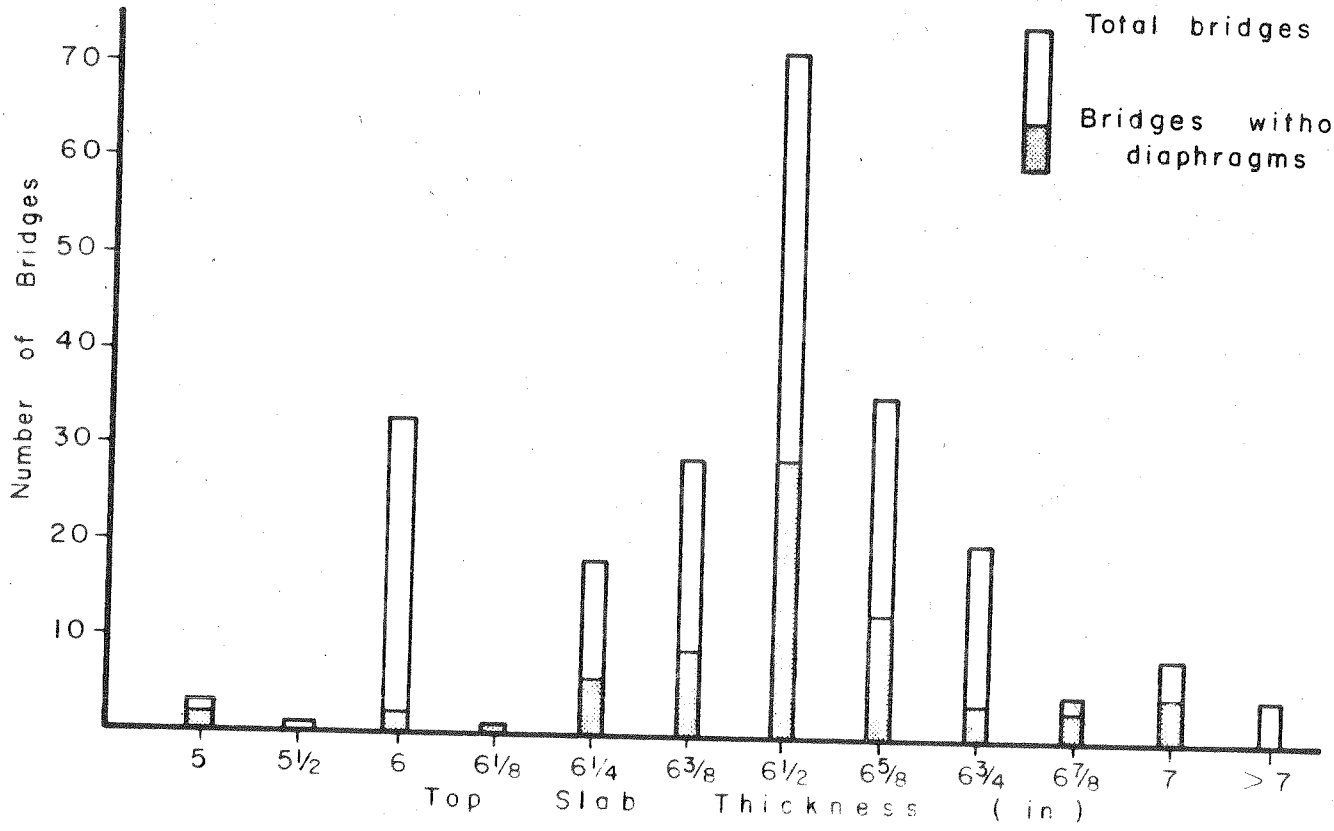

FIG. 23 TOP SLAB THICKNESSES

BOTTOM SLAB THICKNESS (in)	4½	5	5½	5¾	6	6⅛	6½	8	10
TOTAL NUMBER OF BRIDGES	1	2	198	1	24	3	2	1	1
BRIDGES WITHOUT DIAPHRAGMS	-	2	64	-	6	2	-	-	-

FIG. 24 BOTTOM SLAB THICKNESSES

WEB THICKNESS (in)	8	9	10
TOTAL NUMBER OF BRIDGES	221	8	4
BRIDGES WITHOUT DIAPHRAGMS	72	1	1

FIG. 25 WEB THICKNESSES

VI. PARAMETER STUDIES

1. General Remarks

The behavior of box girder bridges subjected to concentrated wheel loads is influenced by a number of parameters. Among these are those reviewed and tabulated for existing bridges in the preceding chapter. Based on this review, a number of cases involving a typical range of the important parameters were selected and analyzed using the computer. Because of the large amount of information output by the computer it was decided to concentrate the study of the results on those internal forces and moments which are most important in terms of the design of box girder bridges. Thus, in general, only the midspan values of longitudinal stresses σ_x, percentage distribution of the total midspan moment to each girder, transverse slab moments M_y, and longitudinal slab moments M_x are presented and discussed in this chapter.

The cases studied included two spans - 60 or 80 ft; four cross-sections - 3, 4, 6, or 8 cells; and four transverse positions of a single 1000 lb. concentrated load at midspan. In all cases the concentrated load was assumed to be a line load having a length of 1 ft. to approximate a wheel load. In each computer solution the concentrated line load was represented by the sum of the first 99 harmonics of the Fourier series. This involved 50 non-zero harmonics since the load was symmetrical with respect to midspan. Results for the above cases were obtained for simply supported bridges without diaphragms. These are presented and discussed first. In addition, for the case of the 60 ft. span, 6 cell bridge, analyses were run for a case of one rigid diaphragm added at midspan and also for a case in which the bottom slabs only were sliced longitudinally to eliminate the transverse continuity of the box girders at these sections. Results for these special cases are presented and discussed in the latter part of the chapter.

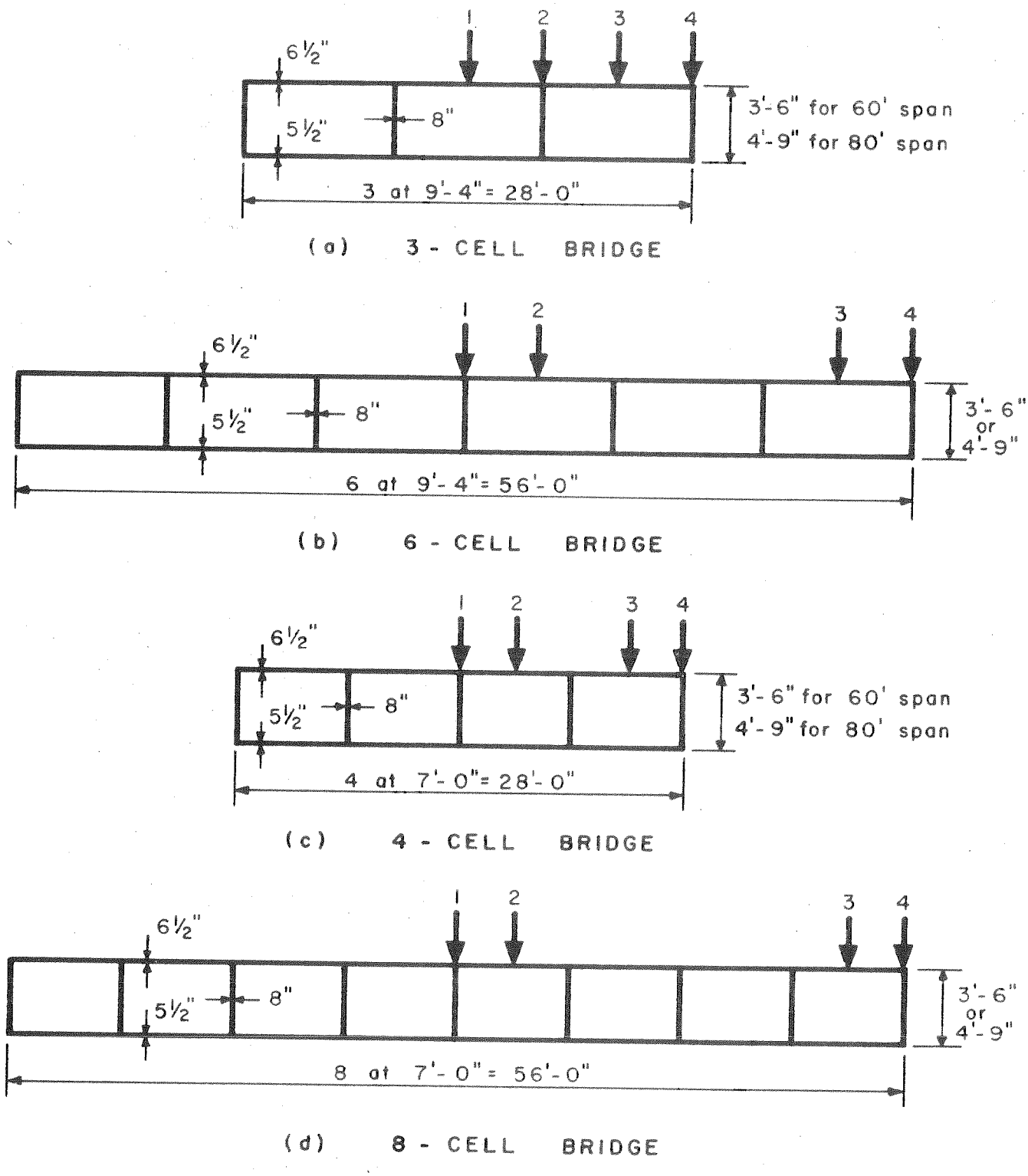

FIG. 26 CENTERLINE DIMENSIONS AND LOAD POSITIONS FOR EXAMPLE BRIDGES

The cross-sectional dimensions for each example bridge together with the four transverse load positions at midspan and the girder designations are shown in Fig. 26. Two overall bridge widths, 28 and 56 ft., and two cell widths, 7 ft. -0 in. and 9 ft.-4 in., were used resulting in the 3, 6, 4, and 8 cell bridges shown. Note that the 3 and 6 cell bridges have similar cell dimensions as also do the 4 and 8 cell bridges. The 60 ft. span bridges had an overall depth of 3 ft.-6 in. and a depth-span ratio of .0583, while similar quantities for the 80 ft. span bridges were 4 ft.-9 in. and .0594. All of the example bridges had dimensions for the top (deck) slab, bottom slab, and web thicknesses equal to 6-1/2, 5-1/2, and 8 in. respectively. For ease in discussion each case analyzed will be designated by three numbers: the span-number of cells-load position, for example Case 60-3-1.

2. Longitudinal Stresses, σ_x

Midspan values of longitudinal stresses σ_x in psf are plotted in Figs. 27 through 34 for the four transverse load positions for each example bridge. These and all remaining figures are presented at the end of this chapter. A study of the results indicates several points of interest.

a. For any given cross-section and span, load position 4, over the exterior girder web, produces the maximum longitudinal stress.

b. For any given cross-section and span, a load placed over a girder web produces a larger maximum stress than a similar load placed at the midpoint between webs of an adjacent cell. In the latter case the load has a chance to distribute longitudinally before it is picked up by the web, while in the former case the effect of shear lag tends to produce a concentration of stress at the girder web under the concentrated load.

c. The peak stress for load position 4, over an exterior girder, is almost the same for the 3 and 6 cell or 4 and 8 cell bridges of a given span. This emphasizes the localized nature of this peak stress. This peak stress damps out more rapidly in the wider bridges.

d. Except for webs directly under a concentrated load, the stresses have essentially a linear variation over the depth of the webs.

e. The ability of a bridge to distribute a concentrated load transversely is a function of the ratio of the relative stiffnesses in the transverse and longitudinal directions. As this ratio becomes greater the distribution becomes better. A study of the results in Figs. 27 through 34 bears this out since for any given loading the longer span and narrower bridges have lower ratios of peak to average stress on the cross-section, indicating better load distribution properties.

3. Percentage Distribution of Total Midspan Moment to Each Girder

In present design methods, the actual box girder cross-section is divided into individual girders consisting of a web and a top and bottom flange. The flanges are taken equal in width to the distance between the midspan of the cells on adjacent sides of the web. Thus for the example bridges of the present study all interior girders have flange widths twice those of the two exterior girders.

The girder moment taken by any girder can be found by integrating the stresses in Figs. 27 to 34 over the proper slab and web areas to obtain forces and then multiplying these forces by their respective lever arms to the neutral axis of the section. The girder moments can then be summed to get their contribution to the total midspan moment on the entire cross-section. To this can be added the contribution of the longitudinal slab moments M_x. The total midspan

moment obtained in this way can then be compared with total statical moment as a check on the results. This was done for all cases and excellent checks, within 1 or 2%, were obtained. The contributions of the slab moments M_x to the total moment were very small, again of the order of 1 to 2%.

Each girder moment can be divided by the total moment taken by all girders, which is practically equal to the total midspan moment, to establish the percentage of the total moment taken by each girder. These results are summarized in Tables 2 to 5.

In making comparisons it should be kept in mind that the interior girders have twice the flange widths of the exterior girder. Since these results and those for longitudinal stresses are interdependent, several of the points made for stresses are equally applicable here. In addition the following comments can be made.

a. For a given cross-section the results for both 60 and 80 ft. spans are quite similar, with a slightly better distribution being obtained in the longer span. It should be noted again that the depth-span ratios for both spans were practically the same.

b. For a uniform distribution across the section, the percentage moment taken by each interior girder would be approximately equal to 100% divided by the number of cells in the bridge section. This percentage would thus be 33.3, 16.7, 25.0, and 12.5% for the 3, 6, 4, and 8 cell bridges with the values for exterior girders being approximately one-half of these. Comparing these values for uniform distribution with those in Tables 2 to 5 it is apparent that the bridges with the narrower width of 28 ft. (3 or 4 cells) achieved a more uniform distribution

than those with a 56 ft. width (6 or 8 cells), thus emphasizing that better load distribution is obtained in the narrower bridges, as would be expected.

c. A load at position 4, over the exterior girder web, is the most severe loading condition for the exterior girder in all cases. Comparing the 3 and 6 cell cases or the 4 and 8 cell cases for this loading, it can be seen that the percentages of the total moment taken by the exterior girder differ by only about 3% indicating the localized effect of this loading.

d. For each interior girder, the most severe loading condition exists when the load is placed directly over the web of the girder under consideration.

TABLE 2. PERCENTAGE OF TOTAL MIDSPAN MOMENT TAKEN BY EACH GIRDER FOR 3-CELL BRIDGE

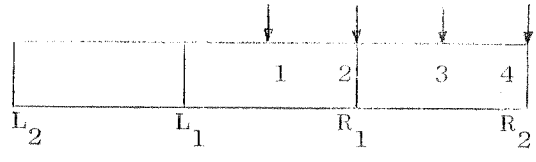

Span	60 ft.				80 ft.			
1000 lb. load at	1	2	3	4	1	2	3	4
Girder L_2	14.0	10.9	9.8	8.9	14.6	11.8	10.8	9.9
Girder L_1	36.0	25.9	23.0	20.4	35.4	27.6	22.1	22.2
Girder R_1	36.0	46.0	39.8	32.3	35.4	43.2	38.8	32.8
Girder R_2	14.0	17.2	27.4	38.4	14.6	17.4	28.3	35.1
Total	100.0	100.0	100.0	100.0	100.0	100.0	100.0	100.0

TABLE 3. PERCENTAGE OF TOTAL MIDSPAN MOMENT TAKEN BY EACH GIRDER FOR 6-CELL BRIDGE

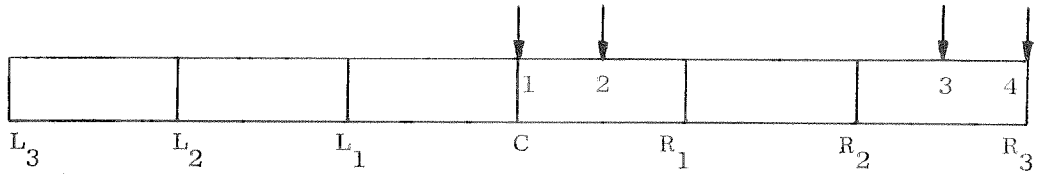

Span	60 ft.				80 ft.			
1000 lb. load at	1	2	3	4	1	2	3	4
Girder L_3	4.7	3.7	1.8	1.6	5.5	4.6	2.6	2.4
Girder L_2	10.6	8.3	4.0	3.7	11.5	9.7	5.5	5.2
Girder L_1	16.6	12.9	5.9	5.5	17.0	13.6	7.4	7.1
Girder C	36.2	26.6	9.6	8.9	32.0	24.7	10.8	10.2
Girder R_1	16.6	27.5	17.0	15.2	17.0	25.3	17.1	15.7
Girder R_2	10.6	14.7	35.3	28.6	11.5	15.2	32.7	27.3
Girder R_3	4.7	6.3	26.4	36.5	5.5	6.9	23.9	32.1
Total	100.0	100.0	100.0	100.0	100.0	100.0	100.0	100.0

TABLE 4. PERCENTAGE OF TOTAL MIDSPAN MOMENT TAKEN BY EACH GIRDER FOR 4-CELL BRIDGE

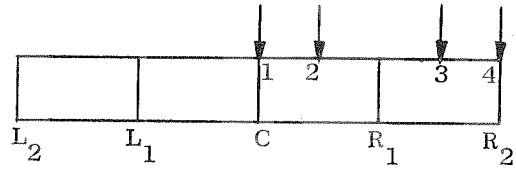

Span	60 ft.				80 ft.			
1000 lb. load at	1	2	3	4	1	2	3	4
Girder L_2	10.2	9.2	7.7	7.2	10.9	9.7	8.4	8.2
Girder L_1	21.9	19.3	15.7	14.7	22.6	19.8	16.7	16.4
Girder C	35.8	28.7	20.1	18.3	33.0	28.1	20.4	19.6
Girder R_1	21.9	30.1	33.1	27.1	22.6	29.7	31.5	27.4
Girder R_2	10.2	12.7	23.4	32.7	10.9	12.7	23.0	28.4
Total	100.0	100.0	100.0	100.0	100.0	100.0	100.0	100.0

TABLE 5. PERCENTAGE OF TOTAL MIDSPAN MOMENT TAKEN BY EACH GIRDER FOR 8-CELL BRIDGE

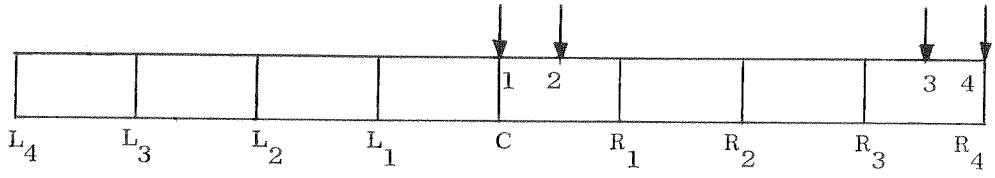

Span	60 ft.				80 ft.			
1000 lb. load at	1	2	3	4	1	2	3	4
Girder L_4	3.9	3.3	1.6	1.6	4.3	3.9	2.3	2.3
Girder L_3	7.9	6.7	3.3	3.2	8.6	7.5	4.6	4.5
Girder L_2	9.8	8.2	4.1	3.9	10.2	8.8	5.2	5.1
Girder L_1	14.5	11.7	5.4	5.1	14.3	11.7	6.4	6.3
Girder C	27.8	21.6	7.4	7.1	25.2	20.3	8.1	8.0
Girder R_1	14.5	21.9	10.7	10.1	14.3	20.6	10.8	10.5
Girder R_2	9.8	12.4	16.3	14.9	10.2	12.3	15.5	14.6
Girder R_3	7.9	9.5	29.0	24.7	8.6	9.9	27.1	23.2
Girder R_4	3.9	4.7	22.2	29.4	4.3	5.0	20.0	25.5
Total	100.0	100.0	100.0	100.0	100.0	100.0	100.0	100.0

4. Slab Moments, M_y and M_x

The transverse distribution of the midspan values of transverse slab moments M_y and longitudinal slab moments M_x in ft-lb/ft are given in Figs. 35 through 50. Values are given for the top and bottom slabs as well as the webs. A study of these Figs. indicates the following:

a. Maximum values of M_y and M_x in the bottom slab are generally very small for all loadings when compared with those in the top slab and the webs.

b. Significant values of M_y and M_x exist only in the cell being loaded for cases in which the load is placed at the mid point between webs and only in the cells on either side of the web for cases in which the load is placed over a web.

c. Loads placed at the midpoints between webs produce much larger (about 3 to 4 times) maximum values of M_y and M_x, then do loads placed over the webs.

A summary of the maximum moments produced in all of the cases in which loads were placed at the midpoint between webs is presented in Table 6. A number of observations can be made from a study of Table 6:

a. Positive values of either M_y or M_x directly under the load for all bridges having the same cell dimensions are practically the same irrespective of the span, number of cells or cell being loaded. Tabulated values of M_y and M_x differ by less than 3% and 6% respectively.

b. Positive values of M_y in the top slab are consistently about 1.5 times those of M_x.

c. Negative values of either M_y or M_x, in the top slab at its juncture with the web for all bridges loaded at the midpoint of the center cell are nearly the same as are also those for all bridges loaded at the midpoint of the exterior cell. The latter loading produces slightly greater negative moments because of its unsymmetrical nature.

d. Negative values of M_y in the top slab are much larger, about 8 or 9 times, than negative values of M_x.

e. The conclusions of paragraph c and d also hold true for the maximum moments in the web which occur at its juncture with the top slab. The ratio cited in paragraph d is about 7 times in this case.

TABLE 6. MAXIMUM SLAB AND WEB MOMENTS (FT-LB/FT)
FOR LOADS AT MIDPOINTS BETWEEN GIRDER WEBS

	Transverse M_y			Longitudinal M_x		
Case	Top Slab Max+M_y	Top Slab Max-M_y	Web Max M_y	Top Slab Max+M_y	Top Slab Max-M_x	Web Max M_x
60-3-1	329.1	138.8	121.7	227.5	15.5	17.9
60-6-2	329.3	139.4	127.4	226.8	16.5	18.7
60-3-3	329.9	152.8	144.7	229.4	17.4	21.5
60-6-3	330.0	153.5	148.1	229.0	17.8	22.0
80-3-1	321.8	135.5	110.7	218.1	16.7	16.3
80-6-2	322.1	136.5	115.4	217.5	17.4	17.0
80-3-3	323.1	147.5	129.6	219.6	18.3	19.3
80-6-3	323.2	148.2	132.7	219.3	18.7	19.8
60-4-2	304.7	136.4	122.4	203.0	14.3	17.9
60-8-2	305.1	134.0	121.1	202.1	14.8	17.7
60-4-3	305.6	147.7	139.1	205.0	15.5	20.5
60-8-3	305.7	148.2	141.7	204.6	16.0	20.9
80-4-2	297.6	133.2	110.1	193.3	15.4	16.1
80-8-2	297.8	131.3	109.0	192.7	15.7	15.9
80-4-3	299.0	142.7	123.6	195.0	16.6	18.3
80-8-3	299.1	143.2	126.1	194.7	17.0	18.7

Longitudinal distributions of M_y and M_x in the top slab for loads placed at the midpoints between webs are shown in Figs. 51 and 52. Distributions along longitudinal lines at the midpoint directly under the load or at the adjacent juncture with a supporting web are both shown for M_y. Several conclusions can be drawn.

a. Distributions of M_y or M_x at midpoint lines for the same span and cell dimensions are essentially identical irrespective of the number of cells in the bridge or the cell being loaded.

b. Distributions of M_y at support lines for the same span and cell dimensions are very similar irrespective of the number of cells in the bridge. Loads placed at the midpoint of the exterior cells (position 3) produce slightly greater values than those placed at the midpoint of the center cells (positions 1 or 2).

c. Both M_y and M_x damp out rapidly in the longitudinal direction especially at midpoint lines. For M_y, at a distance equal to only half the cell width (4 ft. 7-1/2 in.) from midspan, the positive and negative moments have decreased by at least 88 and 66% respectively of their peak values, some decreases being even greater. M_x decreases even more rapidly than M_y and changes sign before damping out to a negligible value.

5. Special Cases

In order to ascertain the effects of a rigid diaphragm placed at midspan or the elimination of transverse continuity by slicing the bottom slabs longitudinally at the midpoint between webs, four additional cases were analyzed for the 60 ft. span, 6 cell bridge. Two cases were for loads over the center web and two cases were for loads over the exterior web. Midspan values of longitudinal stresses σ_x in psf are plotted in Figs. 53 and 54 for these cases as well as for the original cases for the closed box girder bridge without a diaphragm. In addition the percentage of the total midspan moment taken by each girder referred to the neutral axis of the entire section is summarized in Table 7 for these cases.

Several interesting observations may be made:

a. The introduction of a rigid midspan diaphragm improves the load distribution properties of the bridge tremendously for both loading conditions, as should be expected. It should be kept in mind that in an actual bridge the diaphragm will not be absolutely rigid and thus this improvement would be lessened somewhat.

b. Eliminating the transverse continuity in the bottom slab reduces the load distribution effectiveness of the bridge. Comparing this case with the closed box without a diaphragm, in Table 7, the percentage of total moment taken by the most heavily stressed girder increases from 36.2 to 54.0% for a load over the center web and from 36.5 to 60.5% for a load over the exterior web. Clearly the closed box is superior in this respect.

TABLE 7. PERCENTAGE OF TOTAL MIDSPAN MOMENT TAKEN BY EACH GIRDER FOR 60 FT. SPAN, 6-CELL BRIDGE

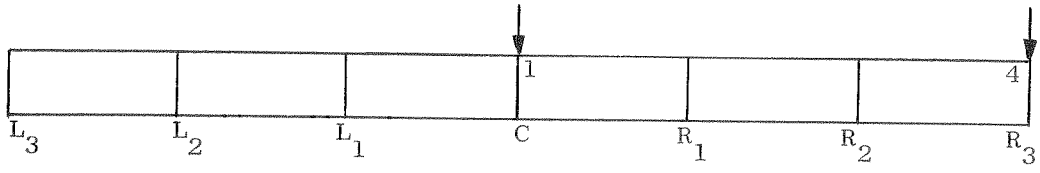

1000 lb. load at	1			4		
Case	(a)	(b)	(c)	(a)	(b)	(c)
Girder L_3	4.7	9.4	1.1	1.6	5.3	-2.0
Girder L_2	10.6	16.2	4.9	3.7	11.3	-1.7
Girder L_1	16.6	16.2	17.0	5.5	13.8	0.2
Girder C	36.2	16.4	54.0	8.9	16.3	2.7
Girder R_1	16.6	16.2	17.0	15.2	18.8	8.6
Girder R_2	10.6	16.2	4.9	28.6	21.2	31.7
Girder R_3	4.7	9.4	1.1	36.5	13.3	60.5
Total	100.0	100.0	100.0	100.0	100.0	100.0

(a) Closed box without midspan diaphragm

(b) Closed box with midspan diaphragm

(c) Bottom slab sliced longitudinally at midpoint between webs, no diaphragm

c. For the cases in which the bottom slab is sliced, both tensile and compressive stresses occur in the bottom flanges of the individual girders due to the inducement of bending of the bottom flanges about vertical axes. These stresses in the bottom slab and also those in the webs are much higher for this case than for the closed box.

6. Computer Times

All of the cases described in this chapter were run using the computer program MULTPL with the exception of the special case of the bridge with a diaphragm at midspan, for which the program MUPDI was used.

For all cases, the concentrated load, taken as a 1 ft. long line load, was represented by the sum of the first 99 harmonics of the appropriate Fourier series. Because of symmetry about midspan this involved 50 non-zero harmonics. Results for all of the internal forces, moments and displacements were output at from 4 to 8 points transversely across the width of each plate and at 7 sections along the span. Average IBM-7094 computer times required to analyze single cases are indicated below:

a. Closed box bridges without diaphragms.

3 cells	1 min. 10 sec.
4 cells	1 min. 30 sec.
6 cells	2 min. 10 sec.
8 cells	2 min. 40 sec.

b. Bridges with bottom slabs sliced longitudinally.

6 cells, full section	4 min. 33 sec.
6 cells, half section	2 min. 09 sec.

c. Closed box bridges with midspan diaphragm.

6 cells, full section	21 min. 13 sec.
6 cells, half section	4 min. 39 sec.

It is apparent from the above that relatively small amounts of computer time are required to obtain solutions for bridges without diaphragms, while for bridges with diaphragms the computer time can become appreciable. The increase in the latter time is related, but not directly proportional, to the number of restraints or interconnections imposed between the bridge and the rigid diaphragms. Restraints imposed at the longitudinal joints only, increase the computer time much less than restraints imposed at the third points between the longitudinal joints of the plates. For the 6 cell, full section bridge, with a midspan diaphragm, 118 restraints were used with 42 being at the joints and 76 being at the third points. Comparable figures for the 6 cell, half section bridge were 58, 20, and 38.

60 FT SPAN
3 CELLS
σ_x PSF

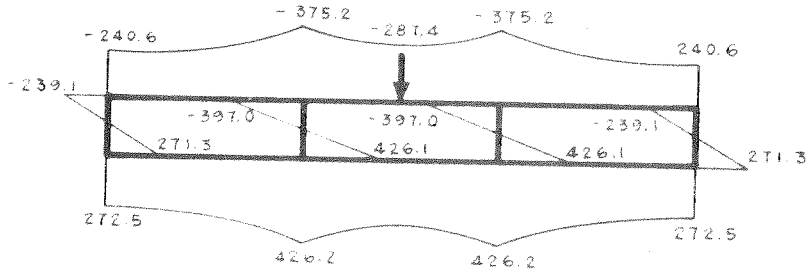

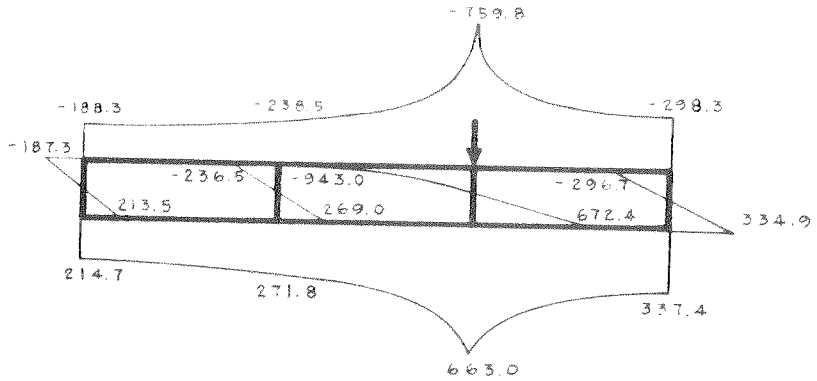

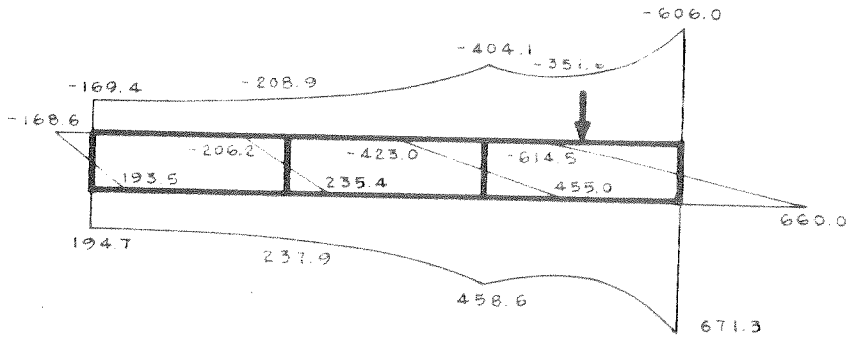

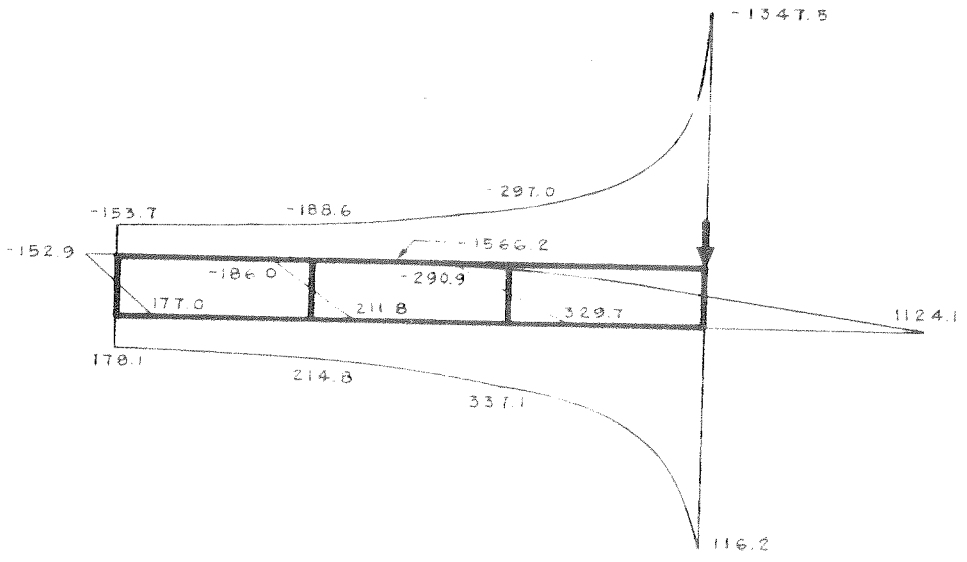

FIG. 27 MIDSPAN LONGITUDINAL STRESSES σ_x (PSF)

60 FT SPAN
6 CELLS
σ_x PSF

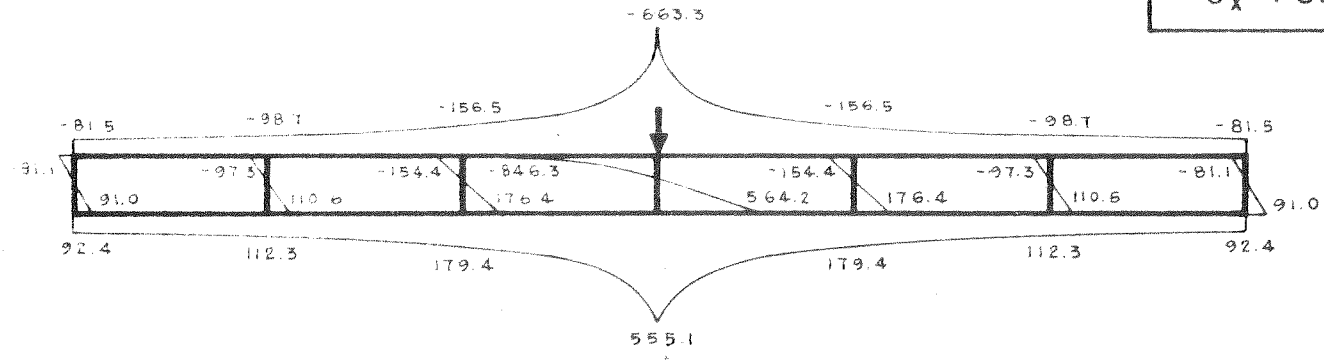

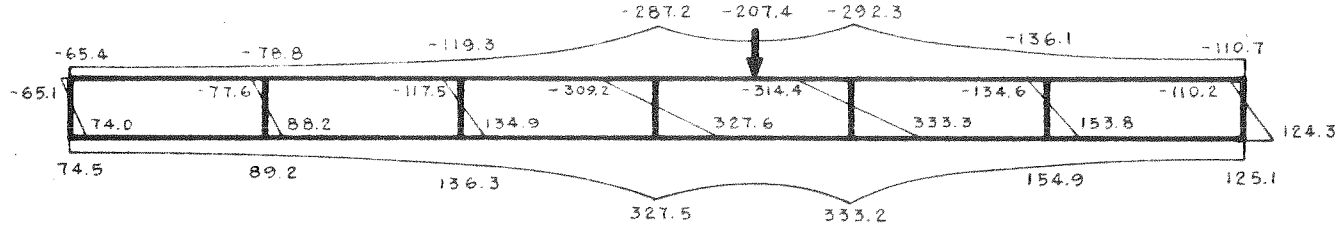

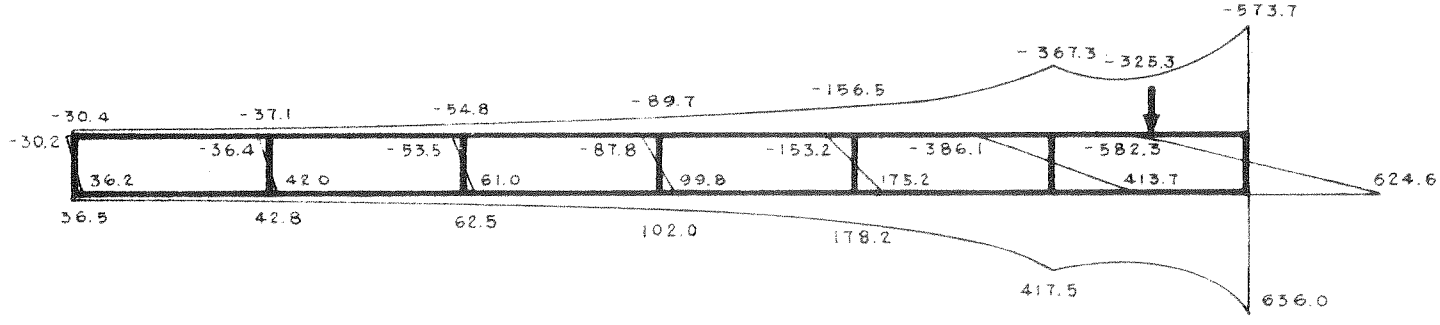

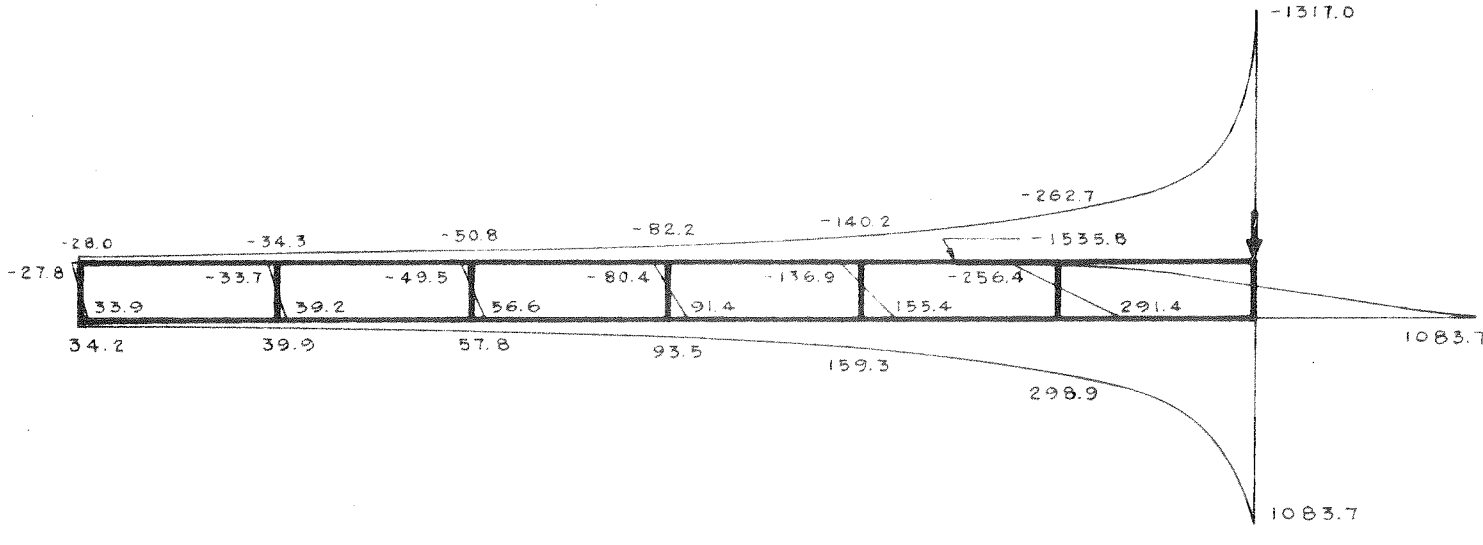

FIG. 28 MIDSPAN LONGITUDINAL STRESSES σ_x (PSF)

60 FT SPAN
4 CELLS
σ_x PSF

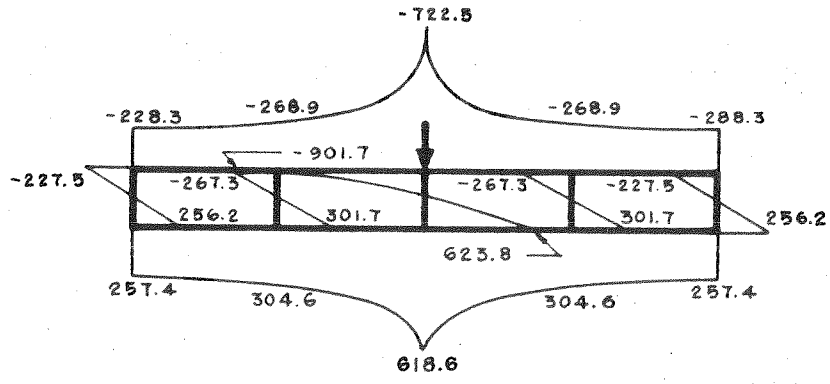

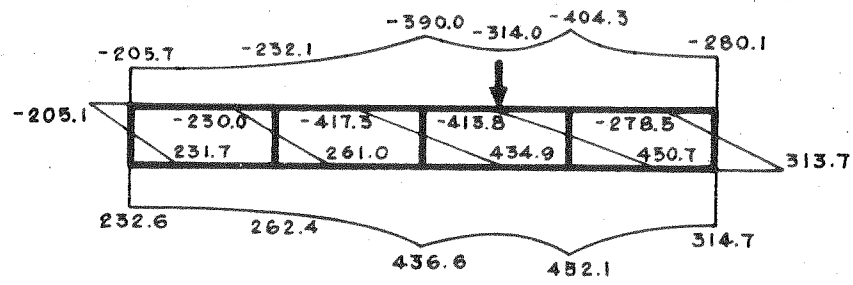

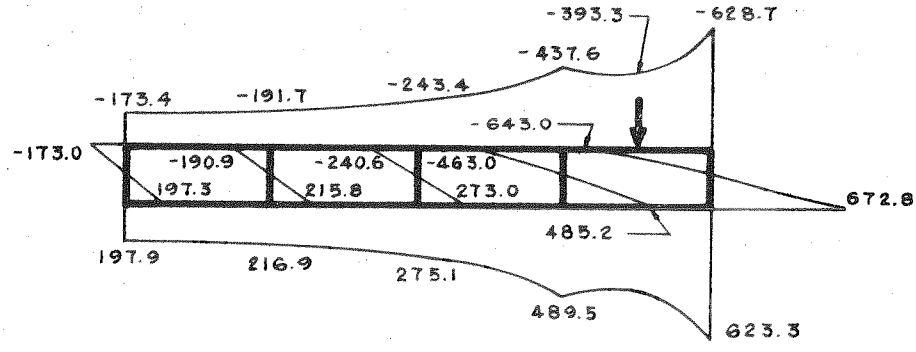

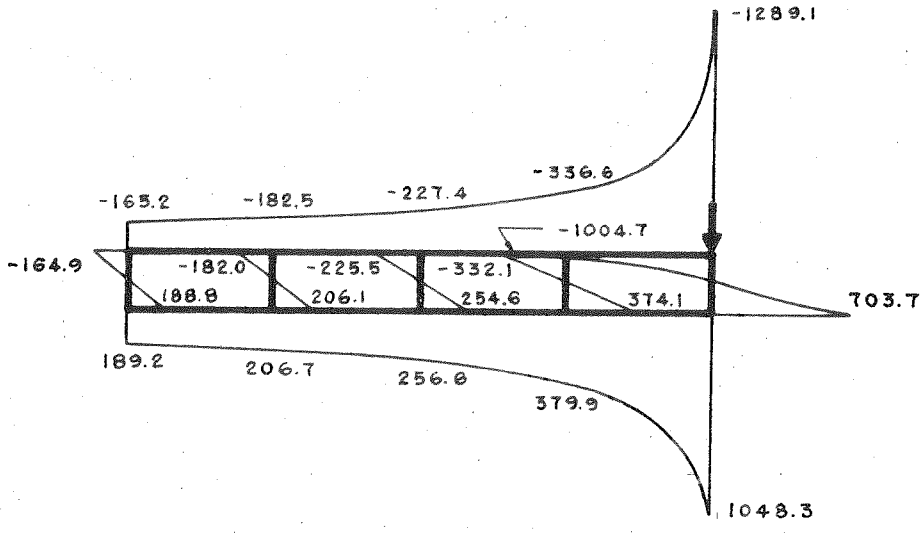

FIG. 29 MIDSPAN LONGITUDINAL STRESSES σ_x (PSF)

60 FT SPAN
8 CELLS
σ_x PSF

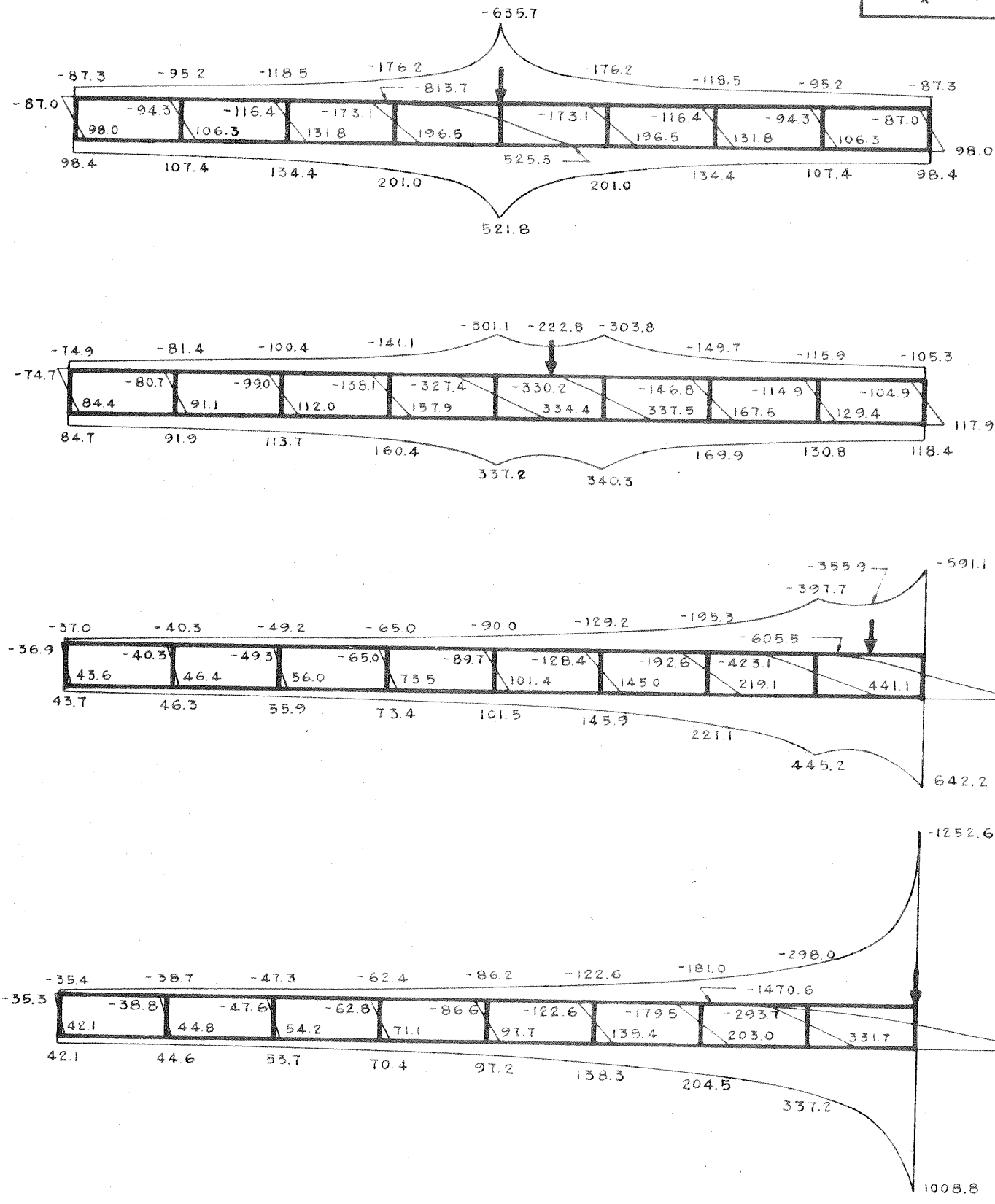

FIG. 30 MIDSPAN LONGITUDINAL STRESSES σ_x (PSF)

80 FT SPAN
3 CELLS
σ_x PSF

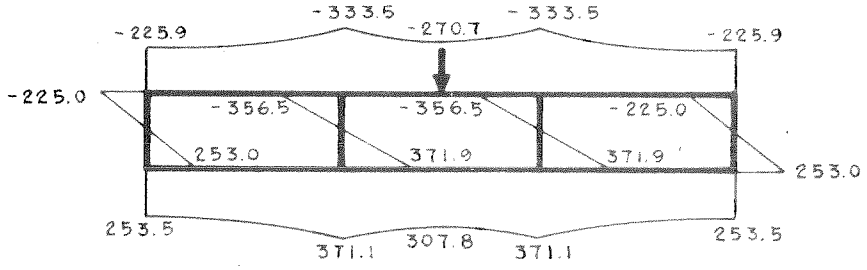

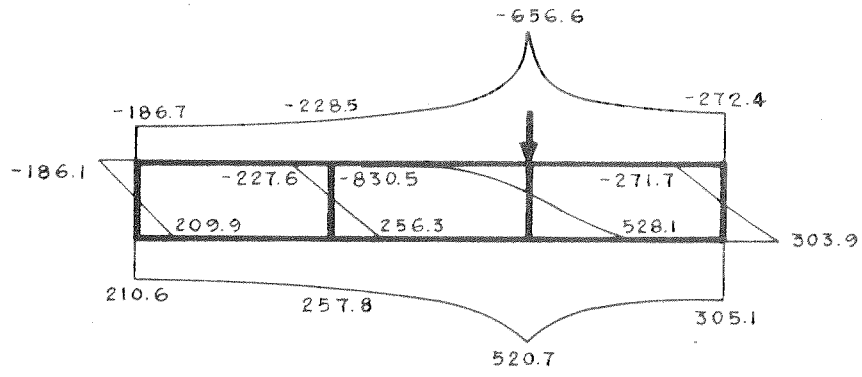

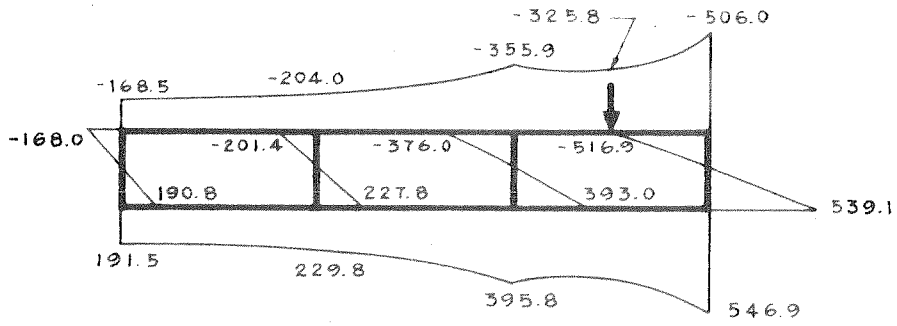

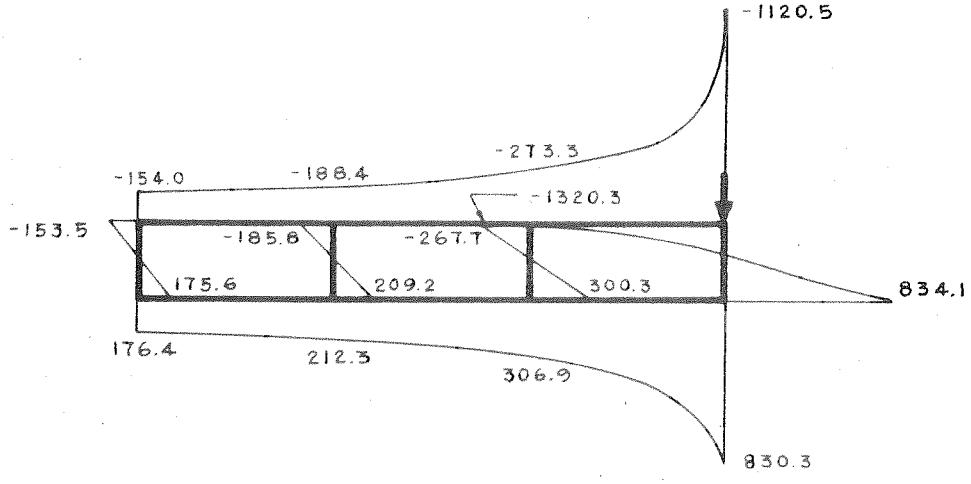

FIG. 31 MIDSPAN LONGITUDINAL STRESSES σ_x (PSF)

80 FT SPAN
6 CELLS
σ_x PSF

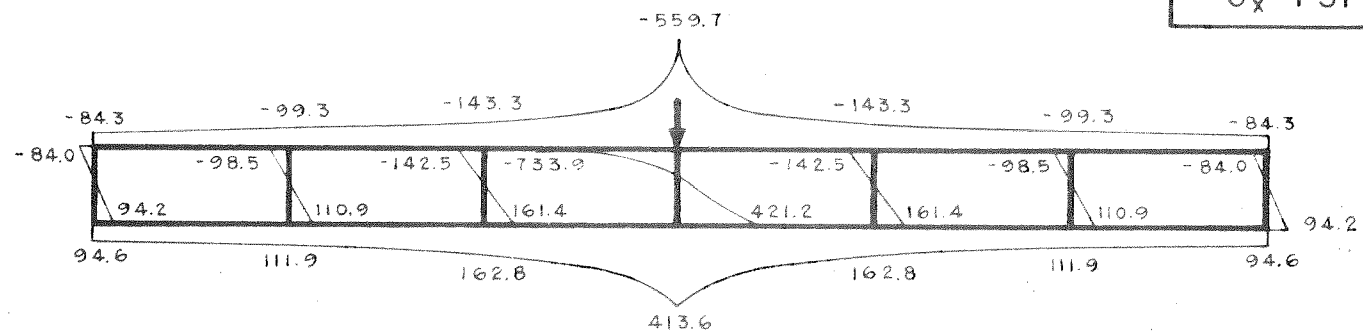

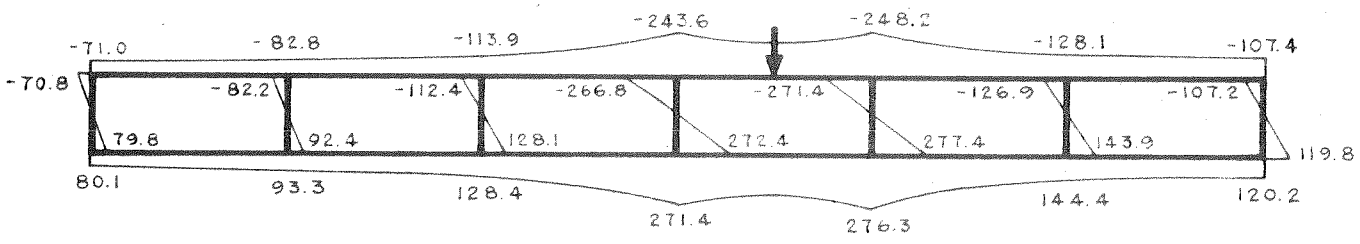

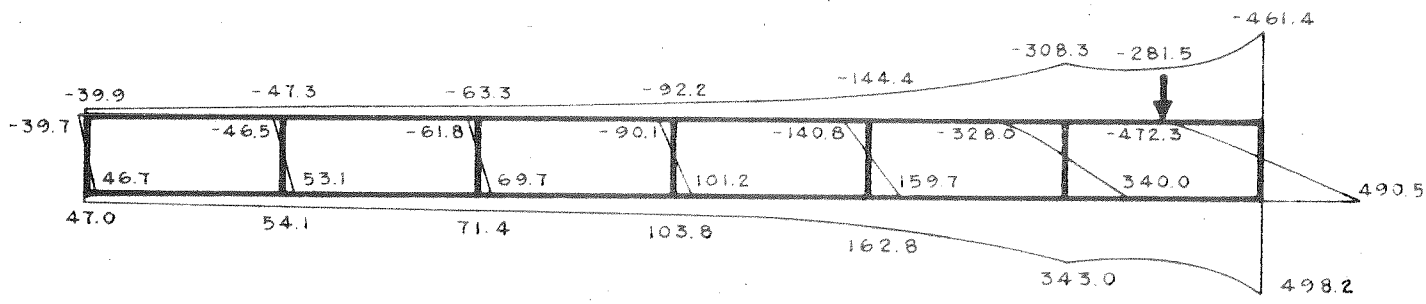

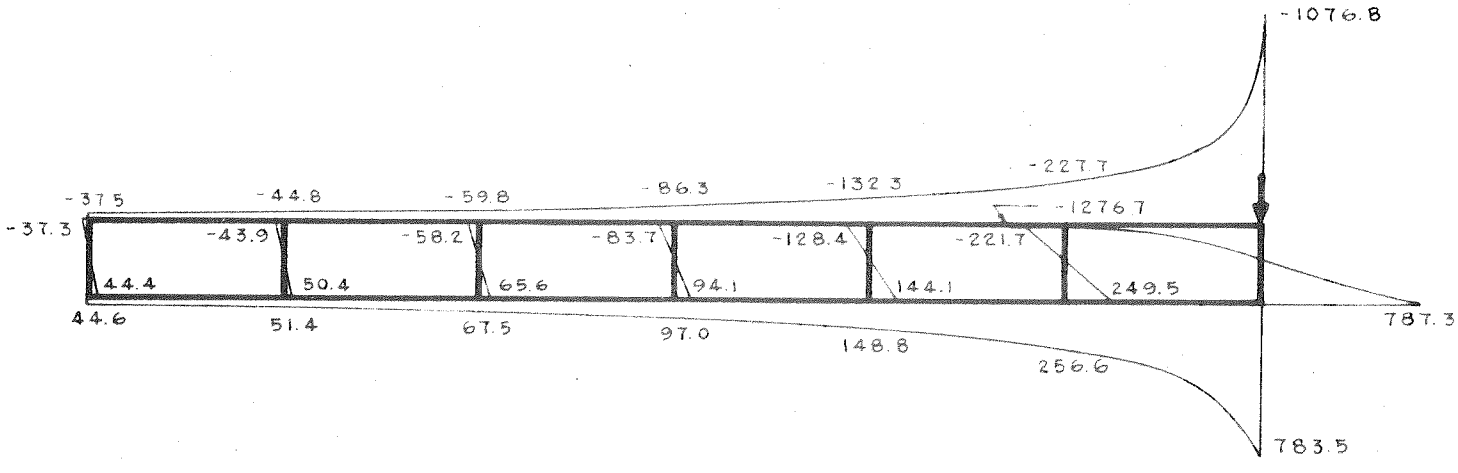

FIG. 32 MIDSPAN LONGITUDINAL STRESSES σ_x (PSF)

80 FT SPAN
4 CELLS
σ_x PSF

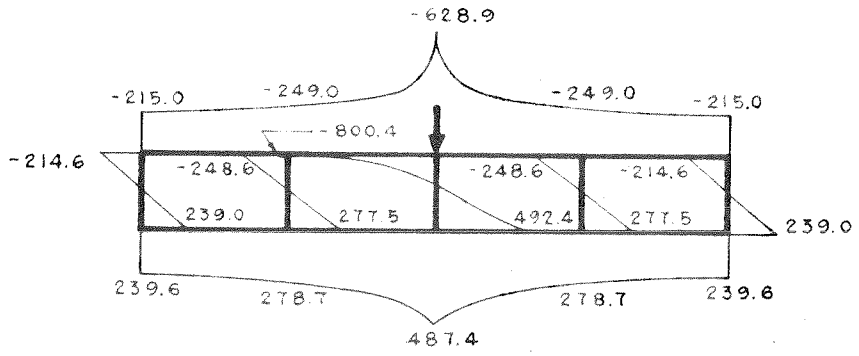

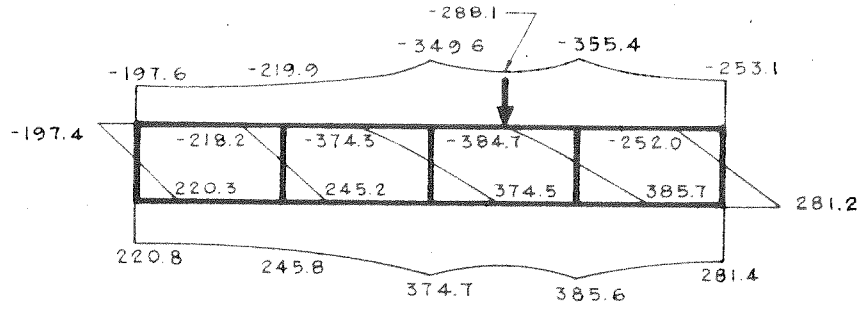

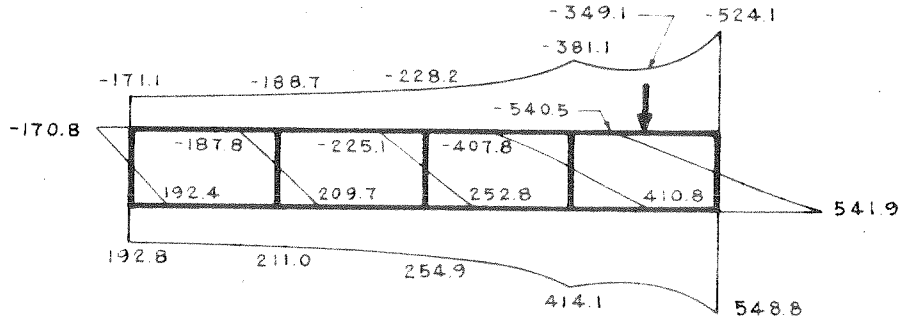

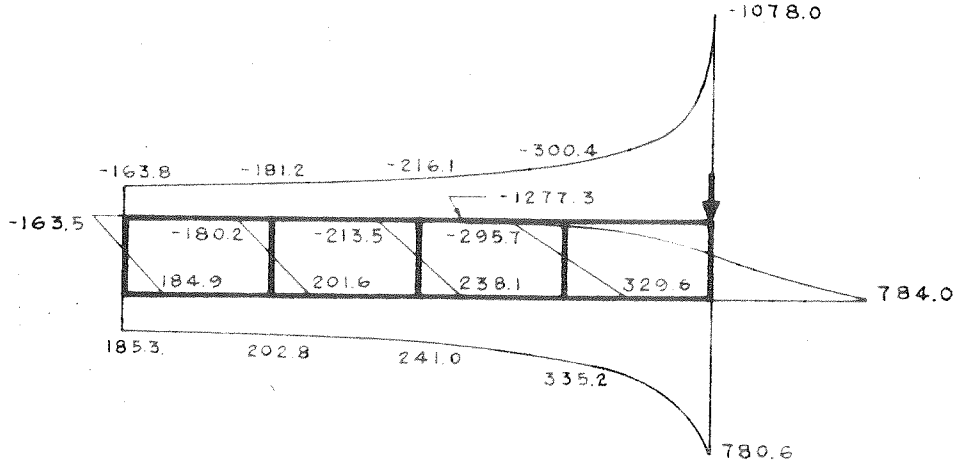

FIG. 33 MIDSPAN LONGITUDINAL STRESSES σ_x (PSF)

80 FT SPAN
8 CELLS
σ_x PSF

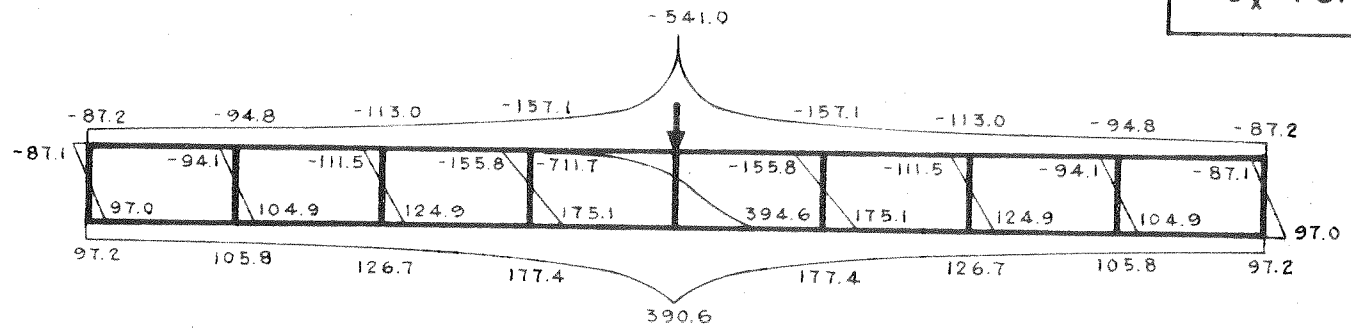

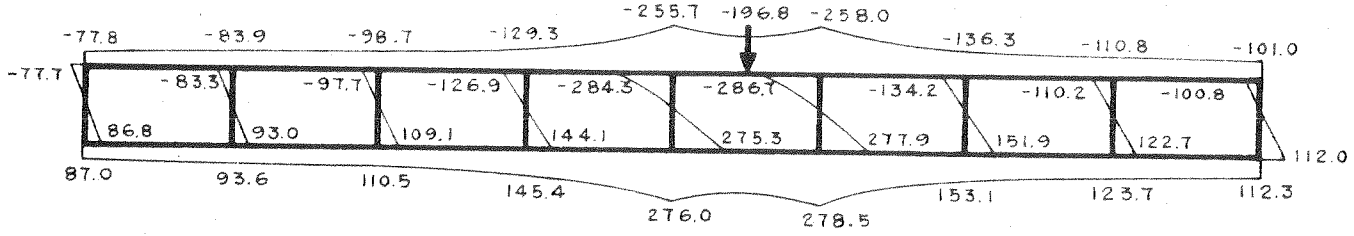

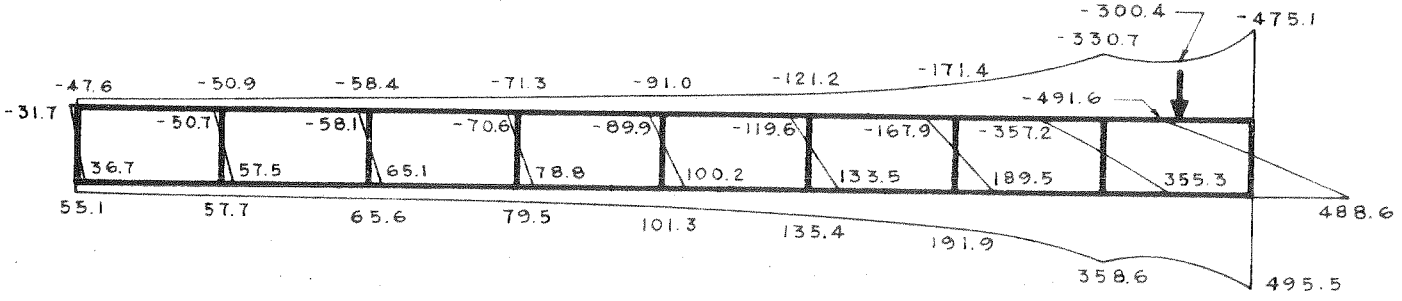

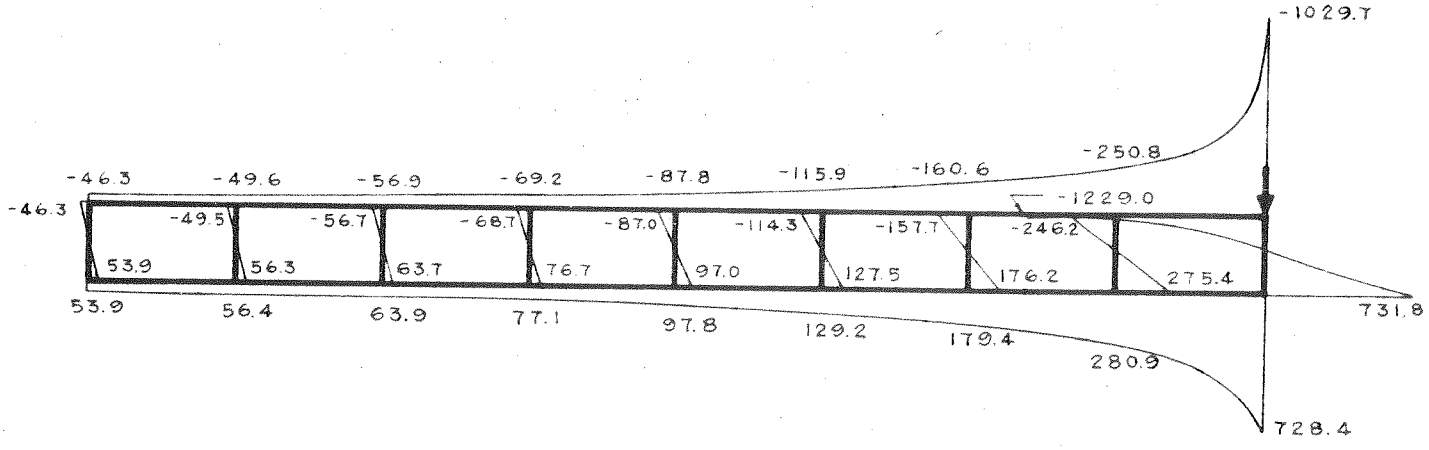

FIG. 34 MIDSPAN LONGITUDINAL STRESSES σ_x (PSF)

60 FT SPAN
3 CELLS
My FT-LB/FT

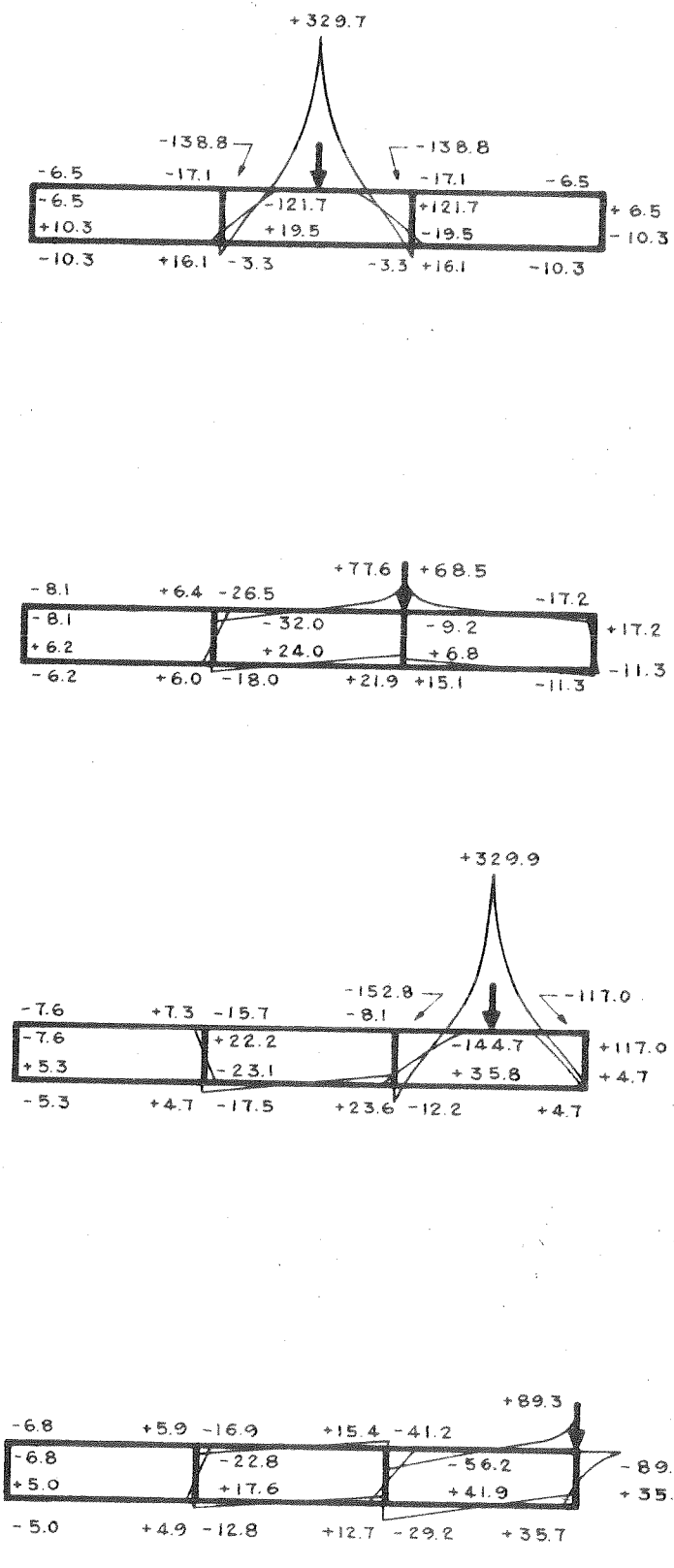

FIG. 35 TRANSVERSE DISTRIBUTION OF TRANSVERSE SLAB MOMENTS M_y (FT-LB/FT) AT MIDSPAN

60 FT SPAN
6 CELLS
My FT-LB/FT

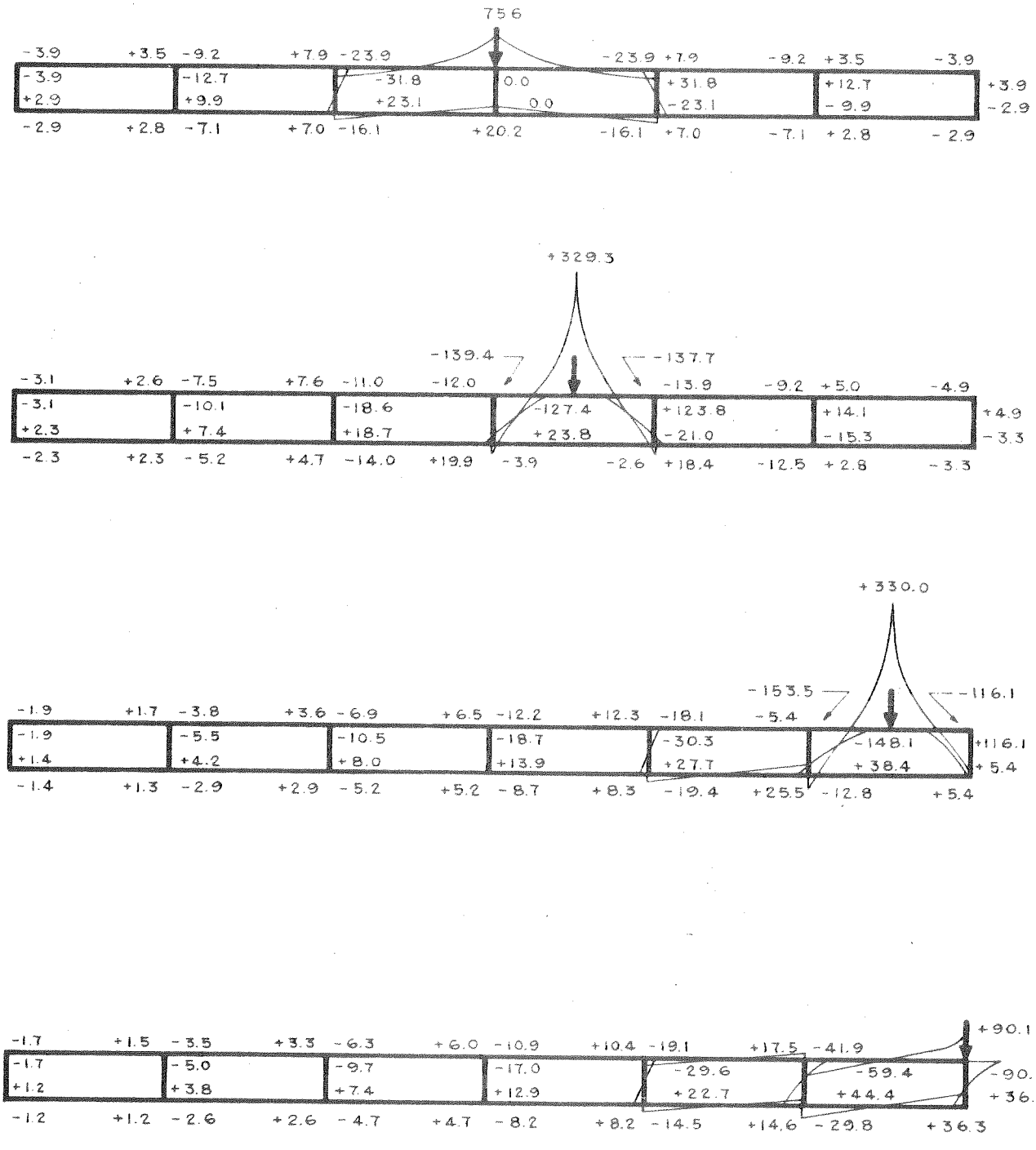

FIG. 36 TRANSVERSE DISTRIBUTION OF TRANSVERSE SLAB MOMENTS My (FT-LB/FT) AT MIDSPAN

60 FT SPAN
4 CELLS
My FT-LB/FT

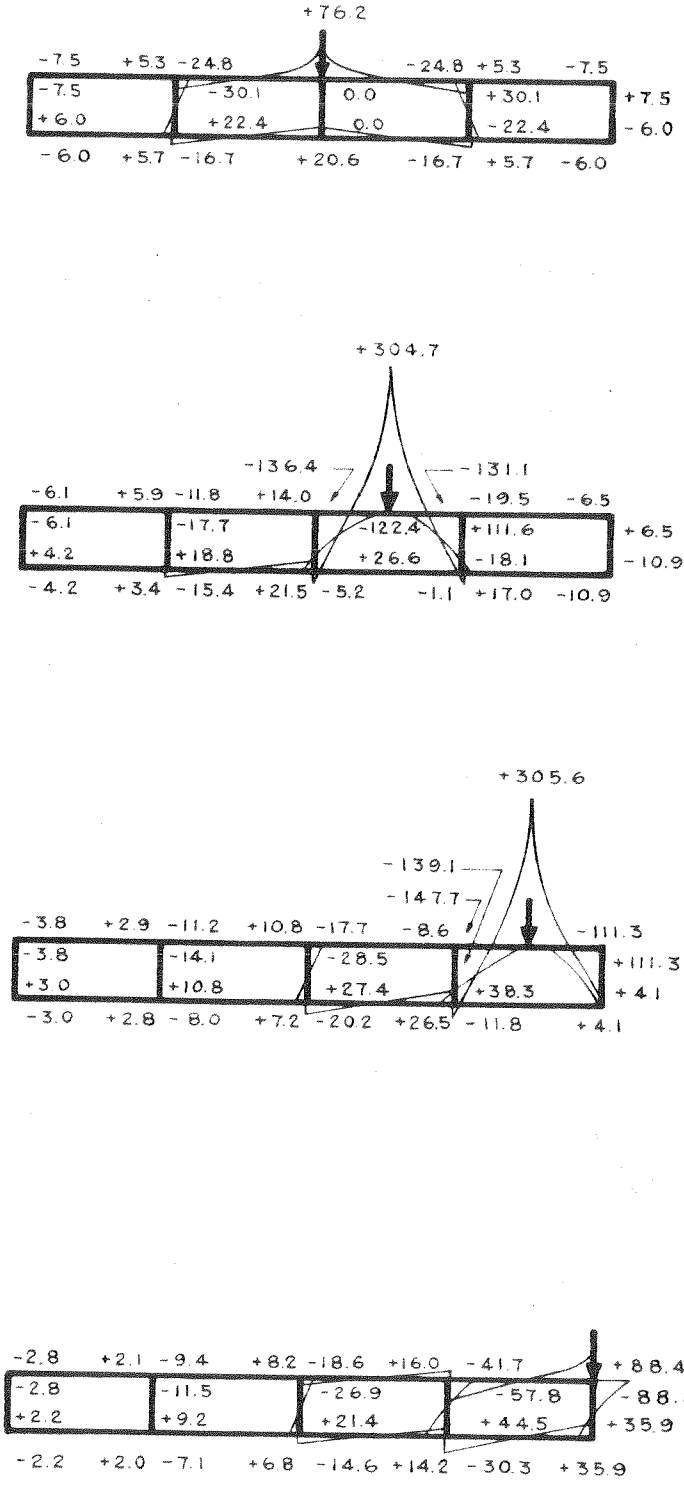

FIG. 37 TRANSVERSE DISTRIBUTION OF TRANSVERSE SLAB MOMENTS My (FT-LB/FT) AT MIDSPAN

60 FT SPAN
8 CELLS
My FT-LB/FT

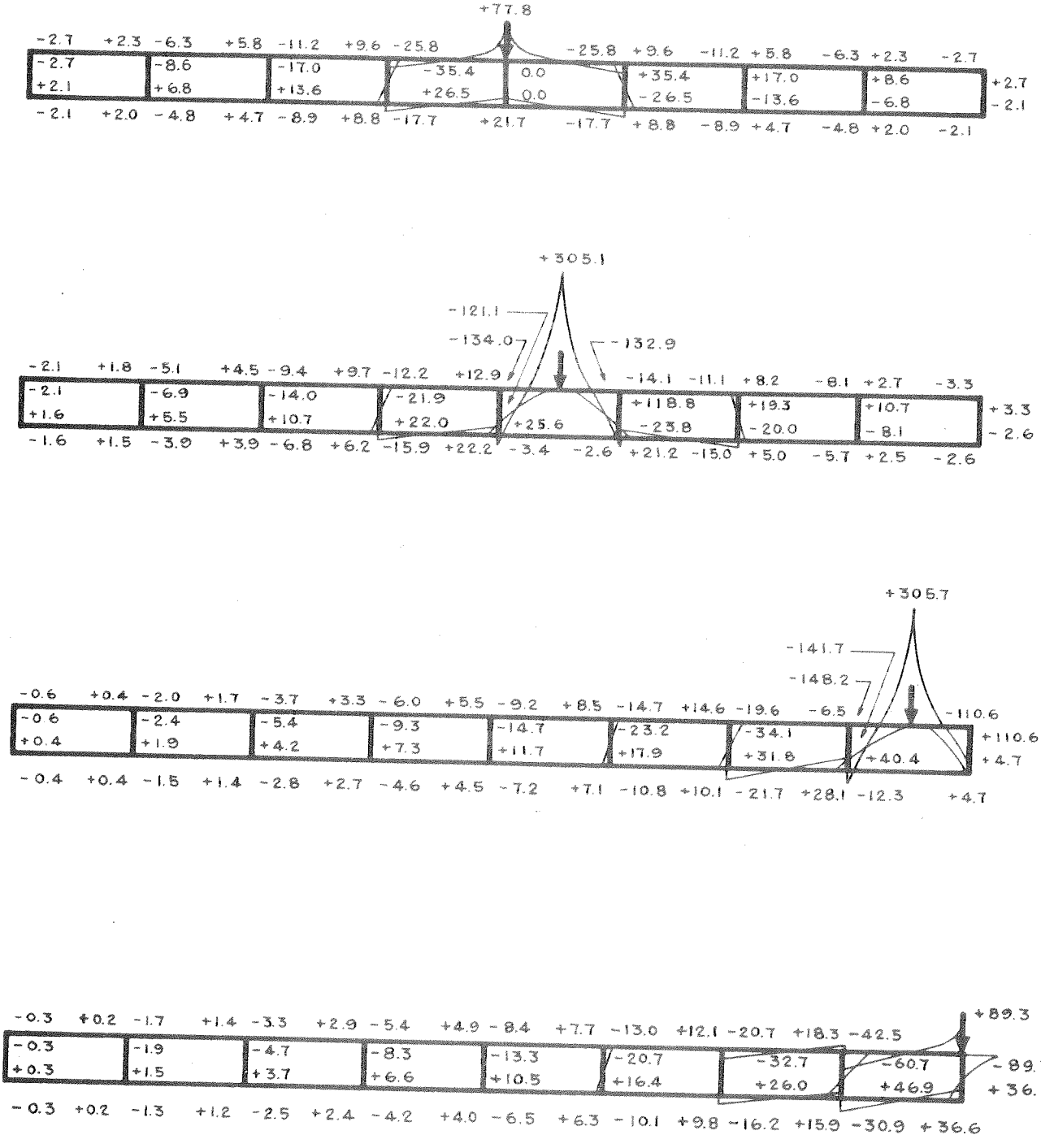

FIG. 38 TRANSVERSE DISTRIBUTION OF TRANSVERSE SLAB MOMENTS My (FT-LB/FT) AT MIDSPAN

80 FT SPAN
3 CELLS
My FT-LB/FT

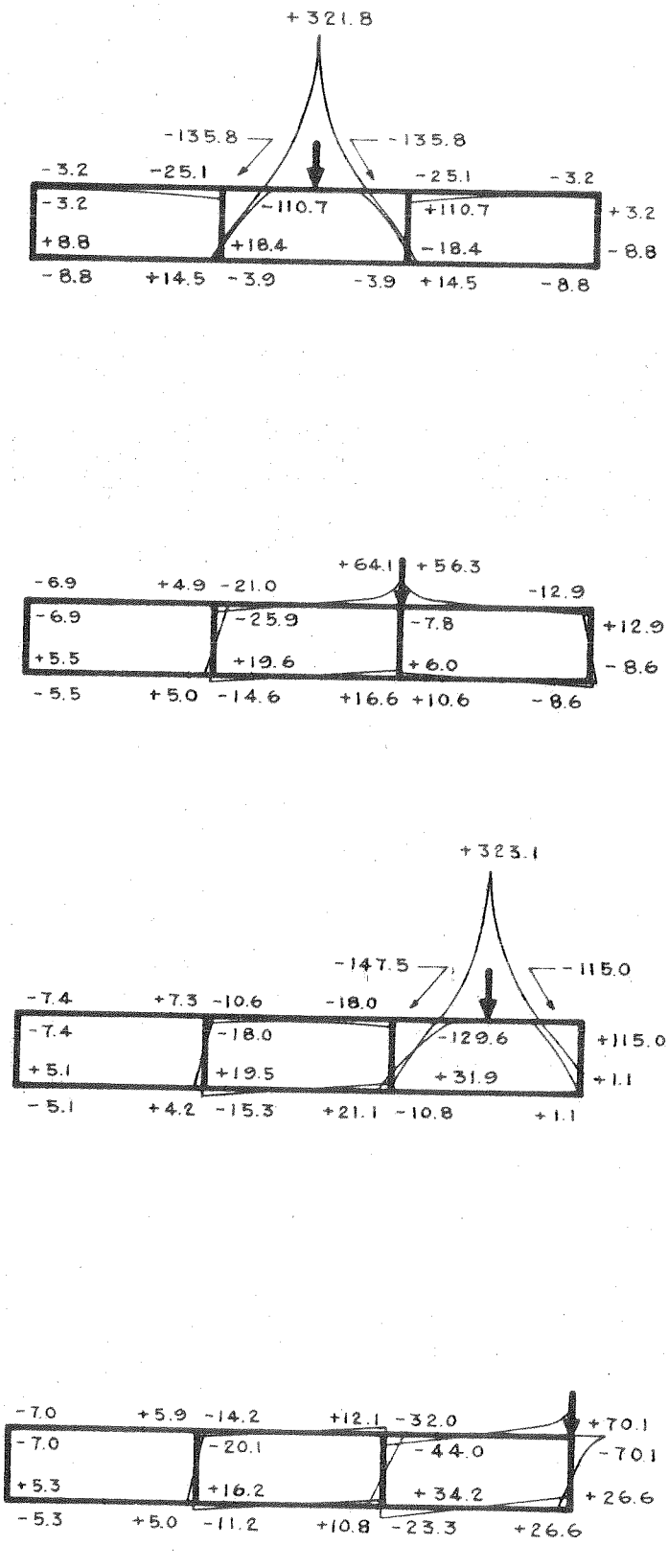

FIG. 39 TRANSVERSE DISTRIBUTION OF TRANSVERSE SLAB MOMENTS My (FT-LB/FT) AT MIDSPAN

80 FT SPAN
6 CELLS
My FT-LB/FT

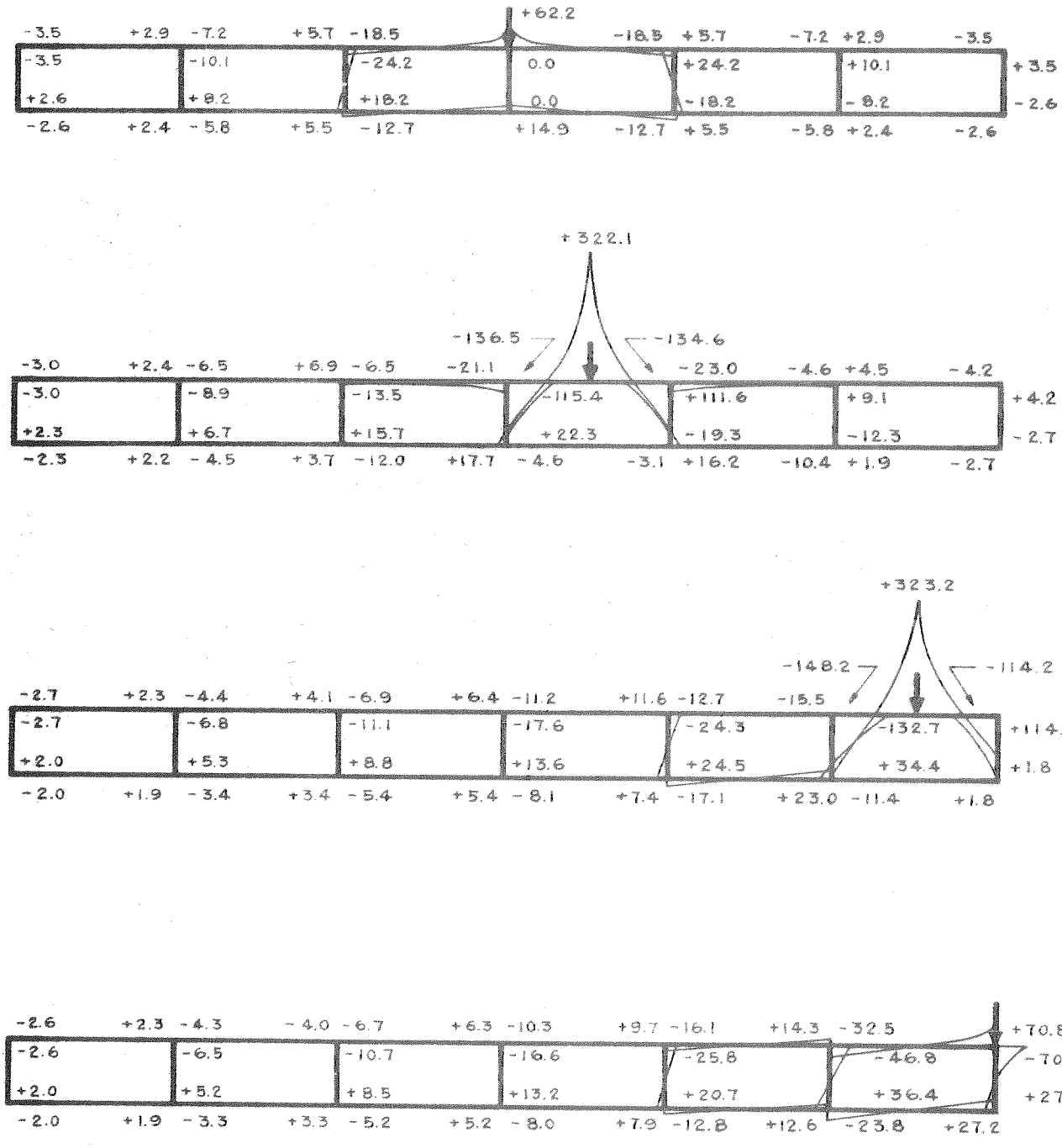

FIG. 40 TRANSVERSE DISTRIBUTION OF TRANSVERSE SLAB MOMENTS My (FT-LB/FT) AT MIDSPAN

80 FT SPAN
4 CELLS
My FT-LB/FT

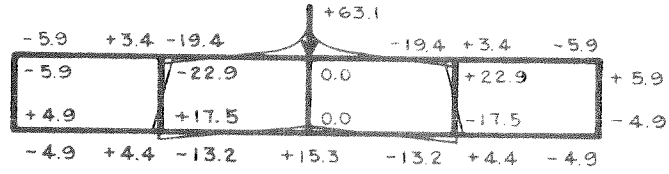

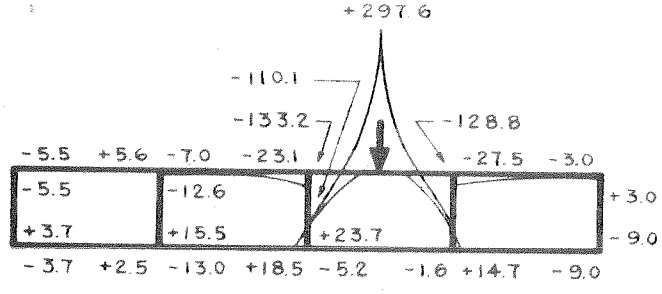

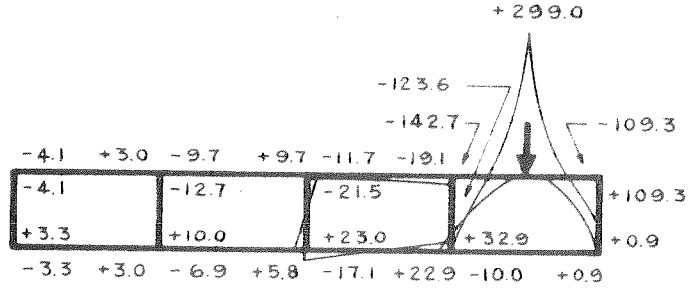

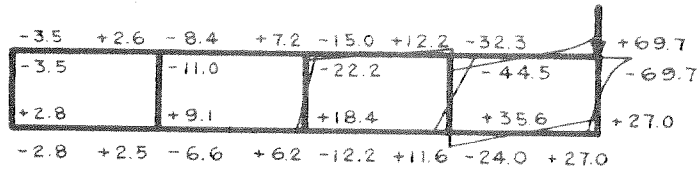

FIG. 41 TRANSVERSE DISTRIBUTION OF TRANSVERSE SLAB MOMENTS My (FT-LB/FT) AT MIDSPAN

80 FT SPAN
8 CELLS
M_y FT-LB/FT

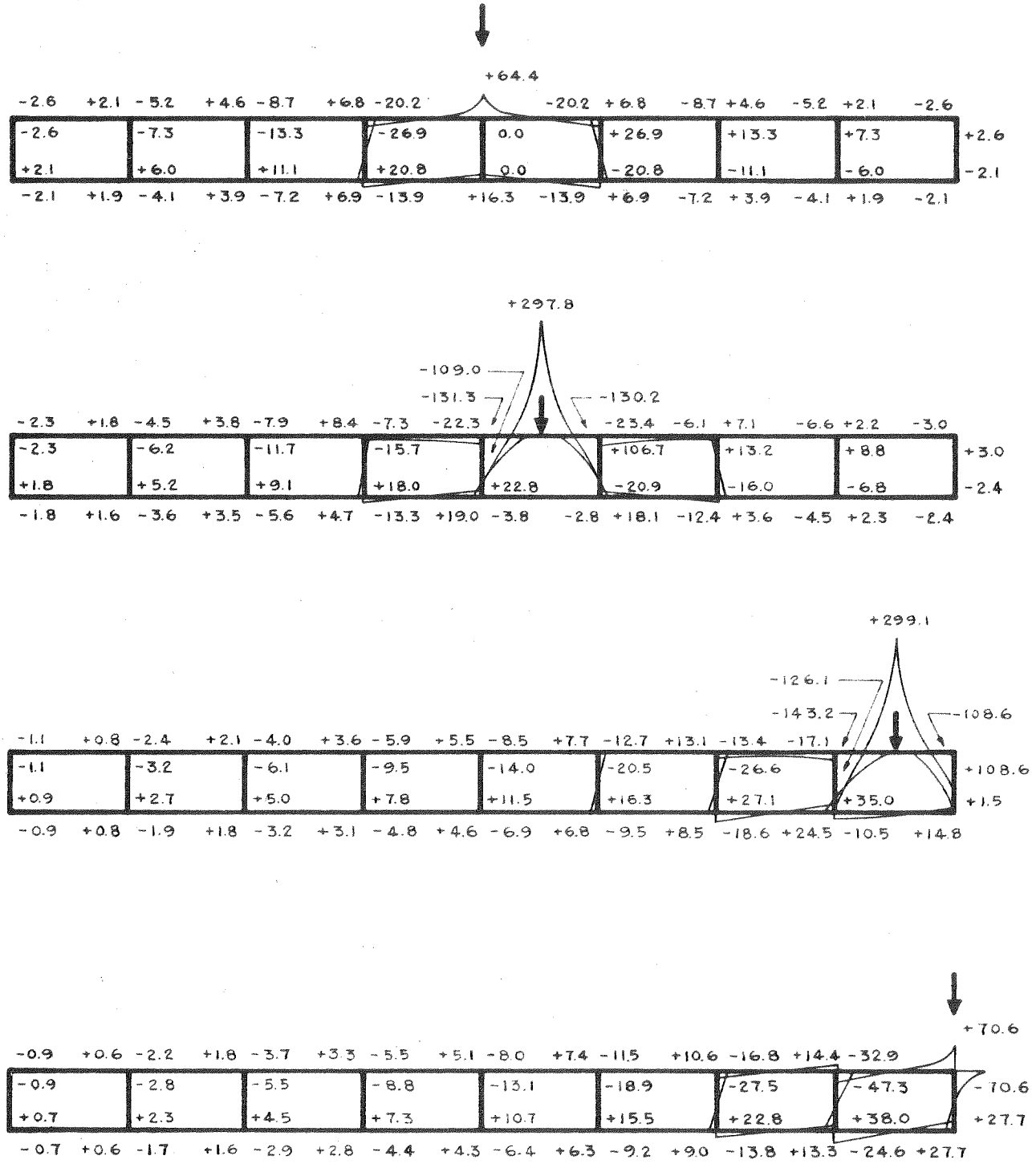

FIG. 42 TRANSVERSE DISTRIBUTION OF TRANSVERSE SLAB MOMENTS M_y (FT-LB/FT) AT MIDSPAN

60 FT SPAN
3 CELLS
M_x FT-LB/FT

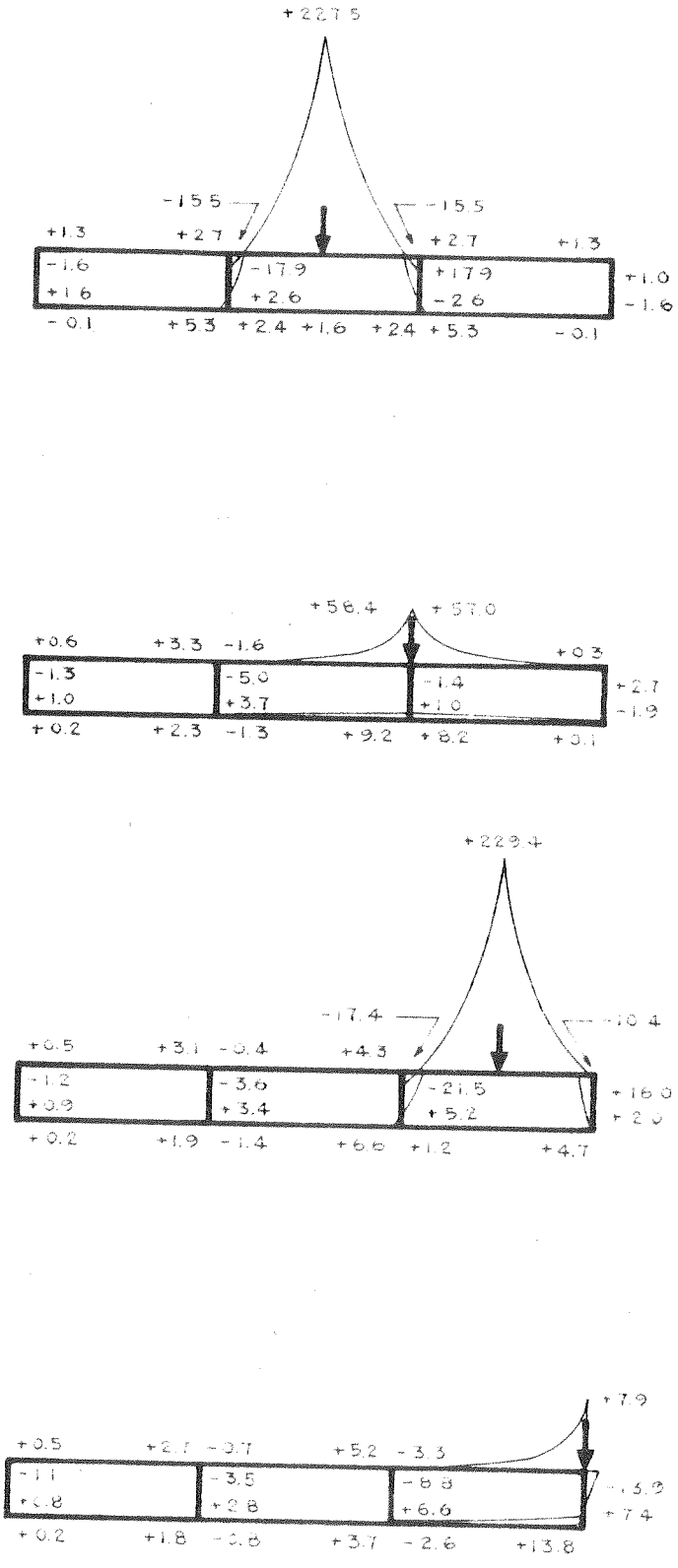

FIG. 43 TRANSVERSE DISTRIBUTION OF LONGITUDINAL SLAB MOMENTS M_x (FT-LB/FT) AT MIDSPAN

60 FT SPAN
6 CELLS
M_X FT-LB/FT

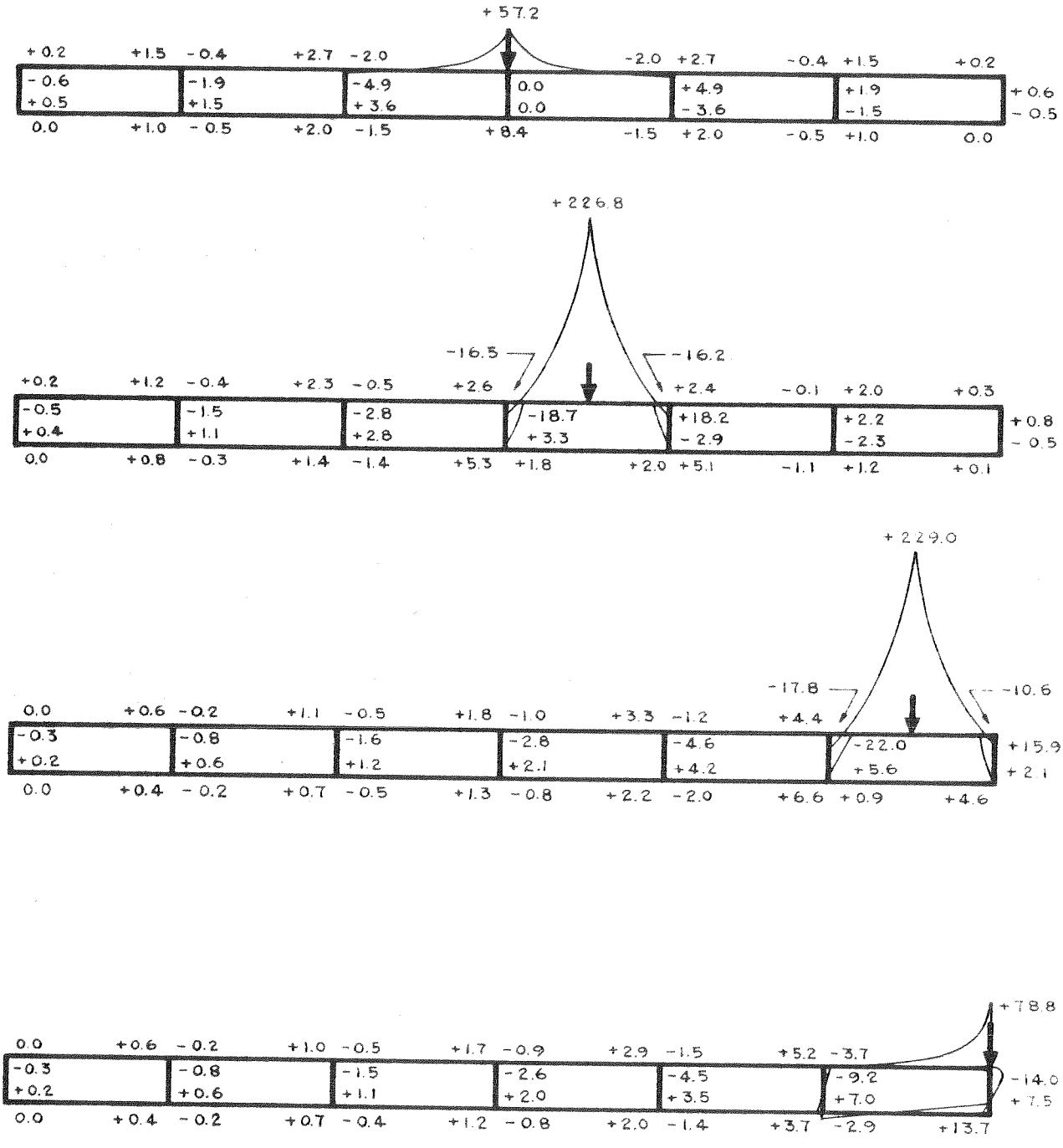

FIG. 44 TRANSVERSE DISTRIBUTION OF LONGITUDINAL SLAB MOMENTS M_X (FT-LB/FT) AT MIDSPAN

60 FT SPAN
4 CELLS
M_x FT-LB/FT

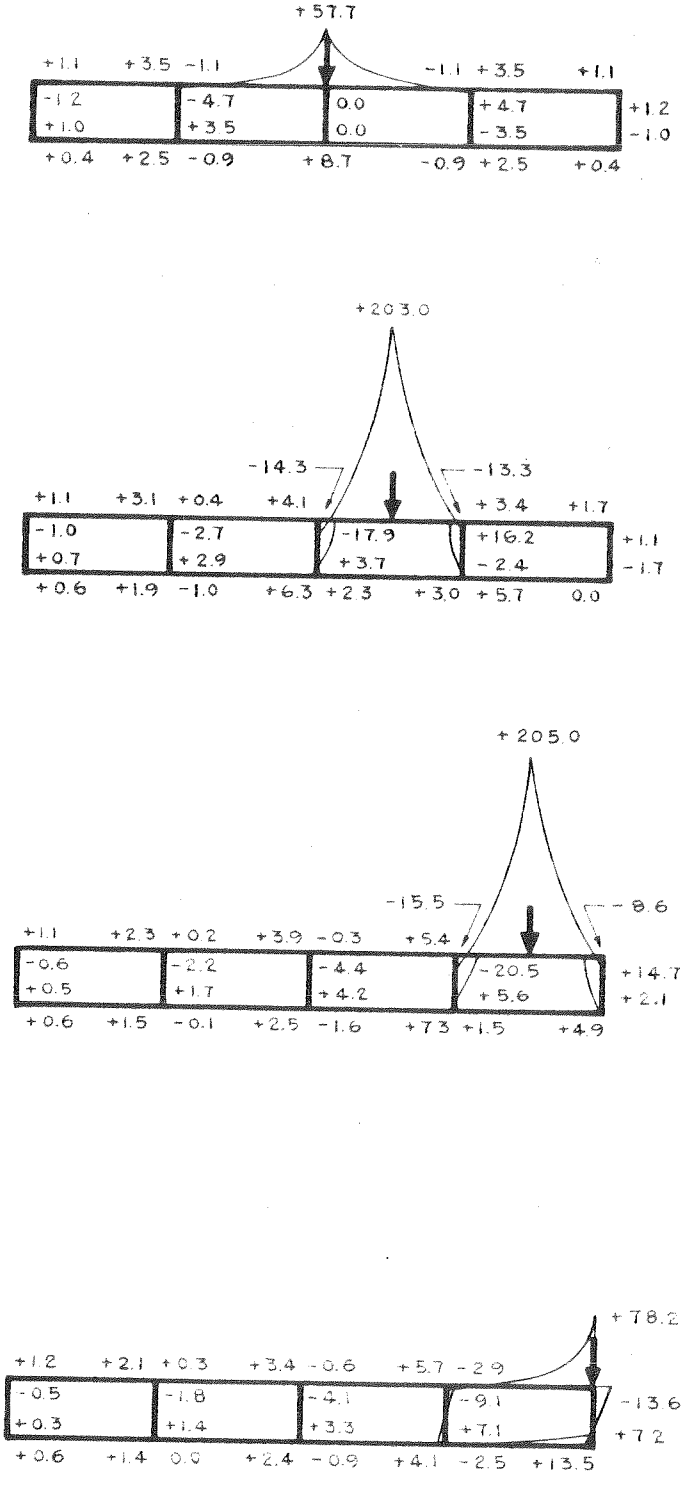

FIG. 45 TRANSVERSE DISTRIBUTION OF LONGITUDINAL SLAB MOMENTS M_x (FT-LB/FT) AT MIDSPAN

60 FT SPAN
8 CELLS
M_x FT-LB/FT

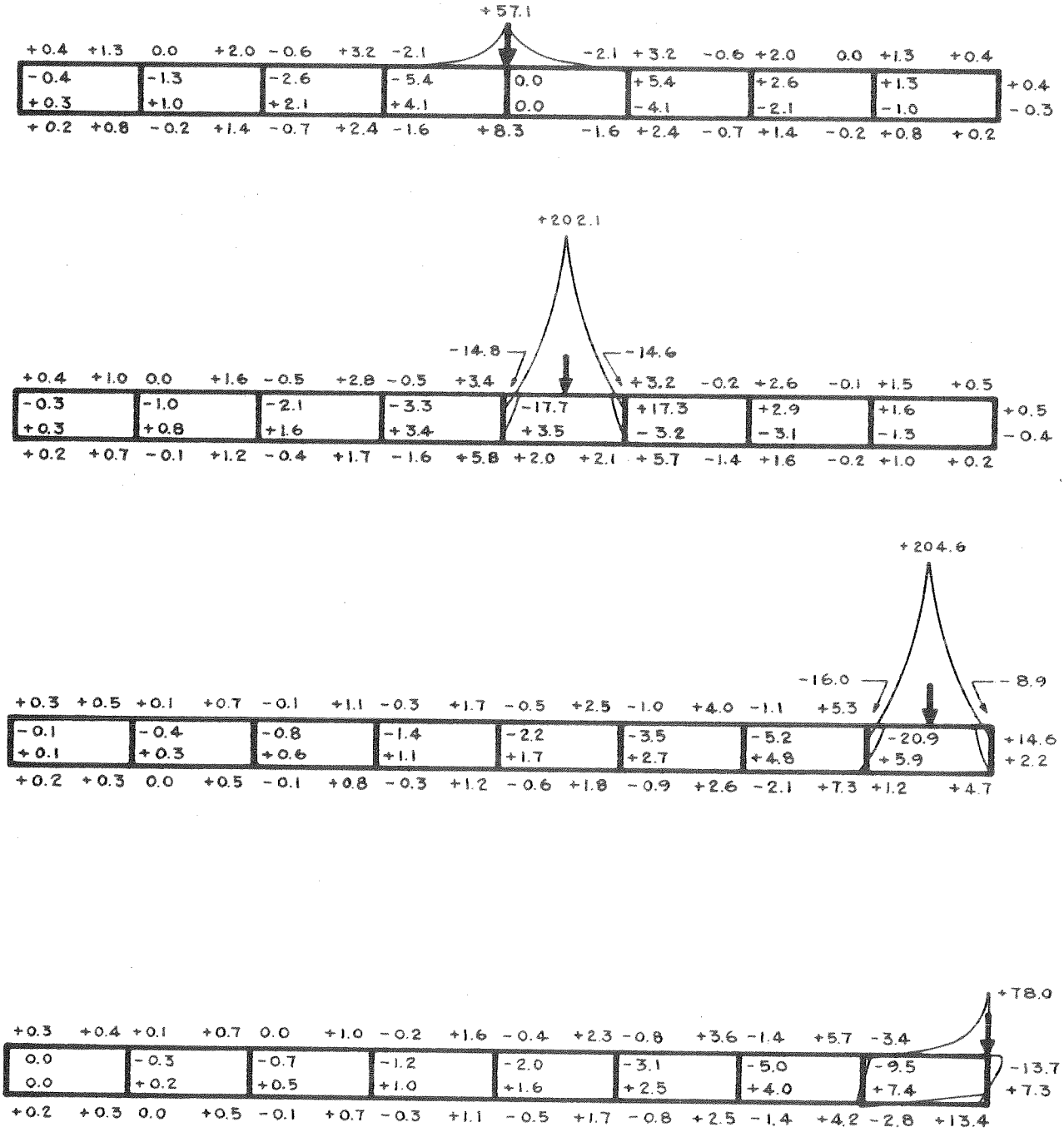

FIG. 46 TRANSVERSE DISTRIBUTION OF LONGITUDINAL SLAB MOMENTS M_x (FT-LB/FT) AT MIDSPAN

80 FT SPAN
3 CELLS
M_X FT-LB/FT

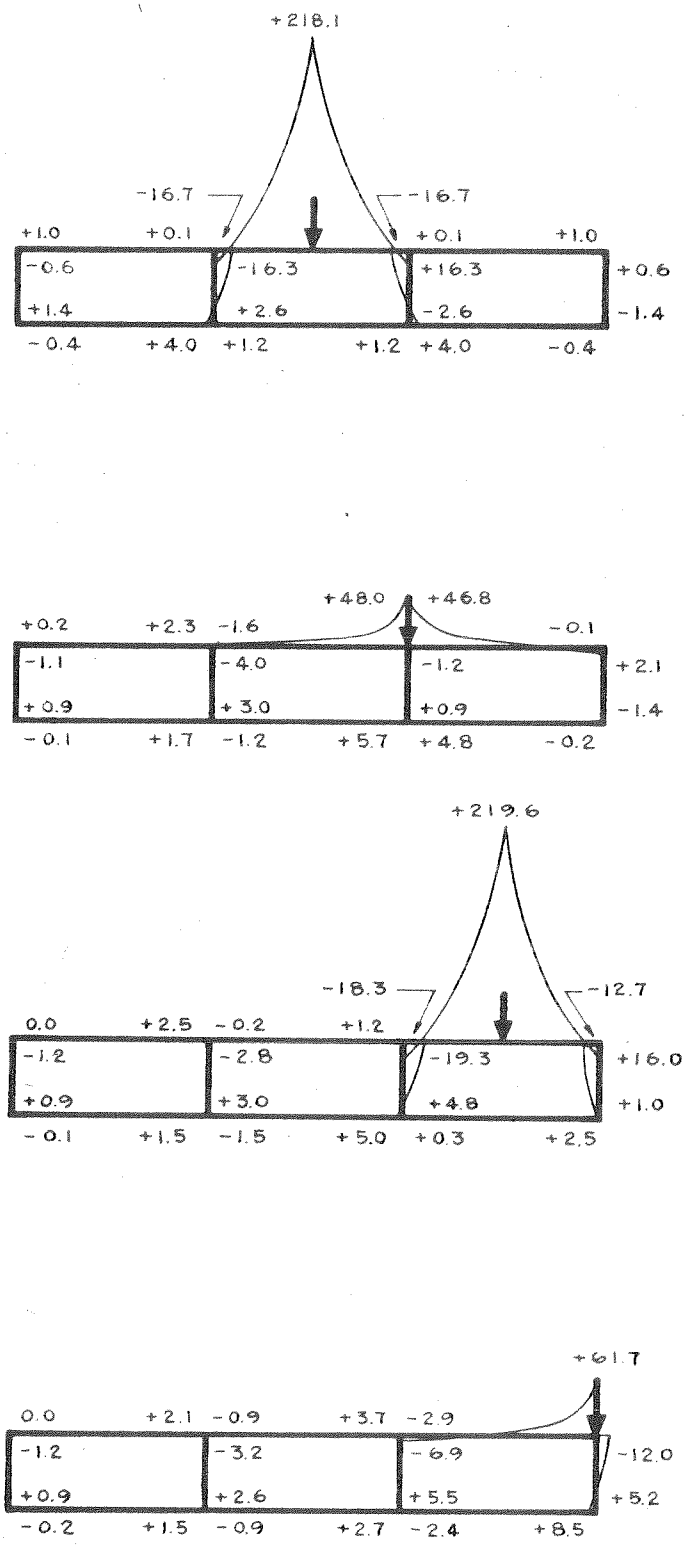

FIG. 47 TRANSVERSE DISTRIBUTION OF LONGITUDINAL SLAB MOMENTS M_X (FT-LB/FT) AT MIDSPAN

80 FT SPAN
6 CELLS
M_X FT-LB/FT

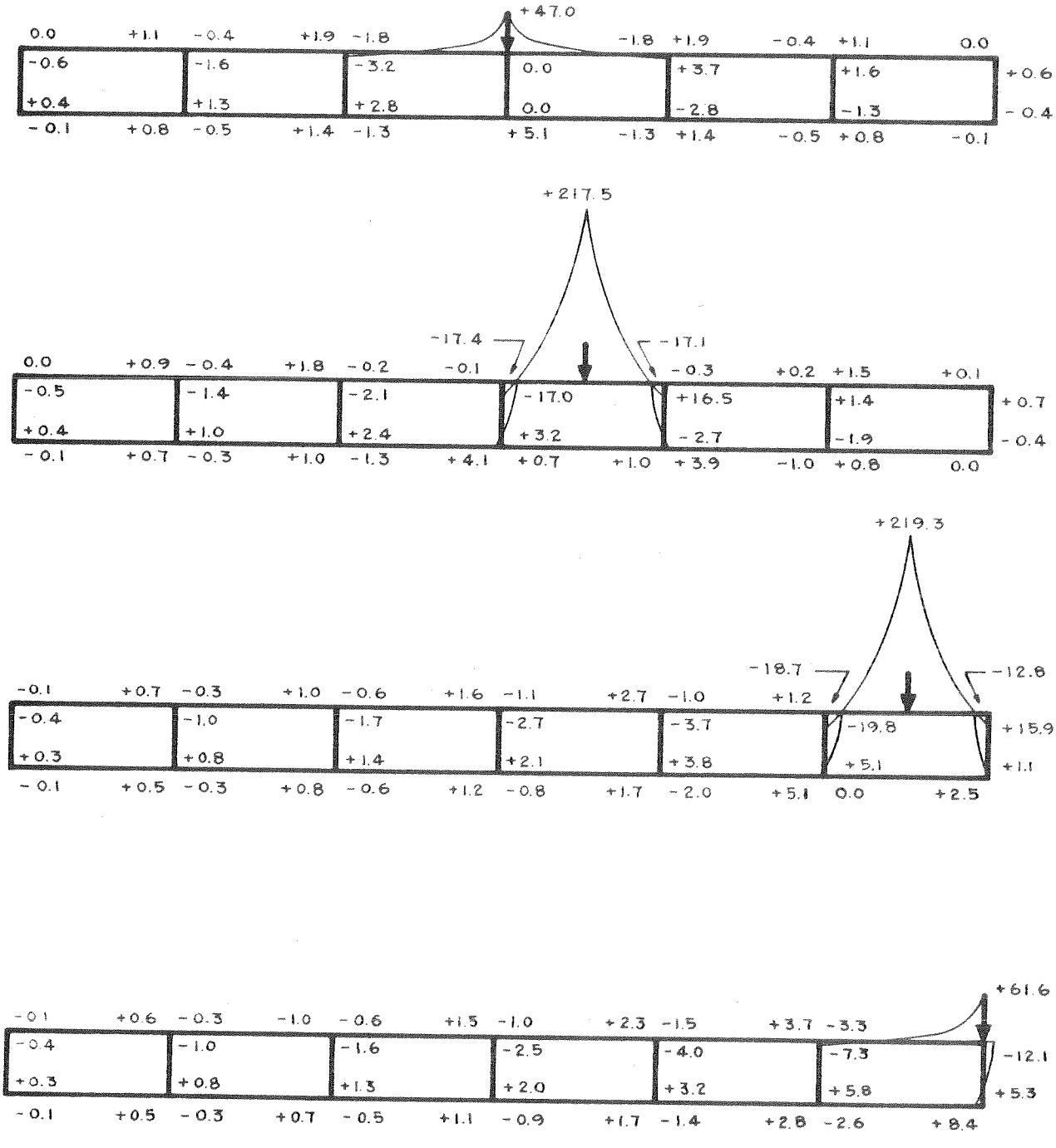

FIG. 48 TRANSVERSE DISTRIBUTION OF LONGITUDINAL SLAB MOMENTS M_X (FT-LB/FT) AT MIDSPAN

80 FT SPAN
4 CELLS
M_X FT-LB/FT

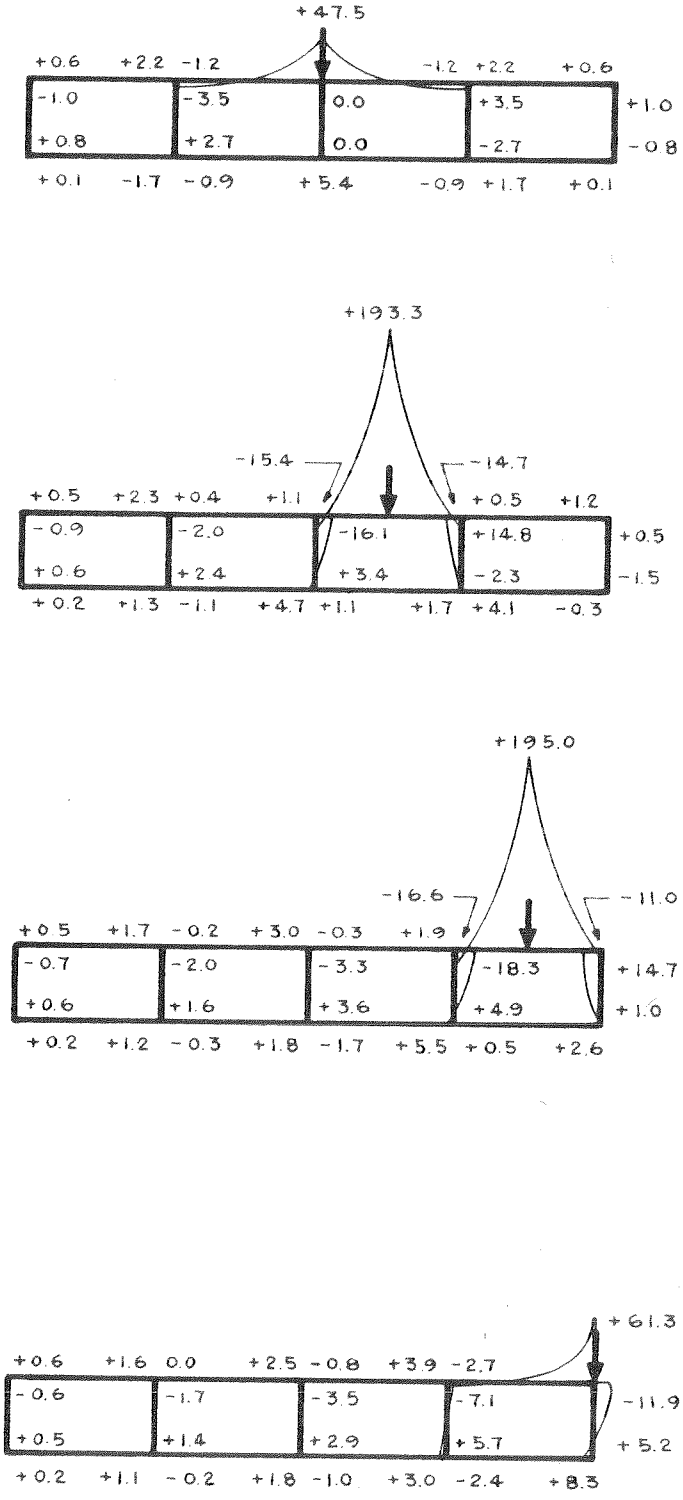

FIG. 49 TRANSVERSE DISTRIBUTION OF LONGITUDINAL SLAB MOMENTS M_X (FT-LB/FT) AT MIDSPAN

80 FT SPAN
8 CELLS
M_x FT-LB/FT

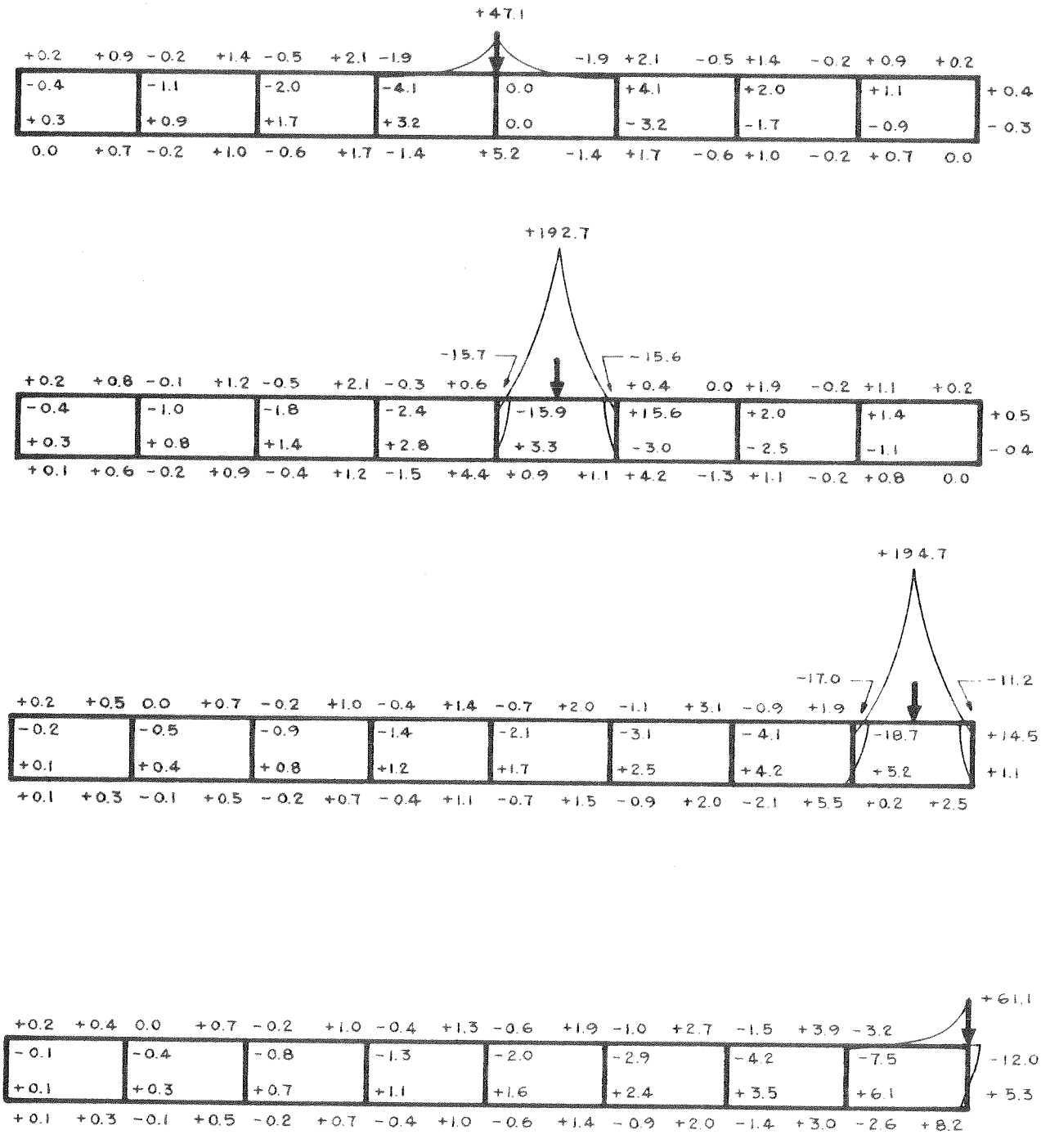

FIG. 50 TRANSVERSE DISTRIBUTION OF LONGITUDINAL SLAB MOMENTS M_x (FT-LB/FT) AT MIDSPAN

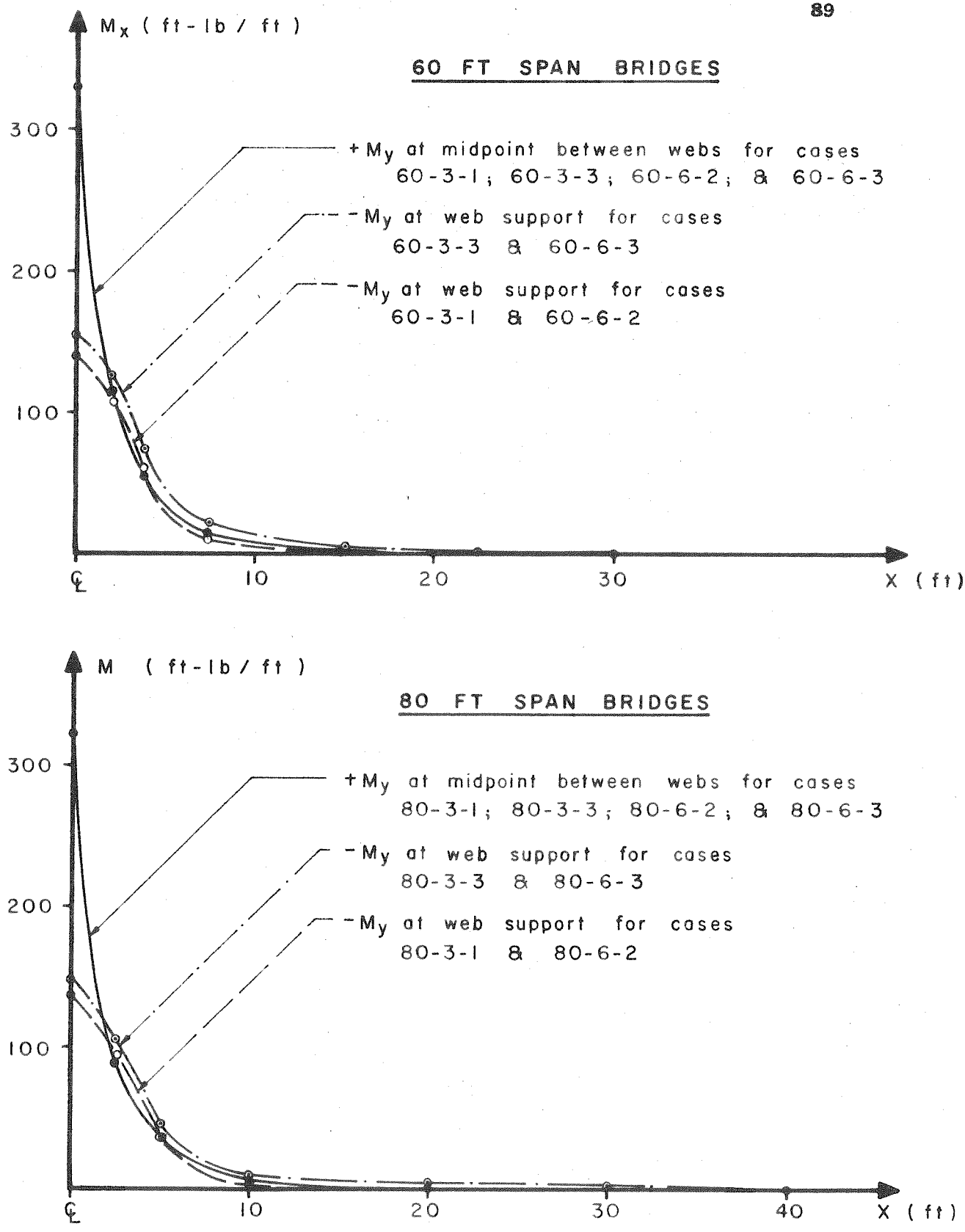

FIG. 51 LONGITUDINAL DISTRIBUTION OF TRANSVERSE SLAB MOMENTS My IN TOP SLAB

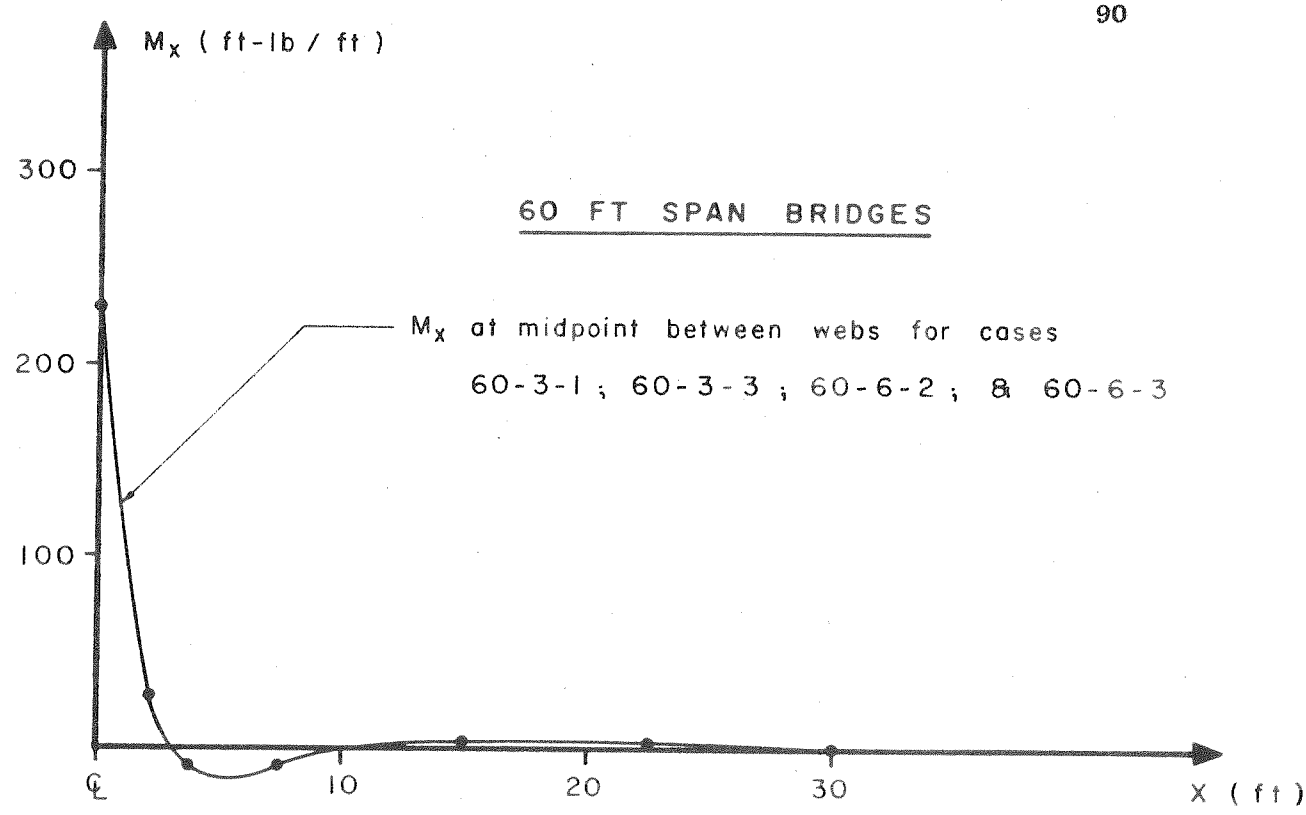

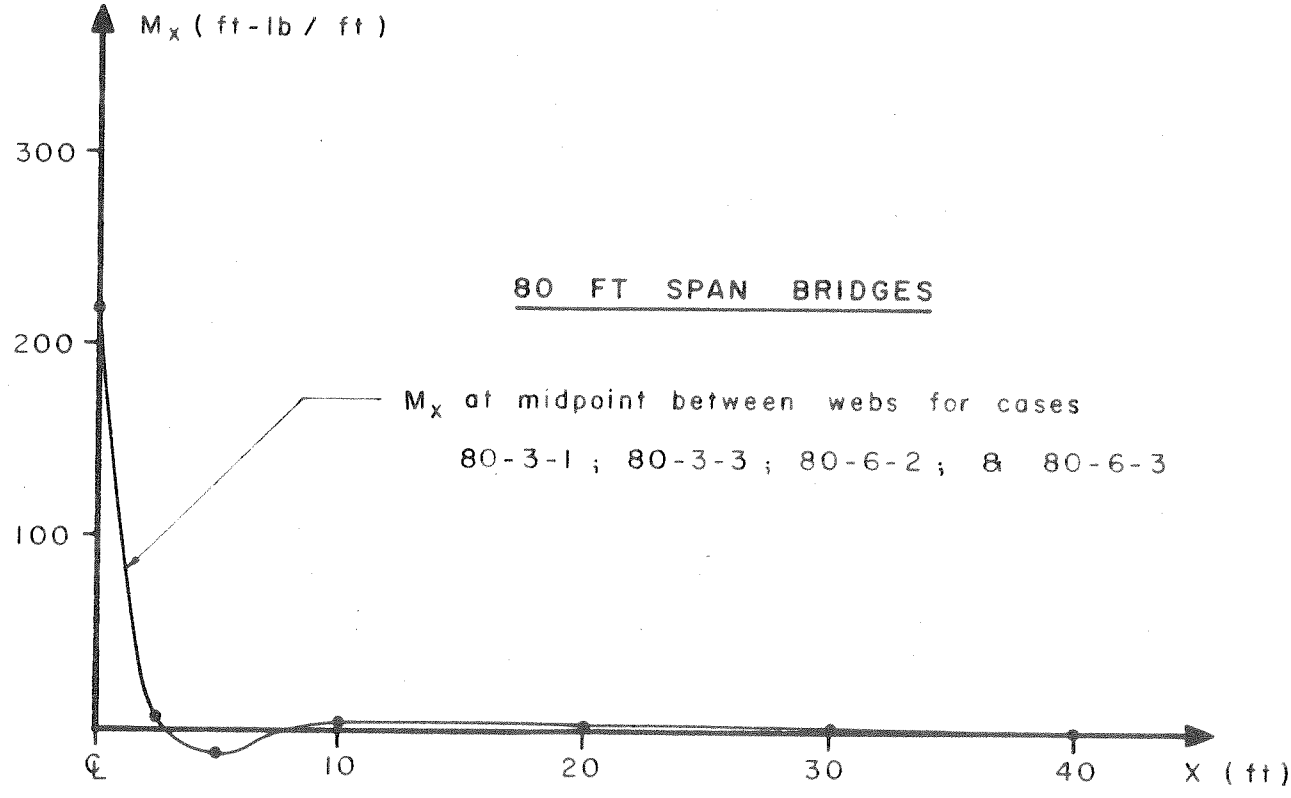

FIG. 52 LONGITUDINAL DISTRIBUTION OF LONGITUDINAL SLAB MOMENTS M_x IN TOP SLAB

60 FT SPAN
6 CELLS
σ_x PSF

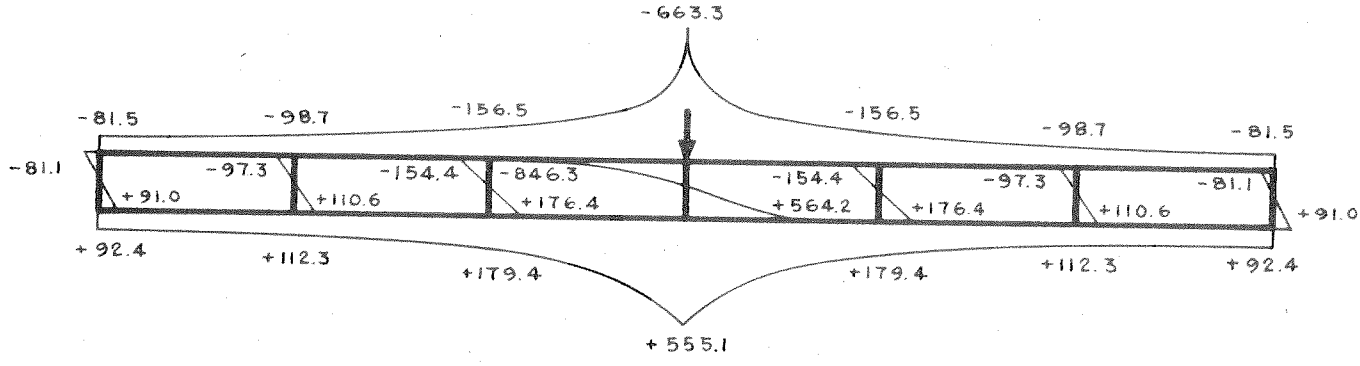

(a) CLOSED BOX WITHOUT DIAPHRAGM

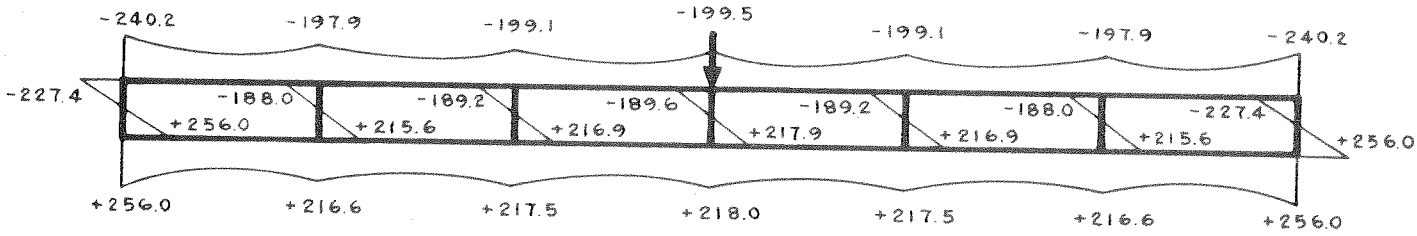

(b) CLOSED BOX WITH ONE RIGID DIAPHRAGM AT MIDSPAN

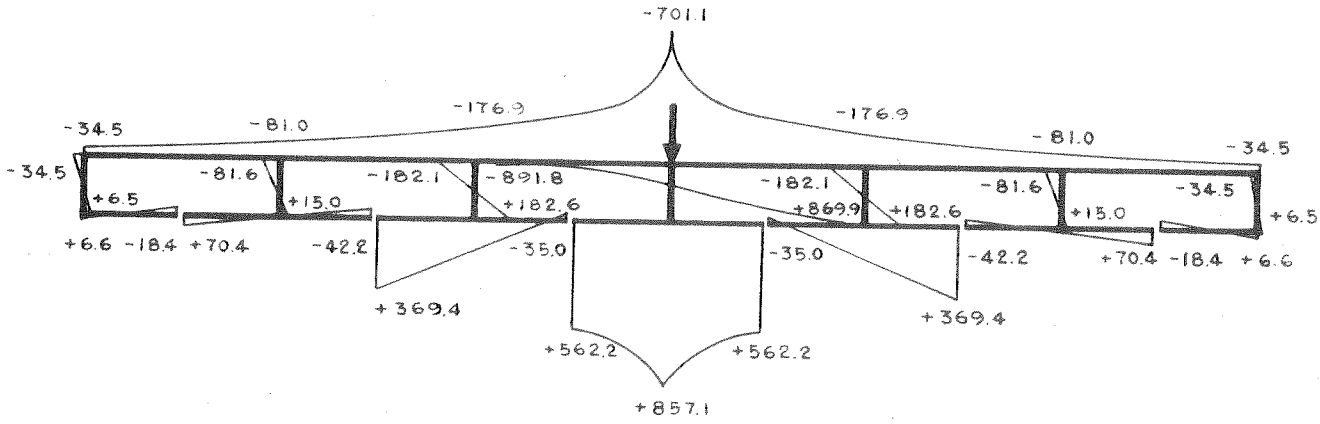

(c) BOTTOM SLAB SLICED LONGITUDINALLY AT MIDPOINT BETWEEN WEBS

FIG. 53 MIDSPAN LONGITUDINAL STRESSES σ_x (PSF) FOR LOAD OVER CENTER WEB

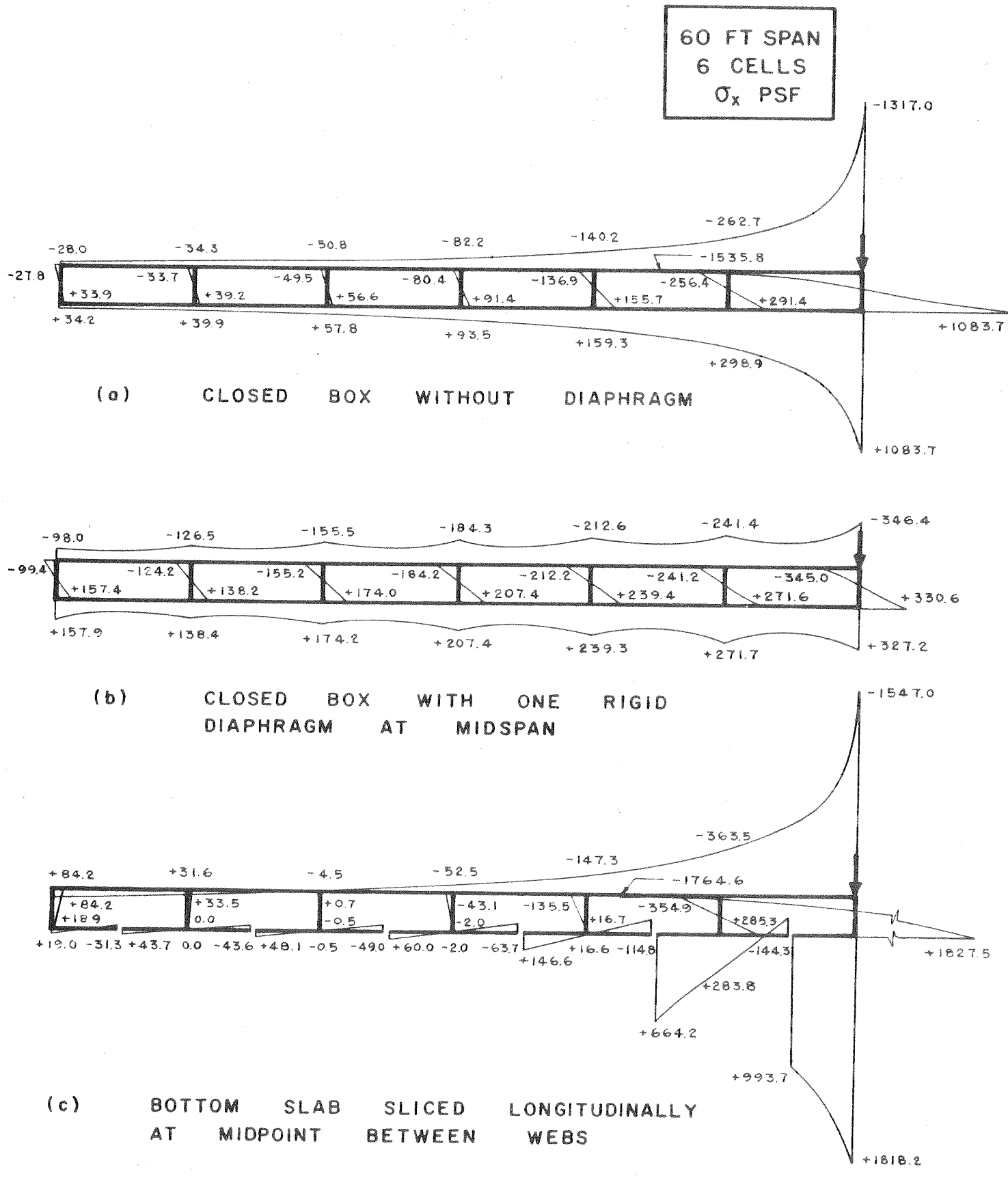

FIG. 54 MIDSPAN LONGITUDINAL STRESSES σ_x (PSF) FOR LOAD OVER EXTERIOR WEB

VII. CONCLUSIONS

A direct stiffness solution using folded plate theory and a harmonic representation of the loading has been presented which makes it possible, with the aid of a digital computer, to analyze simply supported box girder bridges with or without interior diaphragms for virtually any loading. The computer programs, MULTPL and MUPDI, developed in this investigation reduce this complex problem to a simple matter of preparing basic input data on cards, which when used with the programs will yield the detailed output of all internal forces, moments and displacements at selected points. These solutions require a relatively small amount of computer time.

From the examples and parameter studies described, it is apparent that this tool may be used in several ways. First, it may be used as a direct method for the elastic analysis of a specific bridge under a given loading, shrinkage condition, or temperature change. In this case it, and similar programs, might eventually be used to replace present semi-empirical methods used in analyzing complex bridge systems. Second, it may be used as an aid in studying the effect of different parameters on certain internal forces, moments, or load distribution properties. This use might provide a means for developing improved simplified analysis procedures similar to those presently being used for design.

Present design procedures for bridges have evolved over a long period of time and are partially the results of analytical studies, experimental studies, engineering judgement and perhaps most important of all, experience. In studying the criteria for live load distribution to girders in various types

of bridges in present specifications it is difficult from an analytical basis to justify the formulae and factors being used. No attempt has been made to make a critical evaluation of these criteria in this report, however, it is evident that the present method of basing load distribution in bridges only on the girder spacing and type of bridge is a relatively crude approach to the problem. Certainly for box girder bridges, load distribution is influenced by the number and the dimensions of cells, depth-span ratio, width-span ratio, number of diaphragms as well as other factors. Also it is apparent that a box girder bridge is inherently stiffer in a transverse direction than are slab on beam bridges which lack the same transverse continuity in the bottom flange. With the aid of new and more complete analyses using a digital computer, it is possible to obtain a more accurate determination of the load distribution properties of various bridges.

In all live load analyses, the starting point must be the number, types and positions of the vehicles which should be placed on the bridge as design loads. While this subject has received some attention in the past, it would appear that a thorough review of it should be made using modern statistical techniques to arrive at realistic and consistent design loads for all types of bridges.

The present study on box girder bridges was restricted to simply supported structures with or without interior diaphragms. Additional studies are now being conducted on continuous box girder bridges. Studies involving skew bridges, curved bridges, and bridges with plates having orthotropic properties are also being considered for the future.

VIII. ACKNOWLEDGEMENTS

This research investigation was conducted under the sponsorship of the Division of Highways, Department of Public Works, State of California, and the Bureau of Public Roads with the author as the Faculty Investigator. The opinions, findings, and conclusions expressed in this report are those of the author and not necessarily those of the Bureau of Public Roads.

Close liaison and support from the Bridge Department, Division of Highways, State of California, was provided by Mr. J. G. Standley, Supervising Bridge Engineer, Special Studies and Research Section and Mr. R. E. Davis, Senior Bridge Engineer. Their assistance is gratefully acknowledged, especially for providing the material for the review of existing box girder bridges in Chapter V and the examples of actual bridges under design described and analyzed in Chapter IV.

Mr. C. A. Meyer, Graduate Student in Civil Engineering, was responsible for the reduction of data and plotting of much of material in the parameter studies in Chapter VI. Mr. D. Ngo, Graduate Student in Civil Engineering, prepared the ink drawings of all of the figures included in the report.

Finally the author would like to express his sincere appreciation to Mr. K. S. Lo, Graduate Student in Civil Engineering, who has worked closely with the author for several years and who contributed substantially to the research program. The detailed theoretical development of the analytical methods described in Chapter III will form a portion of Mr. Lo's Ph.D. dissertation, which is presently being written under the direction of the author.

IX. BIBLIOGRAPHY

1. Hetenyi, M., "A Method for Calculating Grillage Beams," Contribution on the Mechanics of Solids, Dedicated on the 60th Birthday of S. P. Timoshenko, New York, 1938.

2. Leonhardt, F., "Die vereinfachte Berechnung zweiseitig gelagerter Trägerroste," (Simplified Analysis of Grillages Supported at Two Sides) (In German), Die Bautechnik, September 1938.

3. Leonhardt, F., and Andra, W., "Die vereinfachte Trägerrostberechnung," (Simplified Analysis of Grillages) (In German), Julius Hoffman Press, Stuttgart, 1950.

4. Pippard, A.J.S., and de Waele, J.P.A., "The Loading of Interconnected Bridge Girders," Journal of the Institution of Civil Engineers, 1938.

5. Guyon, Y., "Calcul des Ponts Larges a Poutres Multiples Solidarisees par des Entretoises," Annales Des Ponts et Chaussees, No. 24, Paris 1946.

6. Massonnet, C., "Methode de Calcul des Ponts a Poutres Multiples Tenant Compte de Leur Resistance a la Torsion," Publications, International Association for Bridge and Structural Engineering, Vol. 10, 1950.

7. Massonet, C., "Contribution au Calcul des Ponts a Pourtres Multiples," Trauvaux Publiques de la Belgique, 1950.

8. Massonnet, C., "Complements a la Methode de Calcul des Ponts a Poutres Multiples," Annales des Travaux Publiques de Belgique, No. 5, 1954.

9. Morice, P.B. and Little, G., "Load Distribution in Prestressed Concrete Bridge Systems," Journal of the Institution of Structural Engineers, March 1954.

10. Morice, P.B., and Rowe, R.E., "Load Distribution in Right Highway Bridges," Paper presented to the Fifth Congress of the International Association for Bridge and Structural Engineering, held at Lisbon, 1956.

11. Rowe, R.E., "A Load Distribution Theory for Bridge Slabs Allowing for the Effect of Poisson's Ratio," Magazine of Concrete Research, Vol. 7, No. 20, 1955.

12. Little, G., "The Distribution of a Load in a Box Section Bridge from Tests on a Xylonite Model," Magazine of Concrete Research, No. 18, December 1954.

13. Little, G., and Rowe, R.E., "Load Distribution in Multi-Webbed Bridges from Tests on Plastic Models," Magazine of Concrete Research, No. 21, November 1955.

14. Morice, P.B., "The Minimum Transverse Strength of Slab Bridges," Magazine of Concrete Research, No. 23, August 1956.

15. Rowe, R.E., "Load Distribution in Bridge Slabs," Magazine of Concrete Research, No. 27, November 1957.

16. Hendry, A.W., and Jaeger, L.G., "A General Method for the Analysis of Grid Frameworks," Proceedings, Part III, Institution of Civil Engineers, December 1955.

17. Hendry, A.W. and Jaeger, L.G., "The Load Distribution in Interconnected Bridge Girders with Special Reference to Continuous Beams," Publications, International Association for Bridge and Structural Engineering, Vol. XV, 1955.

18. Hendry, A.W. and Jaeger, L.G., "The Analysis of Interconnected Bridge Girders by the Distribution of Harmonics," Journal of the Institution of Structural Engineers, July 1956.

19. Hendry, A.W. and Jaeger, L.G., "The Load Distribution in Highway Bridge Decks," Proceedings, American Society of Civil Engineers, July 1956.

20. Hendry, A.W. and Jaeger, L.G., "The Analysis of Grid Frameworks and Related Structures," Publishers, Chatto and Windus, London 1958.

21. Niles, A.S. and Newell, J.S., "Airplane Structures," John Wiley and Sons Inc., New York, N.Y., 3rd Edition, 1943.

22. Bruhn, E.F., "Analysis and Design of Airplane Structures," John S. Swift and Co., Cincinnati, Ohio, 1943.

23. Neiman, A.S., "Shearing Stress Distribution in Box Girders with Multiple Webs," Trans. ASCE, Vol. 114, 1949, pp. 162-180.

24. "Phase I Report on Folded Plate Construction," Task Committee on Folded Plate Construction, Journal of the Structural Division, ASCE, Vol. 89, No. ST6, Proc. Paper 3741, December 1963, pp. 365-406.

25. Goldberg, J.E., and Leve, H.L., "Theory of Prismatic Folded Plate Structures," IABSE, Zurich, Switzerland, No. 87, 1957, pp. 59-86.

26. DeFries-Skene, A., and Scordelis, A.C., "Direct Stiffness Solution for Folded Plates," Journal of the Structural Division, ASCE, Vol. 90, No. ST4, Proc. Paper 3994, August 1964, pp. 15-47.

27. Davis, R.E., J.J. Kozak, C.F. Scheffey, "Structural Behavior of Concrete Box Girder Bridge," Nat. Research Council-Highway Research Board-Research Rec. No. 76, 1965, p. 32-82.

28. Drew, F.P., "Studies of Box Beams for Railway Bridges," PCI-Journal, Vol. 10, No. 3, June 1965, p. 46-51.

29. Hass, B., "Die vereinfachte Berechnung der Lastverteilung sehr drillsteifer Brücken (Hohlkästen) (Simplified Calculation of Load Distribution in Box-Type Bridges with High Torsional Rigidity) (in German), Bauingenieur, V. 40, No. 4, April 1965, p. 166-8.

30. Itoh, F., "Stresses of Box Girder and Deck Plate Girder in Torsion Bending," Tokyo, Ry. Tech. Research Inst., Quarterly Report V. 4, No. 3, Sept. 1963, p. 3-7.

31. Studzinski, S.H., "Some Examples of Box Girder Bridges in California," Structural Engineer, Vol. 41, No. 8, Aug. 1963, p. 253-7.

32. Sakurai, S., K. Ito, M. Naruoka, "Experimental Study on Multi-Cell Structures," Japan Soc. Civ. Engrs - Trans. No. 87, Nov. 1962, p. 1-8, (in Japanese with English Abstract).

33. Swamy, N., "Behavior and Ultimate Strength of Prestressed Concrete Hollow Beams in Bending," Instit. Engineers (India) - Journal, Vol. 43, No. 1, Pt CI 1, Sept. 1962, p. 27-50.

34. Zaslavsky, A., "Shearing Stresses in Box-Section Beams with One Axis of Symmetry and in Multicell Sections," Israel Research Council - Bull. Sec. C, Technology, V. 11C, No. 3, Oct. 1962, p. 265-74.

35. Gifford, F.W., "Test on Prestressed Concrete Hollow-Box Bridge Deck," Magazine of Concrete Research, V. 13, No. 39, Nov. 1961, p. 149-56.

36. Heilig, R., "Beitrag zur Theorie der Kastenträger beliebiger Querschnittsform," (Extension of Theory of Closed Box Girders of any Cross Section), (in German). Stahlbau, V. 30, No. 11, Nov. 1961, p. 333-49.

37. Homberg, H., W.R. Marx, N. Zahlten, "Modelluntersuchung an einem schiefen Kasten" (Model Investigation of a Skewed Box Member) (in German). Bautechnik, V. 38, No. 4, April 1961, p. 118-23.

38. Laszlo, F. and N. Nolle, "On Torsional Stiffness of Box Girder Sections," Structural Engineer, V. 39, No. 5, May 1961, p. 163-73.

39. Walker, B.A., "Distribution of Shear Stress in Box Beam," Engineer, V. 209, No. 5448, June 24, 1960, p. 1067-9.

40. Clymer, A.B., "Operational Analog Simulation of Vibration of Beam and Rectangular Multicellular Structure," IRE-Trans. on Electronic Computers, V.EC-8, No. 3, Sept. 1959, p. 381-391.

41. Kubitzki, H.H., "Biege und Verdrehbeanspruchung unsymmetrischer Kastenträger, (Flexural and Torsional Stresses in Unsymmetrical Box Girders) (in German). Technische Mitteilungen, Krupp, V. 17, No. 5, Dec. 1959, p. 207-29.

42. Saeckel, R., "Beitrag zur Spannungsverteilung in Kastenprofilen gekrümmter Träger," (Stress Distribution in Box Sections of Curved Beams) (in German), Dresden, Hochschule für Verkehrswesen, Wissenschaftliche Zeit, V. 7, No. 1, 1959-60, p. 173-83.

43. "Highway Bridge of Light-Gauge Aluminum Cellular Construction," Engineer, V. 207, No. 5385, Apr. 10, 1959, p. 592-4.

44. Esslinger, M., "Deformationen und Spannungen eines torsionsbeanspruchten Kastenträgers," (Deformation and Stresses of Box Beam in Torsion) (in German) Stahlbau, V. 25, No. 7, July 1956, p. 164-6.

45. Jaeger, K., "Stahlbeton-Brückenträger mit mehrzelligem Kastenquerschnitt," (Reinforced Concrete Bridge Girder with Multicell Box-Section), (in German). Österreichische Bauzeitschrift, V. 11, No. 2, Feb. 1956, p. 17-25.

46. Morandi, R. and F. Piccinin, "Two Prestressed Bridges with Hollow Girders of Precast Vacuum Treated Elements," Journal of ACI, Vol. 52, No. 46, March 1956, p. 757-66.

47. Preston, H.K., "Design of Prestressed Hollow-Box Girder Bridges," Eng. News Rec., Vol. 157, No. 26, Dec. 27, 1956, p. 34-6.

48. Benscoter, S.U., "Theory of Torsion Bending for Multicell Beams," Am. Soc. of Mech. Engrs. (Journ. Appl. Mech.) V. 21, No. 1, March 1954, p. 25-34.

49. Chapman, J.C., "Behavior in Pure Bending of Box Girders," Engineer, V. 198, No. 5143, Aug. 20, 1954, p. 253-7.

50. Mueller, P., "Torsion von Kastenträgern mit elastisch verformbarem symmetrischem Querschnitt," (Torsion of Box Girders with Elastic Symmetrical Deformable Sections), (in German). Schweizer Bauzeitung, V. 71, No. 46, Nov. 14, 1953, p. 673-6.

51. "Long Box Girder Bridge Combines Concrete and Steel," Eng. News Rec., V. 148, No. 2, Jan. 10, 1952, p. 42.

52. Foley, E.R., and G.D. Gilbert, "Box Girder on Single Columns Supports Curved Bridge Deck," Eng. News Rec. Vol. 140, No. 24, June 10, 1948, p. 942-4.

53. Williamson, R.A., "Torsion-Bending Stresses in Box Beams," J. Aeronautical Sciences, V. 15, No. 7, July 1948, p. 427-34.

54. Kempner, F., "Recurrence Formulas and Differential Equations for Stress Analysis of Cambered Box Beam," Nat. Advisory Committee Aeronautics-Tech. Note No. 1466, Oct. 1947.

55. Kruszewski, E.T., "Bending Stresses Due to Torsion in Tapered Box Beams," Nat. Advisory Committee Aeronautics, Tech. Note No. 1297, May 1947.

56. Reissner, E., "Analysis of Shear Lag in Box Beams by Principle of Minimum Potential Energy," Brown Univ. - Quarterly Appl. Math., V. 4, No. 3, Oct. 1946, p. 268-78.

57. "Box Members Distinguish Concrete Bridge," Eng. News Rec., V. 136, No. 26, June 27, 1946, p. 996-7.

58. Newton, R.E., "Shear Lag and Torsion Bending of Four-Element Box Beams," Journ. of Aeronautical Sciences, V. 12, No. 4, Oct. 1945, p. 461-7.

59. E. Gruber, "Hohlträger als Faltwerke," (Box-Girders as Folded Plate Structures), (in German), Abh. I.V.B.H. Band VII, Zurich, 1944.

60. Kuhn, P. and P.T. Chiarito, "Shear Lag in Box Beams Methods of Analysis and Experimental Investigations," Nat. Advisory Committee Aeronautics Report No. 739, 1942.

61. Reissner, E., "Note on Some Secondary Stresses in Thin-Walled Box Beams," Journ. Aeronautical Sciences, V. 9, No. 14, Dec. 1942, p. 538-42.

62. "Curved Box Girders for Highway Overpass," Eng. News Rec., V. 129, No. 21, Nov. 19, 1942, p. 698-9.

63. Murray, V.S., "Long-Span Box-Girder Grade-Separation Bridges for Queen Elizabeth Way Extension," Roads and Bridges, V. 79, No. 4, Apr. 1941, p. 15-7.

64. Panhorst, F.W., "How Cellular Concrete Bridge Acts Under Traffic," Eng. News Rec., V. 126, No. 25, June 19, 1941, p. 941-3.

65. Hadley, H.M., "Precast Box Beams for High Strength," Eng. News Rec., V. 125, No. 25, Dec. 19, 1940, p. 838-9.

66. Minelli, C., "Sulle travi a cassone sottoposte a torsione," (Theoretical Mathematical Discussion of Stresses and Strains in Box Beams Subjected to Torsion, Computation of Stresses in Diaphragm of Box Beams), (in Italian). Richerche di Ingegneria, V. 7, No. 5, Sept-Oct. 1939, p. 143-7,

67. Cambilargiu, E., "Berechnung der Verdrehung kastenförmiger Träger, denen eine Wand fehlt," (Torsion of Box Beams with One Side Lacking, Nat. Advisory Committee Aeronautics, Tech. Memo No. 939, Apr. 1948), (in German). Luftfahrtforschung, V. 16, No. 8, Aug. 20, 1939, p. 403-11.

68. Clough, R.W., Wilson, E.L., and King, I.P., "Large Capacity Multistory Frame Analysis Programs," Journal of the Structural Division, ASCE, Vol. 89, No. ST4, Proc. Paper 3592, August 1963, p. 179.

69. Timoshenko, S. and Woinowsky-Krieger, S., "Theory of Plates and Shells," 2nd Ed., New York, McGraw-Hill, 1959.

70. "Manual of Bridge Design Practice," State of California, Department of Public Works, Division of Highways, Bridge Department, 2nd Ed., 1963.

71. Lo, K.S., "Analysis of Cellular Folded Plate Structures," Thesis under preparation to be presented to the University of California, Berkeley, in January 1967 in partial fulfillment of the requirements for the degree of Doctor of Philosophy.

APPENDIX A

Description of IBM 7094 Computer Program for Analysis of Simply Supported Cellular Folded Plate Structures (MULTPL).

UNIVERSITY OF CALIFORNIA
October 1965

Department of Civil Engineering
Faculty Investigator: A. C. Scordelis

IBM 7094 Computer Program for Analysis of Simply Supported Cellular Folded Plate Structures

IDENTIFICATION

MULTPL - Analysis of Cellular Folded Plate Structures by the Elasticity Method
Programmed by: Kam-Shing Lo
University of California, October 1965

PURPOSE

The program provides a rapid solution for cellular or open folded plate structures having simple spans. Uniform or partial surface loads as well as line loads and concentrated loads may be applied anywhere on the structure and the resulting joint displacements together with the internal forces, moments and displacements in each plate element at selected points may be found.

RESTRICTIONS

Restrictions as to the maximum number of plates, joints, loads, etc. are given under input data.

DESCRIPTION

The computer solution uses a direct stiffness method for the analysis. The Goldberg-Leve equations are used to evaluate plate fixed edge forces, stiffnesses, and final internal forces, moments and displacements. A harmonic analysis with up to 100 non-zero terms of the appropriate Fourier Series is used for the loads. The program is written in FORTRAN IV language.

FORM OF INPUT DATA

A. Input data is key punched on data cards. Program deck should be followed by data deck. The normal FORTRAN MONITOR SYSTEM control cards should be used in running the program.

B. A fixed point number (I conversion) is an integer or a series of integers without a decimal point; for example 3, 4, 23, etc. They must be written to the extreme right of the field allotted to them.

C. A floating point number (F conversion) is a number containing a decimal point.

12357.845 0.000346 .123 3000000.

These may be written anywhere within the field allotted to them.

MULTPL, IBM 7094 Computer Program, page 2

D. The program deck should be followed by the data cards indicated below with the information described.

1. FIRST CARD

Col. 2 to 72 - title of the problem to be printed with output

2. SECOND CARD - control card (F10.0,6I4)

Col. 1 to 10 - span length = SPAN
Col. 11 to 14 - number of types of plate = NPL, maximum 15
Col. 15 to 18 - number of elements = NEL, maximum 150
Col. 19 to 22 - number of joints = NJT, maximum 100
Col. 23 to 26 - number of points along x-axis at which results are desired = NXP, maximum 10
Col. 27 to 30 - maximum Fourier series limit = MHARM, maximum 100 for NCHECK = 0; maximum 200 for NCHECK = +1 or -1
Col. 31 to 34 - check on odd or even harmonics = NCHECK
+1 to work on odd series only (sym.)
0 to include all series
-1 to work on even series only (anti-sym.)

3. THIRD CARD - x-coordinates at which results are desired (10F7.3) = XP

4. NEXT CARDS - one card for each type of plate (I10,5F10.0)

Col. 1 to 10 - type number = I
Col. 11 to 20 - horizontal projection of plate = H(I)
Col. 21 to 30 - vertical projection of plate = V(I)
Col. 31 to 40 - plate thickness = TH(I)
Col. 41 to 50 - modulus of elasticity = E(I)
Col. 51 to 60 - Poisson's ratio = FNU(I)

5. NEXT CARDS - one card for each element (5I4,3F10.0)
Uniform loads given below exist over entire plate.

Col. 1 to 4 - element number = I
Col. 5 to 8 - joint I = NPI(I)
Col. 9 to12 - joint J = NPJ(I)
} maximum absolute difference = 4
Col. 13 to 16 - type of plate used = KPL(I)
Col. 17 to 20 - number of transverse sections for internal forces and displacements output = NSEC(I), maximum 16, if NSEC = 0 no internal forces or displacements will be output
Col. 21 to 30 - dead load (P/PL-area; force per unit surface area) = DL(I)
Col. 31 to 40 - uniform horizontal load (P/V-area; force per unit vertical projected area) = HL(I)
Col. 41 to 50 - uniform vertical load (P/H-area; force per unit horizontal projected area) = VL(I)

MULTPL, IBM 7094 Computer Program, page 3

6. NEXT CARD

Col. 1 to 4 - number of partial surface loads (I4) = NSURL, maximum 50

7. NEXT CARDS - one card for each partial surface load (I10,4F10.0). No cards required if NSURL = 0.
Loads given below are uniform over plate width and have a length equal to that given under SURDEL.

Col. 1 to 10 - element number = LEL
Col. 11 to 20 - horizontal load, P/V-area (P/V-length if transverse line load is applied) = SURHL
Col. 21 to 30 - vertical load, P/H-area (P/H-length if transverse line load is applied) = SURVL
Col. 31 to 40 - location from left support to center of distributed length = SURXI
Col. 41 to 50 - distributed length in x-direction (=0 for line load) = SURDEL
If SURDEL $\neq$ 0, input SURHL and SURVL as force/unit area
If SURDEL = 0, input SURHL and SURVL as force/unit width

8. NEXT CARDS - one card for each joint (I10,4F10.0,4I2). All joints require a card.

Col. 1 to 10 - joint number = I
Col. 11 to 20 - applied horizontal joint force or displacement = AJFOR (1,I)
Col. 21 to 30 - applied vertical joint force or displacement = AJFOR (2,I)
Col. 31 to 40 - applied joint moment or rotation = AJFOR (3,I)
Col. 41 to 50 - applied longitudinal joint force or displacement = AJFOR (4,I)
Col. 52 - index for horizontal force or displacement, (can be 0,1,2 or 3) = LCASE (1,I)
Col. 54 - index for vertical force or displacement, (can be 0,1,2, or 3) = LCASE (2,I)
Col. 56 - index for moment or rotation, (can be 0,1,2, or 3) = LCASE (3,I)
0 for given zero force
1 for uniformly distributed force (input uniform force/unit length for AJFOR)
2 for concentrated force at midspan (input total force for AJFOR)
3 for given zero displacement

Col. 58 - index for longitudinal force or displacement, (can be 0,2, or 3) =LCASE (4,I)
0 for given zero force
2 for prestress P at each end (input total force at one end for AJFOR, + away from midspan)
3 for given zero displacement

9. NEXT CARD

Col. 1 to 4 - number of concentrated joint loads (I4) = NCONL, maximum 50

10. NEXT CARDS - one card for each conc. joint load (I10,6F10.0). No cards required if NCONL = 0.
More than one location along a joint may be loaded, but each location requires a separate card.

Col. 1 to 10 - joint number = LJT
Col. 11 to 20 - total horizontal force = CONHL
Col. 21 to 30 - total vertical force = CONVL
Col. 31 to 40 - total moment = CONM
Col. 41 to 50 - total longitudinal force P (NOTE - it must be balanced by one -P somewhere along the same joint) =CONS
Col. 51 to 60 - location from left support to center of load = CONXI
Col. 61 to 70 - distributed length in x-direction (=0 for concentrated load) = CONDEL

11. All of the above data cards are repeated for next problem to be solved.

12. Two blank cards are added at the end of the data deck.

REMARKS

1. Number all elements of the same plate type in consecutive groups if possible. This will save some computer time when calculating internal forces.

2. Select joint numbering so as to minimize maximum absolute difference between joint numbers for any plate element. See sketches on page 6.

OUTPUT DESCRIPTION

The output consists of two parts:

a) Input check printout
b) Results

a) Input check printout

The complete input is properly labelled and printed, and may be used to check up on possible errors in punching, field specifications, and order of the cards.

b) Results

The final results consist of the following quantities:

1. Resulting displacements at joints.
Horizontal, vertical, rotational, and longitudinal displacements are given successively for each joint at x-coordinates specified in input.

2. Internal element forces and displacements.
For each element the following quantities are printed:

1) Longitudinal moment per unit length; M_x
2) Transverse moment per unit length; M_y
3) Torsional moment per unit length; M_{xy}
4) Normal shear on transverse section per unit length; Q_x
5) Normal shear on longitudinal section per unit length; Q_y
6) Longitudinal membrane force per unit length; N_x
7) Transverse membrane force per unit length; N_y
8) Membrane shear per unit length; N_{xy}
9) Longitudinal displacement; u
10) Transverse displacement; v
11) Normal displacement; w

MULTPL, IBM 7094 Computer Program, page 6

Sign Convention for Internal Forces of Plate Element

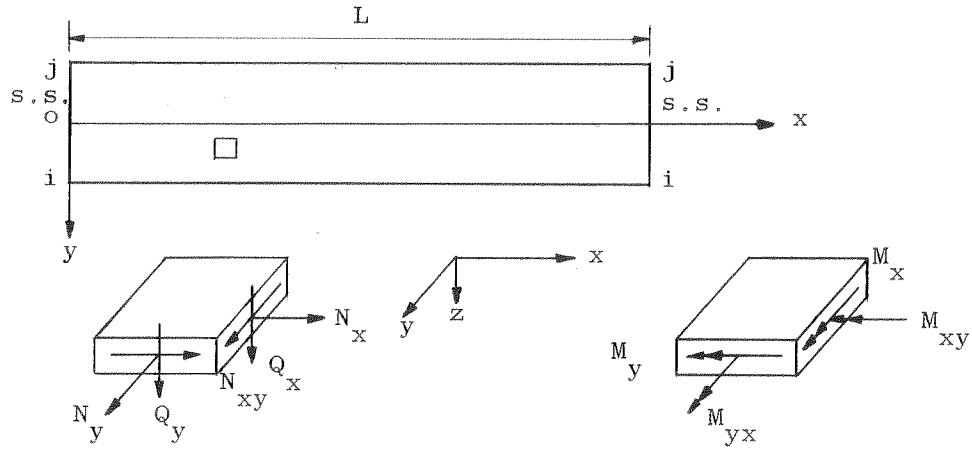

Sign Convention for Surface Loads and Projections of Plate Element

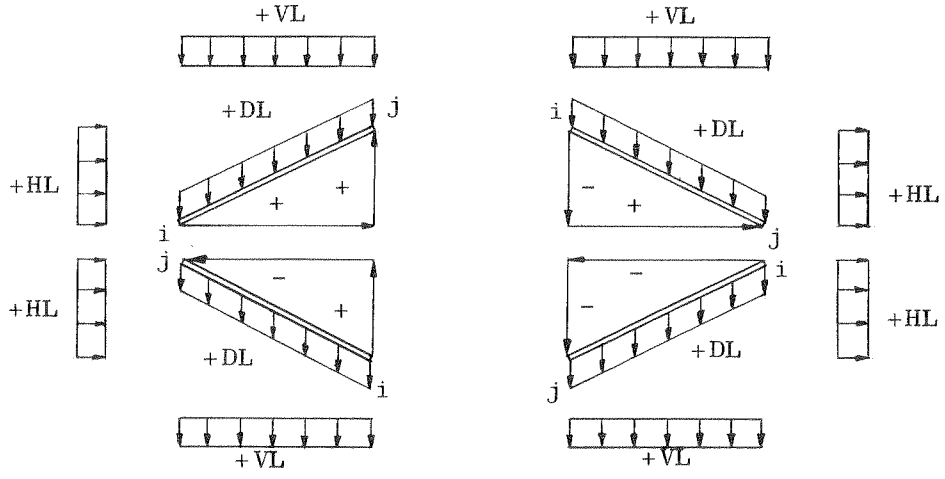

Sign Convention for Joint Forces or Displacements

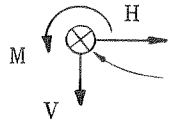

S positive when towards the origin of the plate system.

Alternate Methods of Numbering Joints

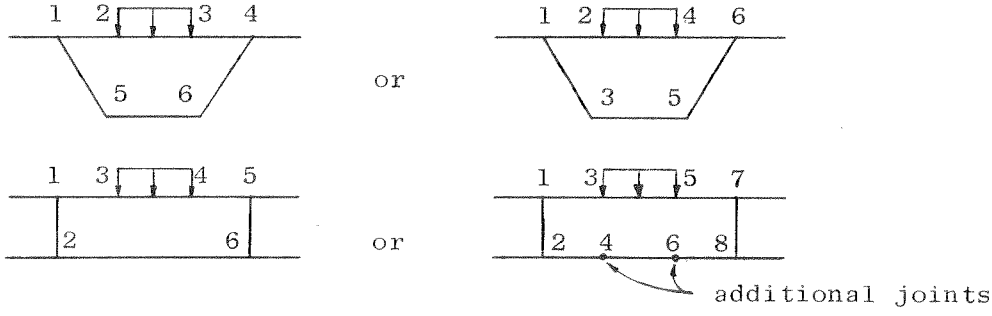

APPENDIX B

Description of IBM 7094 Computer Program for Analysis of Folded Plates Simply Supported at the Ends with Interior Rigid Diaphragms or Supports (MUPDI)

UNIVERSITY OF CALIFORNIA
February 1966

Department of Civil Engineering
Faculty Investigator: A. C. Scordelis

IBM 7094 Computer Program for Analysis of Folded Plates Simply Supported at the Ends with Interior Rigid Diaphragms or Supports

IDENTIFICATION:

MUPDI - Analysis of Folded Plate Structures with Interior Rigid Diaphragms or Supports by the Elasticity Method
Programmed by: Kam-Shing Lo
University of California, February 1966

PURPOSE:

The program provides a rapid solution for cellular or open folded plate structures simply supported at the two ends and having up to four interior rigid diaphragms or supports between the two ends. Uniform or partial surface loads as well as line loads and concentrated loads may be applied anywhere on the structure and the resulting joint displacements together with the internal forces, moments and displacements in each plate element at selected points may be found.

RESTRICTIONS:

Restrictions as to the maximum number of plates, joints, diaphragms, loads etc. are given under input data and remarks.

DESCRIPTION:

The computer solution uses a direct stiffness method for the folded plate system. Compatibility at the interior rigid diaphragms or supports is accomplished by a force (flexibility) method of analysis. The Goldberg-Leve equations are used to evaluate plate fixed edge forces, stiffnesses and final internal forces, moments, and displacements. A harmonic analysis with up to 100 non-zero terms of the appropriate Fourier Series is used for the loads. The program is written in FORTRAN IV language.

FORM OF INPUT DATA:

1. FIRST CARD

   Col. 1 to 72 - title of the problem

2. SECOND CARD - CONTROL CARD (F10.0,7I4)

   Col. 1 to 10 - span length = SPAN
   Col. 11 to 14 - number of types of plate = NPL, maximum 15

MUPDI IBM 7094 Computer Program, page 2

Col. 15 to 18 - number of elements = NEL, maximum 30
Col. 19 to 22 - number of joints = NJT, maximum 20
Col. 23 to 26 - number of diaphragms = NDIAPH, maximum 4
Col. 27 to 30 - number of x-coord. at which results are desired = NXP, maximum 14
Col. 31 to 34 - maximum Fourier series limit = MHARM, maximum 100 for NCHECK = 0; maximum 200 for NCHECK = +1 or -1
Col. 35 to 38 - check on odd or even harmonics = NCHECK
+1 to work on odd series only (sym.)
0 to include all series
-1 to work on even series only (anti-sym.)

3. THIRD CARD

x-coordinates at which results are desired (14F7.3) = XP use second card if needed

4. NEXT CARDS - One card for each diaphragm (I10,2F10.0). No cards required if NDIAPH = 0.

Col. 1 to 10 - diaphragm number = I
Col. 11 to 20 - x-coordinate at which diaphragm exists = DIAPHX(I)
Col. 21 to 30 - diaphragm thickness (width of restraint forces) = DIADEL(I)

5. NEXT CARDS - One card for each type of plate (I10,5F10.0)

Col. 1 to 10 - type number = I
Col. 11 to 20 - horizontal projection of plate = H(I)
Col. 21 to 30 - vertical projection of plate = V(I)
Col. 31 to 40 - plate thickness = TH(I)
Col. 41 to 50 - modulus of elasticity = E(I)
Col. 51 to 60 - Poisson's ratio = FNU(I)

6. NEXT CARDS - One card for each element (5I4,3F10.0,2I2)
Uniform loads given below exist over entire plate

Col. 1 to 4 - element number = I
Col. 5 to 8 - joint I = NPI(I)
Col. 9 to 12 - joint J = NPJ(I)
} maximum absolute difference = 4
Col. 13 to 16 - type of plate used = KPL(I)
Col. 17 to 20 - number of transverse sections, for internal forces and displacements output = NSEC(I), maximum 12, if NSEC = 0 no internal forces or displacements will be output.

Col. 21 to 30 - dead load (P/PL-area; force per unit surface area) = DL(I)
Col. 31 to 40 - uniform horizontal load (P/V-area; force per unit vertical projected area) = HL(I)
Col. 41 to 50 - uniform vertical load (P/H-area; force per unit horizontal projected area) = VL(I)

Restraint Conditions (from diaphragms)

Col. 52 - index for in plane shear restraint = ISHEAR(I)
Col. 54 - index for normal load restraints = IWLOAD(I)
zero punch to consider restraint from diaphragms
non-zero punch to neglect restraint from diaphragms

7. NEXT CARD - Col. 1 to 4 - number of partial surface loads (I4) = NSURL, maximum 50

8. NEXT CARDS - One card for each partial surface load (I10,4F10.0) no cards required if NSURL = 0. Loads given below are uniform over plate width and have a length equal to that given under SURDEL.

Col. 1 to 10 - element number = LEL
Col. 11 to 20 - horiz. load, P/V-area (P/V-length if line load is applied) = SURHL
Col. 21 to 30 - vertical load, P/H-area (P/H-length if line load is applied) = SURVL
Col. 31 to 40 - location from left support to center of distributed length = SURXI
Col. 41 to 50 - distributed length in x-direction (=0 for line load) = SURDEL
If SURDEL $\neq$ 0, input SURHL and SURVL as force/unit area
If SURDEL = 0, input SURHL and SURVL as force/unit width

9. NEXT CARDS - One card for each joint (I10,4F10.0,4I2,2X,3I2). All joints require a card.

Col. 1 to 10 - joint number = I
Col. 11 to 20 - applied horizontal joint force or displacement = AJFOR (1,I)
Col. 21 to 30 - applied vertical joint force or displacement = AJFOR (2,I)
Col. 31 to 40 - applied joint moment or rotation = AJFOR (3,I)
Col. 41 to 50 - applied longitudinal joint force or displacement = AJFOR (4,I)
Col. 52 - index for horizontal force or displacement, (can be 0,1,2, or 3) = LCASE (1,I)
Col. 54 - index for vertical force or displacement, (can be 0,1,2, or 3) = LCASE (2,I)

MUPDI IBM 7094 Computer Program, page 4

Col. 56 - index for moment or rotation, (can be 0,1,2, or 3) = LCASE (3,I)
0 for given zero force
1 for uniformly distributed force (input uniform force/unit length for AJFOR)
2 for concentrated force at midspan (input total force for AJFOR)
3 for given zero displacement

Col. 58 - index for longitudinal force or displacement, (can be 0,2, or 3) = LCASE (4,I)
0 for given zero force
2 for prestress P at each end (input total force at one end for AJFOR, + away from midspan)
3 for given zero displacement

Joint Restraint Conditions (from diaphragms)

Col. 62 - index for horizontal restraint = JFOR (1,I)

Col. 64 - index for vertical restraint = JFOR (2,I)

Col. 66 - index for rotational restraint = JFOR (3,I)
zero punch to consider restraint from diaphragms
non-zero punch to neglect restraint from diaphragms

10. NEXT CARD - Col. 1 to 4 - number of concentrated joint loads (I4) = NCONL, maximum 50

11. NEXT CARDS - One card for each concentrated joint load (I10,6F10.0) No cards required if NCONL = 0. More than one location along a joint may be loaded, but each location requires a separate card.

Col. 1 to 10 - joint number = LJT
Col. 11 to 20 - total horizontal force = CONHL
Col. 21 to 30 - total vertical force = CONVL
Col. 31 to 40 - total moment = CONM
Col. 41 to 50 - total longitudinal force P (Note-it must be balanced by one -P somewhere along the same joint) = CONS
Col. 51 to 60 - location from left support to center of load = CONXI
Col. 61 to 70 - distributed length in x-direction (=0 for concentrated load) = CONDEL

12. NOTE - The next 3 cards are not needed if number of diaphragms = 0.

13. NEXT CARD - Diaphragms which are over rigid external support (4I4) = NDIA
Input numbers in ascending order as needed in Col. 1 to 4; 5 to 8; 9 to 12; 13 to 16.
Use a blank card if no such diaphragms

14. NEXT 2 CARDS - To indicate how the diaphragms are initially connected to the plate system (I4,3(3X,I1))

    Col. 1 to 4 - joint number at which the diaphragms are initially connected = JNUM(I)
    Col. 8 - index for horizontal connection = IC (1,I)
    Col. 12 - index for vertical connection = IC (2,I)
    Col. 16 - index for rotational connection = IC (3,I)
    0 if it is not connected
    1 if it is connected
    NOTE - if only one joint is connected, use 1 in all three indices on one card, put data on 1st card and leave 2nd card blank.
    if two joints are connected, use any combinations of three 1 indices in the horizontal and vertical connection indices, but the rotational connection index must be zero for both joints.

15. All above data cards are repeated for next problem to be solved.

16. Two blank cards are added at the end of the data deck.

REMARKS:

1. Number all elements of the same plate type in consecutive groups if possible. This will save some computer time when calculating internal forces.

2. Select joint numbering so as to minimize maximum absolute difference between joint numbers for any plate element.

3. By using a zero punch for ISHEAR and/or IWLOAD in a plate element card, compatibility between the plate and the diaphragm is maintained at the one third points between the two longitudinal edges of plate. Interaction shear or normal forces between the plate and the diaphragm are assumed to vary linearly over the plate width and uniformly over the diaphragm thickness. A line interaction is assumed if DIADEL = 0.

4. The maximum total number of connections between the folded plate system and all of the diaphragms must be equal to or less than 120. Therefore, assuming there are a total of N zero indices for ISHEAR and IWLOAD and a total of M zero indices for JFOR, horizontal, vertical or rotational joint restraints, then $(2N + M) \times NDIAPH \leq 120$.

OUTPUT DESCRIPTION

The output consists of two parts:

a) Input check printout
b) Results

a) Input check printout

The complete input is properly labelled and printed, and may be used to check up on possible errors in punching, field specifications, and order of the cards.

b) Results

The final results consist of the following quantities:

1. If NDIAPH is not zero the interaction (restraint) joint and plate forces between each diaphragm and the folded plate system are printed.

   The positive directions of shear and normal plate forces are the same as the positive y and z axis of the plate element.

2. Resulting displacements at joints.
   Horizontal, vertical, rotational, and longitudinal displacements are given successively for each joint.

3. Internal element forces and displacements.
   For each element the following quantities are printed:

   1) Longitudinal moment per unit length; M_x
   2) Transverse moment per unit length; M_y
   3) Torsional moment per unit length; M_{xy}
   4) Normal shear on transverse section per unit length; Q_x
   5) Normal shear on longitudinal section per unit length; Q_y
   6) Longitudinal membrane force per unit length; N_x
   7) Transverse membrane force per unit length; N_y
   8) Membrane shear per unit length; N_{xy}
   9) Longitudinal displacement; u
   10) Transverse displacement; v
   11) Normal displacement; w

   Each of these quantities is printed for each transverse section specified across the plate width and at the x-coordinates specified along the plate length.

SIGN CONVENTIONS

The sign conventions for internal forces of plate elements, surface loads, plate dimensions, and joint forces or displacements are the same as those shown for MULTPL on page A6.